THESIS ON NATURAL AND EXACT SCIENCES B191

Analysis of ADP Compartmentation in Cardiomyocytes and Its Role in Protection Against Mitochondrial Permeability Transition Pore Opening

NIINA KARRO

TUT
PRESS

TALLINN UNIVERSITY OF TECHNOLOGY
Institute of Cybernetics
Laboratory of Systems Biology

This dissertation was accepted for the defense of the degree of Doctor of Philosophy in Gene Technology on 24 August 2015.

Supervisor: Rikke Birkedal, PhD
Laboratory of Systems Biology, Institute of Cybernetics,
Tallinn University of Technology, Tallinn, Estonia

Opponents: Prof. Uwe Schlattner, PhD
Laboratory of Fundamental and Applied Bioenergetics,
Joseph Fourier University, Grenoble, France

Margus Eimre, dr. med.
Institute of Biomedicine and Translational Medicine, Department of Pathophysiology,
University of Tartu, Tartu, Estonia

Defense of the thesis: 5 October 2015

Declaration:
I hereby declare that this doctoral thesis, submitted for the doctoral degree at Tallinn University of Technology, is my original investigation and achievement and has not been submitted for the defense of any academic degree elsewhere.

Niina Karro

Colophon: This thesis was typeset with LaTeX 2ε using André Miede's *classicthesis* style with modifications by David Schryer and Ardo Illaste to conform with Tallinn University of Technology style guidelines. The main font is Libertine (Times compatible). Biolinum is used for sans-serif text.

ISSN 1406-4723
ISBN 978-9949-23-836-1 (publication)
ISBN 978-9949-23-837-8 (PDF)

LOODUS- JA TÄPPISTEADUSED B191

ADP kompartmentatsiooni analüüs südamelihasrakkudes ja selle roll mitokondriaalse suure läbitavusega poori avanemise eest kaitsmisel

NIINA KARRO

TTÜ KIRJASTUS

CONTENTS

SUMMARY

This dissertation employed different interdisciplinary methods and approaches in order to study energetic compartmentation of cardiomyocytes and the role of adenosine diphosphate (ADP) in protection against mitochondrial permeability transition pore (mPTP) opening.

New insights into aspects of intracellular ADP diffusion restrictions in cardiac myocytes are gained by using rainbow trout and guanidinoacetate methyltransferase deficient (GAMT-/-) mice as animal models. Although this work revealed the existence of diffusion restrictions in trout cardiomyocytes, the modeling results suggest different metabolic compartmentation and regulation compared to mammalian cardiomyocytes. Results show that trout cardiac cells lack the coupling between a fraction of adenosine triphosphatases (ATPases) and endogenous pyruvate kinase (PK) that was found in rat. The coupling of hexokinase (HK) to mitochondrial respiration in trout cardiomyocytes suggests that they have different metabolic regulation compared to mammalian cardiomyocytes. In addition, no coupling of creatine kinase (CK) to respiration is found. Based on the results, another explanation of diffusional restriction at the mitochondrial outer membrane (MOM) level may be proposed. This thesis considers the view that in part it might be not due to the MOM itself, but due to the close proximity and interactions between the sarcoplasmic reticulum (SR) and mitochondria. This hypothesis also may explain why mice with a disabled CK-system show near-normal function and no structural changes in energetic compartmentalization as well as mitochondrial organization. In vivo, the mitochondria-SR coupling creates the structural key basis for the optimal regulation of mitochondrial respiration, excitation-contraction coupling (ECC), Ca^{2+} and reactive oxygen species (ROS) signaling, thus avoiding the danger of mitochondrial Ca^{2+}-overload and irreversible opening of the mPTP.

This dissertation also demonstrates that ADP is a potent inhibitor of mPTP in severely stressed mitochondria and that this mechanism is not related to its effect on ROS production. The results imply that ADP may regulate mPTP via some other mechanism, in addition to its regulation via adenine nucleotide translocase (ANT) and reduction in ROS production. This work also discusses the physiological implications of ADP diffusional barriers considering the role of ADP in mPTP regulation.

KOKKUVÕTE

Käesoleva väitekirja eesmärk on ADP difusioonitakistuste analüüs südamelihasrakkudes ning ADP rolli uurimine mitokondriaalse suure läbitavusega poori (mPTP) avanemise eest kaitsmisel patofüsioloogilistes tingimustes. Rakendades erinevaid interdistsiplinaarseid meetodeid ning lähenemisi saadakse uusi teadmisi rakusisese energeetilise kompartmentatsiooni valdkonnas kasutades vikerforelli ja GAMT-puudulikkusega hiiri.

Üheltpoolt katsetulemused näitavad rakusiseste difusioonitakistuste olemasolu vikerforelli südamelihasrakkudes, siis modelleerimistulemused vihjavad erineva metaboolse kompartmentatsiooni ja regulatsiooni olemasolule võrreldes imetajate südamelihasrakkudega. Analüüsides tulemusi matemaatilise mudeli kaasabil näidati, et forelli südamelihasrakkudes puudub funktsionaalne sidestus endogeense püruvaatkinaasi (PK) ja teatava osa rakusiseste ATPaaside vahel, seevastu, on selline seos leitud rotti südamelihasrakkudes. Funktsionaalne sidestus heksokinaasi (HK) ja mitokondriaalse hingamise vahel vihjab erineva metaboolse regulatsiooni olemasolule võrreldes imetajate südamelihasrakkudega. Lisaks leiti, et vikerforelli südamelihasrakkudes puudub funktsionaalne sidestus kreatiinkinaasi (CK) ja mitokondriaalse hingamise vahel. Saadud tulemuste põhjal võib esitada alternatiivse selgituse difusioonitakustustele mitokondriaalse välise membraani (MOM) tasemel. Antud töö esitab arvamuse, et osaliselt difusioonitakustused võivad mitte olla tingitud MOMist, vaid hoopis sarkoplasmaatilise retikulumi (SR) ja mitokondrite lähestikku paiknemisest ja koostoimest. Selline hüpotees võib seletada, miks ei erine energeetiline kompartmentatsioon ja mitokondriaalne organisatsioon metsiktüüpi ning GAMT-puudulikkusega hiirte vahel, kellel funktsionaalne CK-süsteem puudub. In vivo, mitokonder-SR seostus loob struktuurse aluse elektromehaanilise sidestuse (ECC), mitokondriaalse hingamise, Ca^{2+} ning reaktiivsete hapniku radikaalide (ROS) signaalkaskaadi optimaalse reguleerimise jaoks, seega vältides Ca^{2+}-ülekoormust mitokondris ja pöördumatut mPTP avanemist.

Lisaks rakusisese ADP kompartmentatsiooni uurimisele on antud töö raames uuritud ADP rolli mPTP avanemise eest kaitsmisel patofüsioloogilistes tingimustes. Saadud tulemused näitavad, et ADP inhibeerib mPTPt ka tõsiselt kahjustatud mitokondrites, ning et see efekt ei ole tõenäoliselt seotud tema võimaliku mõjuga ROS tootmisele. Selline tulemus demonstreerib, et ADP võib reguleerida mPTPt mõne muu mehhanismi kaudu, kui regulatsioon läbi ANT ning ROS tootmise vähendami-

se kaudu. Doktoritöö samuti arutab ADP difusioonibarjääride füsioloogilist mõju arvestades ADP rolli mPTP reguleerimisel.

LIST OF PUBLICATIONS

List of publications by Niina Karro (formely Sokolova)

I **Sokolova N**, Vendelin M, Birkedal R; **Intracellular diffusion restrictions in isolated cardiomyocytes from rainbow trout.** *BMC Cell Biology*, Volume 10, Issue 90, December 2009

II **Karro N**, Sepp M, Jugai S, Laasmaa M, Vendelin M, Birkedal R; **Metabolic compartmentation and regulation in rainbow trout cardiomyocytes.** *Submitted, (2015)*

III Branovets J, Sepp M, Kotlyarova S, Jepihhina N, **Sokolova N**, Aksentijevic D, Lygate CA, Neubauer S, Vendelin M, Birkedal R; **Unchanged mitochondrial organization and compartmentation of high-energy phosphates in creatine deficient GAMT-/- mouse heart.** *The American Journal of Physiology: Heart and Circulatory Physiology*, 305: 506-520, August 2013

IV **Sokolova N**, Pan S, Provazza S, Beutner G, Vendelin M, Birkedal R, Sheu S-S; **ADP protects cardiac mitochondria under severe oxidative stress.** *PLoS One*, Volume 8, Issue 12, December 2013

Summary of author's contributions

I In Publication I the author performed all the experimental work, the data analysis, prepared the figures and contributed to the text.

II In Publication II the author performed all the experimental work and live cell imaging, the raw data analysis, prepared some of the figures and contributed to the text.

III In Publication III the author performed a part of the oxygraphic and spectrophotometric experiments.

IV In Publication IV, which consists of work carried out at the University of Rochester Medical Center, the author participated in design and coordination of the study, performed all the experimental work, the data analysis, prepared all the figures and contributed to the text.

LIST OF CONFERENCE PRESENTATIONS

I Sokolova N, Birkedal R, Vendelin M; **Intracellular Diffusion Restrictions in Trout Cardiomyocytes**; Biophysical Society 53rd Annual Meeting 2009, Boston, Massachusetts, USA, February 28 - March 4, 2009

II Birkedal R, Sokolova N, Laasmaa M, Vendelin M; **Using Rainbow Trout Cardiomyocytes to Identify the Diffusion Restrictions Found Specifically in Oxydative Muscles**; Annual Meeting of the Society of Experimental Biology, Glasgow, UK, June 28 - July 1, 2009

III Sokolova N, Birkedal R, Vendelin M; **Intracellular Diffusion Restrictions in Trout Cardiac Fibers and Cells**; 36th International Congress of Physiological Sciences (IUPS 2009), Kyoto, Japan, July 27 - August 1, 2009

IV Sokolova N, Provazza S, Pan S, Beutner G, Birkedal R, Vendelin M, Sheu S-S; **Regulation of Mitochondrial Permeability Transition by ADP**; Biophysical Society 55rd Annual Meeting 2011, Baltimore, Maryland, USA, March 5 - 9, 2011

V Sepp M, Branovets J, Sokolova N, Kotlyarova S, Birkedal R, Vendelin M; **Influence of SERCA and Actomyosin ATPase on Respiration Kinetics in Permeabilized Rat Cardiomyocytes**; Biophysical Society 55rd Annual Meeting 2011, Baltimore, Maryland, USA, March 5 - 9, 2011

VI Gross P, Sokolova N, Provazza S, Beutner G, Sheu S-S; **Comparative Effects of Ryanodine Receptor Inhibitors on Mitochondrial Ca^{2+} Uptake Profiles in Control and Malignant Hyperthermia Mouse Heart**; The 65th Annual Meeting of the Society of General Physiologists: Mitochondrial Physiology and Medicine 2011, Woods Hole, Maryland, USA, September 7 - 11, 2011

VII Sokolova N, Birkedal R, Vendelin M; **Distribution of Intracellular ADP Diffusion Restriction in Trout Cardiomyocytes**; Biophysical Society 56th Annual Meeting 2012, San Diego, California, USA, February 25 - 29, 2012

VIII Gross P, Sokolova N, Pan S, Beutner G, Sheu S-S; **Regulation of Mitochondrial Ca^{2+} Uptake by Mitochondrial Ryanodine Receptor in Control and Malignant Hyperthermia Mouse Heart**; Biophysical Society 56th Annual Meeting 2012, San Diego, California, USA, February 25 - 29, 2012

IX O-Uchi J, Porter GA, Kang SH, Boncompagni S, Sokolova N, Gross P, Jhun BS, Beutner G, Brookes PS, Blaxall BC, Dirksen RT, Protasi F, Pan S, Sheu S-S; **Malignant Hyperthermia Mutation of RyR1 (Y522S) Increases Catecholamine-Induced Cardiac Arrhythmia Through Mitochondrial Injury**; Basic Cardiovascular Sciences, 2012 Scientific Sessions, New Orleans, LA, USA, July 23 - 26, 2012

X Sokolova N, Vendelin M, Birkedal R; **Distribution of Intracellular ADP Diffusion Restriction in Trout Cardiomyocytes**; Biophysical Society 57th Annual Meeting 2013, Philadelphia, Pennsylvania, USA, February 2 - 6, 2013

XI Branovets J, Sepp M, Kotlyarova S, Jepihhina N, Sokolova N, Aksentijevic D, Lygate CA, Neubauer S, Vendelin M, Birkedal R; **Unchanged Mitochondrial Organization and Compartmentation in Creatine Deficient GAMT-/- Mouse Heart**; Biophysical Society 57th Annual Meeting 2013, Philadelphia, Pennsylvania, USA, February 2 - 6, 2013

XII Kotlyarova S, Mandel M, Sokolova N, Aksentijevic D, Lygate CA, Neubauer S, Vendelin M, Birkedal R; **Cardiomyocytes from Creatine-Deficient Mice Lacking L-arginine:glycine amidinotransferase (AGAT) Show no Changes in Mitochondrial Organization and Cellular Compartmentation**; Biophysical Society 57th Annual Meeting 2013, Philadelphia, Pennsylvania, USA, February 2 - 6, 2013

XIII Sokolova N, Sepp M, Kotlyarova S, Laasmaa M, Vendelin M, Birkedal R; **Metabolic compartmentation and regulation in rainbow trout cardiomyocytes**; 37th International Congress of Physiological Sciences (IUPS 2013), Birmingham, UK, July 21 - 26, 2013

PREFACE

This thesis concludes research carried out mainly at the Laboratory of Systems Biology, Institute of Cybernetics at Tallinn University of Technology. The studies were supervised by Dr. Rikke Birkedal, the senior researcher at Institute of Cybernetics. The work presented here is the result of a multidisciplinary project, aiming to study energetic compartmentation and regulation in isolated permeabilized cardiomyocytes. This research resulted in Publication I, Publication II and Publication III. Financial support from the Wellcome Trust (081755), the Estonian Science Foundation (ETF8041) as well as the Archimedes Foundation is very appreciated.

A part of this thesis has been carried out at the laboratory of Prof. Shey-Shing Sheu, University of Rochester Medical Center, New York, USA. The collaboration with Prof. Sheu developed into Publication IV: "ADP protects cardiac mitochondria under severe oxidative stress". The project was financed by NIH grants (RO1HL-033333, RO1HL-093671 and R21HL-110371).

Certainly, I would have never reached the point of finishing my dissertation without the help and support of others. Many inspiring people have been involved in the work leading to my PhD thesis. I would like to acknowledge everyone for their contributions to the studies conducted during my time as a PhD student.

Acknowledgements

It is my pleasure to express my sincere gratitude to all the people who have inspired me during my doctoral study. First and foremost, I would like to give special thanks to my supervisors Dr. Rikke Birkedal and Dr. Marko Vendelin for giving me the opportunity to work in their research group, for their invaluable guidance and help, and for all that they have taught me over the past years. Your great support and encouragement of independent study are greatly appreciated.

I would like to thank all past and present members of the SysBio Lab for the valuable collaborations, discussions, support and for sharing in the highs and lows at every stage of the progress. Thank you all for being good friends and such great people to work with. Many thanks to Dr. Pearu Peterson for his help with Python-related software.

I owe particular thanks to all the members of Bioenergetics lab at KBFI, your help is very much appreciated.

I would like to thank my supervisor at the University of Rochester Prof. Shey-Shing Sheu for providing me with many opportunities to grow. I have learned a lot from his research experience, his great enthusiasm and passion towards science. I would like to thank past and present members of Prof. Sheu lab for their help in my research: Dr. Virendra Sharma, Dr. Gisela Beutner and Dr. Shi Pan for many insightful comments that challenged me to consider my topic from different perspectives. I convey my special thanks to Dr. Sung Hyun Kang, Dr. Bong Sook Jhun, Dr. Jin O-Uchi, Polina Gross and Sarah Provazza, who helped me in so many ways during my time in Rochester. Thank you for your friendship and sharing your time with me, I heartily wish you luck.

Also I would like to thank Prof. Paul S Brookes and everybody in his lab, especially, Dr. Sergiy Nadtochiy and Dr. Andrew Wojtovich, for a great help and sharing their lab, instruments and time with me. I would like to thank everybody in the Mitochondrial Research and Innovation Group (MRIG) at the University of Rochester Medical Center for all their seminars and discussions. I always received help, new ideas, and direction in my project.

I would like to dedicate this dissertation to my family. Without your encouragement and support, I would not have made it this far.

ACRONYMS

ADP	adenosine diphosphate
AK	adenylate kinase
ANT	adenine nucleotide translocase
ATP	adenosine triphosphate
ATPases	adenosine triphosphatases
CK	creatine kinase
Cr	creatine
CRC	Ca^{2+} retention capacity
CsA	cyclosporine A
CypD	cyclophilin D
ECC	excitation-contraction coupling
GAMT	guanidinoacetate methyltransferase
GAMT-/-	guanidinoacetate methyltransferase deficient
GAPDH	glyceraldehyde-3-phosphate dehydrogenase
HK	hexokinase
ICEUs	intracellular energetic units
IMS	mitochondrial intermembrane space
IR	ischemia-reperfusion
$K_{M_{ADP}}$	apparent Michaelis-Menten constant for ADP
MIM	mitochondrial inner membrane
MOM	mitochondrial outer membrane
mPiC	mitochondrial phosphate carrier
mPTP	mitochondrial permeability transition pore
mtCK	mitochondrial creatine kinase
NADH	reduced nicotinamide adenine dinucleotide
NMR	nuclear magnetic resonance
PCr	phosphocreatine
PEP	phosphoenolpyruvate

PGK	3-phosphoglycerate kinase
Pi	phosphate ion
PK	pyruvate kinase
ROS	reactive oxygen species
SERCA	sarco-endoplasmic reticulum Ca^{2+} ATPase
SR	sarcoplasmic reticulum
t-BH	tert-butyl hydroperoxide
VDAC	voltage gated anion channel

THESIS

1

INTRODUCTION

Understanding the mechanisms that regulate the mitochondrial function and energy transfer in normal and pathological cardiac cells is important for the research in the field of cardiac bioenergetics as well as for the diagnosis of many heart diseases. The correct analysis of this regulation has direct implications for the determination of pathophysiological mechanisms and adaptive strategies for a variety of disorders in cardiac muscle.

Heart muscle as a high-energy demanding organ has developed an exceptional capacity for energy production, featuring the highest density of mitochondria per cell among all the other organs. Indeed, approximately 30% of the cardiomyocyte volume is occupied by mitochondria [1], in which oxidative phosphorylation occurs, producing more than 90% adenosine triphosphate (ATP) necessary for normal cardiac function [2]. Cardiac function depends on a well balanced and highly efficient matching of energy supply and demand. A normal heart is able to balance the rate of ATP production with the rate of utilization while maintaining stable cellular pools of ATP, ADP, phosphocreatine (PCr) and other energy metabolites despite the fluctuations in cellular energy demand and workload [3–5]. The mechanisms ensuring sufficient production of ATP in mitochondria, efficient transport of ATP to muscle ATPases of the contractile system, as well as rapid removal of ADP generated in these reactions remain controversial. The most important factors suggested to serve as key regulators of mitochondrial metabolism are ADP, phosphate ion (Pi) and Ca^{2+} (Fig. 1).

ADP and Pi have been suggested as the natural regulatory mechanisms of mitochondrial energy metabolism since they coordinate with both ATP consumption and production via feedback of ADP and Pi from ATPases. As such, ATP utilization in cytosol increases ADP and Pi fluxes to mitochondria via CK-system [6, 7] and consequently the availability of substrates for ATP generation increases. ADP and Pi enter the mitochondria via ANT and mitochondrial phosphate carrier (mPiC), respectively, and stimulate ATP-production by F_1F_0-ATPase (Fig. 1). It has been found that ADP acts not only as a substrate for F_1F_0-ATPase, but also activates the pyruvate dehydrogenase complex [8] and isocitrate dehydrogenase [9]. Pi has been

proposed to play an important role at low and moderate workloads [10]. It activates mitochondrial reduced nicotinamide adenine dinucleotide (NADH) generation, the flux of reducing equivalents in the cytochrome chain, and serves as a substrate for ATP production [11, 12].

To understand the nature of regulation by feedback, it is necessary to take into consideration energetic compartmentalization in cardiomyocytes. It is interesting that in oxidative muscles, which rely on oxidative metabolism to generate ATP, seems to be barriers that restrict ADP diffusion significantly [13, 14]. These local restrictions have been suggested to be overcome by the CK-system acting as a temporal and spatial buffer between sites of energy generation and utilization. Such structural and functional compartmentation is considered to play an essential role in the regulation of heart energy metabolism ensuring optimal metabolic signaling and feedback and in such way avoiding deprivation of cardiac energy during sudden changes in energetic requirements of the heart. These subcellular compartments and their specific localization are the objects of active studies. The identification of diffusion restricting structures is clinically relevant, since compromised energetic balance induced by ischemia-reperfusion (IR) injury is associated with reduced diffusion restriction [15–18].

Another potential regulator of mitochondrial metabolism is Ca^{2+}. In cardiomyocytes, Ca^{2+} mediates ECC and in parallel stimulates Krebs cycle by activating mitochondrial matrix Ca^{2+}-dependent dehydrogenases to maintain the NADH redox potential and the ATP synthetic capacity of the F_1F_0-ATPase [19–23]. This coupling is achieved by mitochondria being located adjacent to SR and the close proximity of Ca^{2+} release units [24]. As a result, the balance between energy demand and supply is maintained during high workloads by correlation between cytosolic and mitochondrial Ca^{2+} via regulation of Ca^{2+} influx and efflux mechanisms across the mitochondrial inner membrane (MIM) [25, 26]. In this way, ADP and Ca^{2+} regulate the rate of ATP hydrolysis in a complementary way as a feedback and feed-forward signaling molecules, thus providing an adequate mitochondrial response to increased cellular energy demand (Fig. 1).

Ca^{2+} and ADP are also two major regulators of the mPTP, a key mechanism for cell death through both apoptosis and necrosis [27]. In the regulation of mPTP opening, Ca^{2+} and ADP have opposite effects. Mitochondrial Ca^{2+}-overload accompanied by excessive production of ROS leads to irreversible opening of mPTP, which is a major cause of cell death. ADP is a well known mPTP inhibitor, since it serves as a substrate for ATP generation and its binding to ANT shifts the latter to "m" (matrix) conformation, which favors the closure of mPTP [28, 29], (see Fig. 1).

Specifically, this dissertation is focused on ADP - its regulation of mitochondrial energy production and protection from mPTP under pathophysiological conditions. The thesis consists of five chapters and four publications. Chapters 2, 3

and 4 give a short theoretical background to a specific research field, provide discussions and outline the main results achieved during my doctoral studies. The first subject explored in this work concerns the study on rainbow trout cardiac muscle energetics, which addresses important questions regarding the ADP compartmentation and metabolic regulation. This work is summarized in Publication I and Publication II. The second topic is related to the study of mitochondrial organization and energy transfer in cardiomyocytes of GAMT-/- mice, lacking functional CK-system. Chapter 3 provides an introduction to the role of CK-system in the heart and the overview of the outcomes and discussion of Publication III. The third study was done in collaboration with prof. Shey-Shing Sheu at the University of Rochester Medical Center. Chapter 4 presents a summary of the main results of Publication IV and discusses the protective effects of ADP from mPTP opening in cardiac mitochondria under severe oxidative stress. Chapter 5 summarizes the main conclusions.

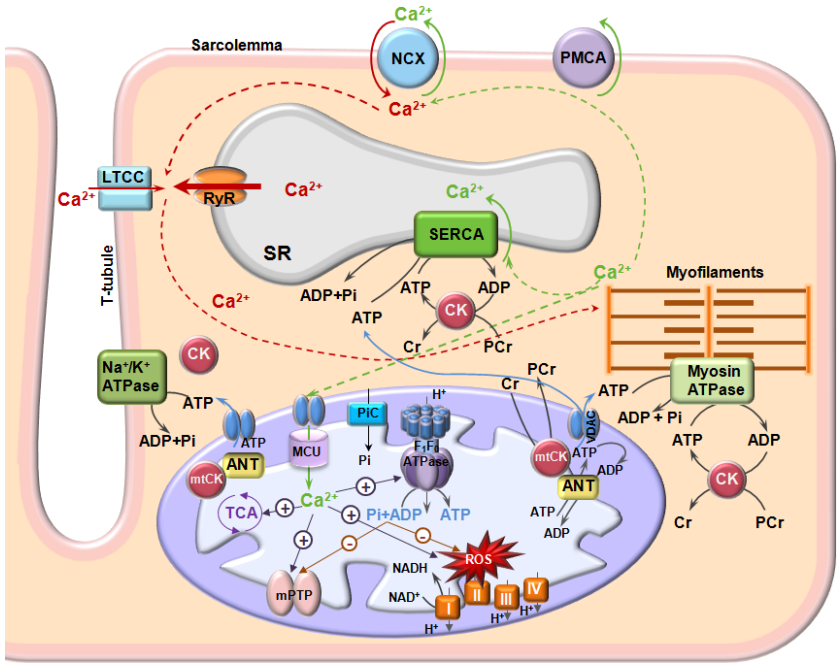

Figure 1 – Schematic presentation of mitochondrial energetics regulation and excitation-contraction coupling. Mitochondrial energetics are regulated by ADP/Pi feedback and parallel Ca^{2+} activation in order for ATP generation to match ATP consumption. ADP and Pi feedback from ATPases via creatine kinase (CK) system stimulates ATP production by F_1F_0-ATPase. It combines Pi and ADP to form ATP, which is then exchanged for ADP across the inner mitochondrial membrane (MIM) by the adenine nucleotide translocase (ANT). The F_1F_0-ATPase reaction is driven by a proton gradient maintained mainly by the respiratory chain (shown as complexes I–IV). The voltage-dependent anion channel (VDAC) is involved in transport of anions, cations, Ca^{2+}, ATP, ADP and other metabolites across the outer mitochondrial membrane (MOM). Pi is transported across the MIM into the mitochondrial matrix by the mitochondrial phosphate carrier (PiC). The energy contained within ATP is then transferred to the cytoplasmic phosphocreatine (PCr) pool through the actions of a mitochondrial creatine kinase (mtCK). PCr is converted back to creatine (Cr) by cytosolic CK. The freed energy is used for ATP formation and driving the peripheral ATPases. Solid blue lines indicate the direct ATP transfer from the mitochondria to the sites of utilization independent of the CK-system. As ATP diffusion is limited, the direct transfer of ATP from the mitochondria to a site of utilization requires close localization between the mitochondria and the peripheral ATPases. Solid red and green lines indicate movement of Ca^{2+} and dotted red and green lines indicate cytosolic Ca^{2+} flux during contraction and relaxation, respectively. During the action potential, Ca^{2+} is transported across the myocyte membrane (sarcolemma or T-tubules) via L-type Ca^{2+} channels (LTCC) and to a lesser extent via the Na^+/Ca^{2+} exchanger (NCX), thereby releasing a larger pool of Ca^{2+} through cardiac ryanodine receptor (RyR) from the sarcoplasmic reticulum (SR). This Ca^{2+} activates contraction of the myofilaments. During relaxation, Ca^{2+} is taken up back into the SR by SR Ca^{2+} ATPase (SERCA) and is pumped out of the cells by NCX. Mitochondrial Ca^{2+} uniporter (MCU) and plasma membrane Ca^{2+} ATPase (PMCA) only contribute by 1% to 2% to fast Ca^{2+} extrusion [30, 31]. In parallel Ca^{2+} activates the tricarboxylic acid (TCA) cycle Ca^{2+}-dependent dehydrogenases and the F_1F_0-ATPase. Ca^{2+} and ADP are also key regulators of mitochondrial permeability transition pore (mPTP) opening, among other things via their regulation of reactive oxygen species (ROS) production. In the regulation of mPTP opening Ca^{2+} and ADP function oppositely. Thus Ca^{2+} and ADP signals must balance to adjust metabolism and avoid opening of the mPTP.

2

INTRACELLULAR COMPARTMENTATION OF CARDIOMYOCYTES

Cardiomyocytes represent a unique and complex architecture. Experimental and model studies suggest that cardiomyocytes are compartmentalized by intracellular diffusion barriers that restrict diffusion of ADP in cytosol and at the level of the MOM. However, the structural and molecular nature of these barriers as well as the exact localization remain uncertain and are the subjects of active research.

Presumably, there may be different levels of energetic compartments. The smallest compartments are represented by coupled enzymes. It is recognized that the coordination between ATP utilization and generation processes can be achieved through a coupled enzymatic network. Examples of functional enzymatic coupling are the coupling of CK-isoenzymes to the energy consuming sites in cytosol such as actomyosin ATPases [14, 32], sarco-endoplasmic reticulum Ca^{2+} ATPase (SERCA) [33, 34], Na^+/K^+ATPases [35] and the energy producing sites (mitochondria, glycolysis). In addition to CK, the concerted action of mitochondrial and cytosolic isoforms of adenylate kinase (AK) [36, 37] or glycolytic enzymes such as PK, glyceraldehyde-3-phosphate dehydrogenase (GAPDH)/3-phosphoglycerate kinase (PGK) or HK [36, 38] also contribute to intracellular phosphotransfer and spatial distribution.

Candidates for the next size level compartments are the membrane-delimited organelles, such as mitochondria and SR (see Fig. 2). Several decades of research on regulation of mitochondrial respiration in rat cardiac cells using permeabilized cell technique [42, 43] have demonstrated that the apparent ADP affinity of mitochondrial respiration for exogenous ADP is much lower in permeabilized cardiomyocytes compared to isolated mitochondria [13, 44–50]. Detailed analysis of the data has indicated a significant diffusion restriction for ADP at the MOM level, permeability of which has been assumed to be regulated by tubulin binding to voltage gated anion channel (VDAC) [51, 52] and might be partially overcome by CK [32, 47]. Besides, the close localization and interactions between SR and mitochondria are essential for the signal transduction, dynamics, regulation of ECC

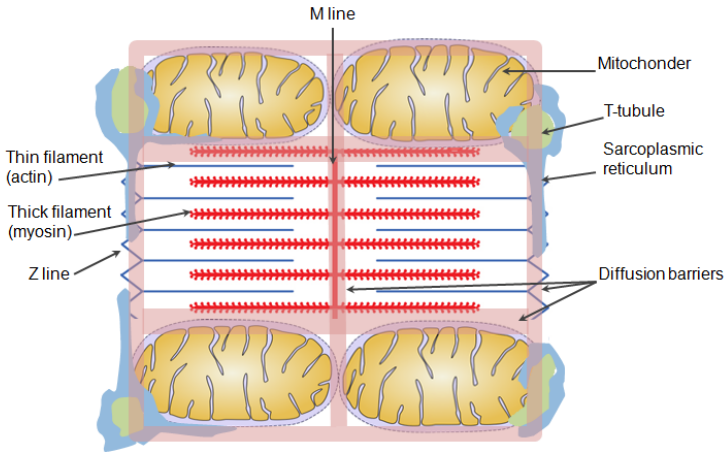

Figure 2 – Schematic organization of diffusional barriers in cardiomyocytes. The scheme is scaled according to [39, 40] and show mitochondria, t-tubules and sarcoplasmic reticulum around a sarcomere. The diffusional barriers (pink lines) are scaled according to [41] and superimposed. In transversal direction, diffusion barriers are formed by mitochondrial and SR membranes, while longitudinal barriers are constituted by protein-dense regions in the myofilaments (z-lines, m-bands) and possibly in part by the junctional SR and t-tubules. The barriers are in agreement with the cell structures, and seem to separate mitochondria and myosin ATPases.

and oxidative energy production in the mitochondria. Moreover, it ensures the energetic coupling between SERCA and mitochondria [53]. It has been suggested that SR and associated cytoskeleton proteins may also act as a diffusion barrier leading to functional coupling of ATPases and mitochondria [54] (see Fig. 2). This assumption gives an alternative explanation of diffusional restriction at the level of MOM. In addition to SR and mitochondria, t-tubules also have been suggested to contribute to diffusion restrictions.

The largest compartments are represented by intracellular energetic units (ICEUs), in which t-tubules, mitochondria and adjacent ATPases of SR and myofibrils are organized into functional complexes [55–57]. Their possible confinement of ADP and ATP into small compartments with reduced diffusion distances is considered to enhance the functional coupling between adjacent energy producing mitochondria and energy consuming ATPases. It has been proposed that in ICEUs a metabolic signaling between sites of ATP production and utilization occurs via two parallel energy transfer systems: via direct channeling of adenine nucleotides [53, 56] and via CK-system. The latter is controlled by ADP and Pi concentration, thus adjusting the mitochondrial ATP generation to the actual ATP turnover in the cytosol without changing the total levels of adenine nucleotides. ICEUs hypothesis was proposed on the basis of experiments that suggest the existence of

cytoplasmic structural barriers restricting the distribution of adenine nucleotides in the cytosol [53, 55, 58]. Mathematical modeling of the data showed that the diffusion restrictions of ADP are localized in certain areas and are not distributed homogeneously in the cardiomyocyte [59].

Several arguments have been raised against the hypothesis of diffusion restrictions. As an alternative explanation, Kongas et al. [60] proposed that the high apparent Michaelis-Menten constant for ADP ($K_{M_{ADP}}$) in fibers might be due to inhomogeneity of skinned fiber preparation as well as the larger diameter of the fibers compared to the cells. In addition to skinned fibers, it is possible that the formation of small cell aggregates in the oxygraph together with unstirred layers surrounding the cells may lead to larger diffusion distances [60]. This hypothesis was tested by comparing cell population and single cell kinetics on isolated permeabilized rat cardiomyocytes [61]. The results of the study and the quantification of the influence of unstirred water layers on the measurements confirmed that diffusion restrictions indeed reside inside the cardiomyocytes and are not an artifact of the preparation [61]. Furthermore, the analysis of measured diffusion coefficients for two fluorescent dyes in rat cardiomyocytes by mathematical model of intracellular diffusion, suggested the presence of an obstructive lattice inside the cell that could cause restrictions of the molecular diffusion [41].

To find out what factors cause the compartmentation, we took advantage of the structural differences between rat and rainbow trout cardiomyocytes. Trout cardiac cells have different morphology and relatively simple cytological architecture. In terms of morphology, energetics and function cardiomyocytes from trout more closely resemble myocytes from neonatal rather than adult mammals [62, 63]. Furthermore, trout cardiomyocytes rely more on glycolytic energy production [64], they are more hypoxia-tolerant and seem to lack a tight functional coupling of mitochondrial creatine kinase (mtCK) to respiration [65]. Most of experiments have been done on mammalian cardiomyocytes, however, experiments on skinned fibers suggest that diffusion restrictions also exist in heart of fish [65–67]. These features make rainbow trout a very good animal model to study ADP diffusion restrictions in low-performance hearts using mathematical models of regulation of mitochondrial respiration.

The results from trout fibers may be affected by clustering of fibers on top of the stirrer during oxygraphic measurements and incomplete separation of the cells, which is avoided when studying isolated permeabilized cardiomyocytes. In Publication I ADP-kinetics of mitochondrial respiration was compared in permeabilized fibers, cardiomyocytes and isolated mitochondria from rainbow trout heart. The measurements were performed at different temperatures to cover the physiological range for rainbow trout and in the absence and presence of creatine (Cr) to

test whether diffusion is facilitated by the CK-system. The study was complicated by the fact that isolated trout cardiomyocytes hypercontracted after permeabilization in the solution used for mammalian cardiomyocytes that seemed to work for fibers. This necessitated the need for the development of an alternative solution, in which isolated trout cardiomyocytes could retain their morphology and show stable steady-state respiration rates throughout an experiment. The results were obtained using a new developed fish respiration solution and demonstrated that $K_{M_{ADP}}$ in trout fibers was higher than in cardiomyocytes. In contrast to fibers, $K_{M_{ADP}}$ in permeabilized cardiomyocytes was independent of temperature and not decreased by Cr. However, $K_{M_{ADP}}$ was still about ten times higher than in isolated mitochondria, suggesting that intracellular diffusion of ADP is indeed restricted in trout cardiomyocytes. This was surprising, because trout cardiac cells are long and thin, lack t-tubules, have a lower SR density and only a single layer of myofilaments surrounding a central core of mitochondria. Publication I discusses the difference between fibers and cardiomyocytes, the effect of temperature and the physiological importance of diffusion restrictions. Publication I concludes that diffusion restrictions also exist in trout cardiomyocytes despite their structural difference and lack of membrane structures penetrating the cytosol, it also points out that the absence of a Cr effect may indicate that trout heart lacks mtCK tightly coupled to respiration.

To study intracellular diffusion restrictions further in Publication II we combined mathematical modeling and specific kinetic experiments to reveal aspects of intracellular compartmentation in trout cardiomyocytes. The main purpose of Publication II was to find the distribution of ADP diffusion restrictions in permeabilized trout cardiomyocytes and to confirm whether they indeed lack the coupling of mtCK to respiration. To reach this goal, sets of experimental data were generated for the further analysis by a series of mathematical models of different complexity as in [68]. We measured mitochondrial respiration stimulated by ADP and ATP, and evaluated the rate of inhibition of ATP stimulated respiration by an ADP-trapping system, consisting of phosphoenolpyruvate (PEP) activating endogenous PK, and exogenous PK, which competes with mitochondria for ADP. In Publication II we found a high activity of HK, which stimulates mitochondrial respiration when activated by glucose. Henceforward, the sets of experimental data were performed 1) under control conditions, 2) in the presence of glucose to study the role of HK in more detail, and 3) in the presence of Cr to assess the role of CK. One of the important outcomes of Publication II is that the apparent $K_{M_{ADP}}$ was more than two times higher than reported in Publication I, indicating the fact that intracellular diffusion restrictions in permeabilized trout cardiomyocytes are more prominent. However, the extent of diffusion restriction in terms of $K_{M_{ADP}}$ is still smaller in trout than in rat cardiomyocytes. The results also showed that the overall meta-

bolic compartmentation is different in trout cardiomyocytes. In contrast to rat cardiomyocytes, the present data were best fit by a simple model, which considered only three compartments: solution, cytosol and mitochondrial intermembrane space (IMS). In comparison, rat cardiomyocytes have an additional fourth compartment, where PK is functionally coupled to a fraction of ATPases [68]. The mathematical model suggests that in the control case, the exchange coefficients between solution and cytosol and IMS and cytosol are roughly similar, indicating that diffusion is restricted to almost same extent by cytosolic factors (~40%) as by the MOM (~60%). It should be noted that the extent of the diffusion restriction at the MOM level is similar to that in rat cardiomyocytes [68]. Publication II also demonstrated that in trout cardiomyocytes instead of CK, HK is functionally coupled to respiration, thus, suggesting that they have a different metabolic regulation compared to mammalian cardiomyocytes.

The lack of CK coupling to respiration may be associated with the smaller diffusion distances and restrictions along with the lower mechanical performance of trout cardiac cells. As was mentioned before, SR in rainbow trout cardiomyocytes is sparsely developed in comparison to adult mammalian cardiac myocytes [69]. Ultrastructural studies have revealed that SR is located in the teleost cardiomyocytes primarily beneath the sarcolemma [70, 71]. In fact, the SR is able of accumulating and releasing considerable amounts of Ca^{2+} in trout cardiomyocytes [72–75]. Moreover, the functional importance of SR in trout heart is dynamic [76–78]. Recent study have shown that, at rest, trout do not require the SR for Ca^{2+} release during ECC, and that external Ca^{2+} is the main trigger of cardiac contraction [79]. This can be mainly attributed to the elongated and narrow shape of the trout cardiomyocytes, which compensates for the absence of a t-tubular system and combined with a higher surface-to-volume ratio, increases the efficacy of sarcolemmal Ca^{2+} flux [70, 71, 80]. In contrast, during β-adrenergic stimulation, SR plays a significant role in cardiac ECC, hence, suggesting that Ca^{2+} stored in the SR of trout cardiomyocytes may act as a reserve or backup mechanism and is released only when extra Ca^{2+} is required to increase the cell contraction and cardiac performance when required, for example, during stress [79]. Taking this into account, it is still possible, that SR and associated cytoskeleton proteins may restrict ADP diffusion to the observed extent in trout cardiac myocytes, leading to a functional coupling of ATPases and mitochondria in the trout heart [54] (also see discussion in the next chapter). The results of Publication II have revealed that the magnitude of diffusion restriction is less in trout than in rat cardiomyocytes. In this case, perhaps, t-tubules and highly developed SR network may contribute further to cytosolic diffusion restriction in rat cardiomyocytes. It seems that the importance of CK and the extent of diffusion restriction in cardiomyocytes relate

to morphology, cardiac metabolism and mechanical performance. This surely requires additional studies.

3

THE ROLE OF CREATINE KINASE SYSTEM IN THE HEART

Compartmentation by the MOM seems to require the presence of a CK-system to facilitate ADP-transport, where cytosolic CK and mtCK are proposed to play a central role in the regulation of energy production [46]. In cardiac muscle, the CK-system serves an important function of energy buffer ensuring optimal ATP/ADP ratio, thus maximizing free energy of ATP hydrolysis near sites of ATP consumption and provides a consistent availability of ATP during transitions to high metabolic demand [32, 37, 81, 82]. In addition to a temporal buffering function, the CK-system has been proposed to be an important spatial buffer that links ATP-producing mitochondria to sites of ATP utilization via Cr/PCr shuttling. In this shuttle system, mtCK, which is bound to the outer surface of the MIM via cardiolipin and functionally coupled to ANT [83], catalyzes the phosphotransfer from ATP to Cr to generate PCr in the reaction: ATP + Cr $\Leftrightarrow$ ADP + PCr. PCr is smaller and more easily diffusible than ATP, it diffuses from the mitochondria to ATPases, where cytosolic isoforms of CK catalyze the reformation of ATP from PCr, the resulting free Cr diffuses back to the mitochondria [32, 46, 84–87]. This facilitated diffusion has been suggested to be necessary to overcome the possible intracellular ADP diffusion restrictions to avoid the inhibition of ATPases and consequently muscle contraction. Nevertheless, this spatial buffer hypothesis and its role in cell functioning has been the subject of intense scientific debates [88].

There are a number of findings that questioned the importance of CK system as a spatial buffer. Meyer et al. [89] suggested that CK-facilitated energy transfer is just a consequence of the CK reaction and its role may be negligible for cardiac function, if the diffusion distances are taken into account. A recent model based on nuclear magnetic resonance (NMR) data proposed that the energetic communication via CK shuttling between mitochondria and ATPases may depend on the workload and could be bypassed at high workload or in pathological conditions [90]. The role of CK-system in the heart has also gained attention by the observation that the down-regulation of CK-activity and total Cr pool in the pathological condition such as heart failure results in PCr depletion, a strong decline in ATP transfer [91–93] and also in a reduction of PCr/ATP ratio [94, 95]. This ratio

serves as a marker of cardiac bioenergetic status and is a predictor of mortality [96, 97]. It has also been demonstrated that disruption of the CK-system in hearts of CK-deficient mice, lacking both the cytosolic and the mitochondrial forms of CK leads to cytoarchitectural rearrangements and alterations in regulation of mitochondrial respiration [53, 98]. At the same time, several studies using knockouts of one or more CK isoforms or where Cr was depleted by feeding rodents with Cr analogue, β-guanidinoproionic acid, have demonstrated different effects on cardiac function. Generally, the hearts seem to compensate for the absence of CK under basal workloads, but they are not able to manage with a large and rapid increase in energy demand, high workload conditions and ischemia [99–105]. Furthermore, deficiency of the enzymes that synthesize Cr can inhibit CK-system. For example, GAMT-/- mice, in which the second of two essential enzymes in the biosynthesis of Cr - guanidinoacetate methyltransferase (GAMT) is knocked out, have a complete deficiency of Cr and PCr in all organs [106, 107]. Recent experiments with GAMT-/- mice have shown that their baseline cardiac function, maximal exercise capacity as well as response to chronic myocardial infarction are not affected by the lack of a functional CK-system [107–109], suggesting the fact that diminished total Cr levels in the failing heart are not pathophysiological. This could be due to compensatory changes similar to those described in hearts of CK-deficient mice [98, 103]. It is possible that other compensatory pathways may provide signal transduction and energy transfer between sites of energy production and consumption. Two mechanisms have been proposed: a support by glycolysis of Ca^{2+} uptake by the SR [110] and a close association between mitochondria and SR [53]. It is well recognized that the glycolytic enzymes can be organized into complexes bound in close proximity of ATPases so that they can directly take part in the regulation of the local ATP/ADP ratio [111, 112].

The aim of the study conducted in Publication III was to determine whether GAMT-deficiency leads to the changes in cardiomyocyte mitochondrial organization, regulation of respiration and intracellular compartmentation as was observed in hearts of CK-deficient mice. Three-dimensional mitochondrial positioning at whole cell level was assessed by confocal microscopy. Kinetic measurements on permeabilized mouse cardiomyocytes included ADP and ATP kinetics of respiration, the competition between mitochondria and PK for ADP produced by ATPases, ADP kinetics of endogenous PK and ATP kinetics of ATPases. Using fluorescence microscopy, ADP kinetics of respiration was confirmed on single permeabilized cardiomyocytes by recording autofluorescence response to changes in ADP. The experimental results were analyzed by mathematical models to estimate intracellular compartmentation. The detailed analysis of morphologic and kinetic data showed no difference between GAMT-/- and wildtype mice. Moreover, modeling results also demonstrated that there was no changes in intracellular com-

partmentation, diffusion across MOM and communication between compartments. Publication III concludes that inactivation of the CK-system in GAMT-/- mice due to the lack of Cr does not lead to alterations in mitochondrial organization and intracellular compartmentation in relaxed cardiomyocytes. Thus, our results suggest that the healthy heart is able to preserve cardiac function at a basal level in the absence of CK facilitated energy transfer without compromising intracellular organization and regulation of mitochondrial energy homeostasis. The lack of compensatory changes in mitochondrial organization and cellular compartmentation in GAMT-/- mice raises questions regarding the importance of the CK-system as a spatial buffer in unstressed cardiomyocytes.

As a matter of fact, CK may not be crucial for spatial energy buffering, if the decreased availability of exogenous ADP to mitochondria is a consequence of close mitochondria-SR association. Compartmentation of CK isoenzymes and their functional coupling is fully developed in adult mammals [14]. This is associated with a higher level of differentiation and structural organization during the maturation process in mammalian cardiac cells. The absence of mtCK in the hearts of neonatal mammals and increased activities of membrane-bound hexokinases imply that neonatal cells are more dependent on glycolysis [113–115]. Likewise, the hearts of lower vertebrates such as frog and fish seem not to have a mtCK functionally coupled to oxidative phosphorylation (see Publication I and Publication II). It can be explained by the fact that they have a lower cardiac performance, body temperature and a reliance on glycolysis for ATP production [14, 65]. The SR also appears to be less developed in lower vertebrates compared to adult mammals [69, 116]. Furthermore, in mammalian heart, the SR is sparse and immature at fetal and neonatal stage, its association with mitochondria increases during postnatal development [24]. During maturation mammalian cardiomyocytes increase in diameter and become terminally differentiated, their structural organization becomes more complex, they develop multiple parallel rows of myofibrils and organize mitochondria in a crystal-like pattern [39, 117, 118]. Mitochondrial oxidative capacity increases, becoming a major source of energy for the heart. The switch from glycolysis to mitochondrial oxidative metabolism during cardiac development increases the activities and significance of functional coupling of cytosolic and mtCK [114, 119]. In view of this the question arises whether CK-system is needed to facilitate ADP transport across the MOM in the heart? Is it possible that the decreased accessibility of exogenous ADP to mitochondria after cardiomyocyte maturation is due to the gradual development of the mitochondria-SR assemblies, and is not associated with the enhancement of energetic communication via the CK-system? Thereby in this context, variations in SR-mitochondria associations and interactions might give an alternative explanation for the species-specific differences and developmental changes in the apparent ADP-affinity of

permeabilized cardiomyocytes [14, 115, 118, 120], see also Publication I and Publication II. Consequently, the extent of diffusion restriction relates to morphology, metabolism and ECC as well, and depends on structural and functional developmental stage of the SR. Nevertheless, this hypothesis is still open for discussions and remains to be carefully tested experimentally.

4

THE ROLE OF ADP IN PROTECTION AGAINST mPTP OPENING

The common premise for the mitochondria-related diseases centers on energy failure, Ca^{2+} dysregulation, and oxidative stress. Dysregulation of the intracellular Ca^{2+} homeostasis and a dramatic decrease in the availability of ATP are characteristics during transient ischemic episodes in the heart and the brain and can lead to opening of the mPTP and enhanced generation of ROS [121–123].

mPTP is a non-specific high-conductance pore in the inner mitochondrial membrane, permeable to small molecules and ions with molecular masses up to 1500 Da. Under physiological conditions transient opening of mPTP may generate "superoxide flashes" for redox signaling [124] and also function as a mitochondrial Ca^{2+}-release channel for the intracellular Ca^{2+} signaling [125–127]. However, under pathological conditions, increase of the mitochondrial Ca^{2+} content above the optimal threshold would be dangerous for the cell, since it results in inhibition of oxidative phosphorylation [128] and irreversible opening of mPTP, ultimately leading to cell death [129–131]. Irreversible pore opening leads to collapse of the membrane potential, matrix swelling and rupture of the MOM, followed by the release of pro-apoptotic mediators [27]. Extensive studies of mPTP in cardiac pathological conditions, including IR, indicate that loss of mitochondrial functions by opening of the mPTP is one of major mechanisms of reperfusion-induced cardiomyocyte necrosis [132–134].

The exact molecular composition of the mPTP remains unknown, although some proteins have been suggested to play important roles. Experiments with ANT and cyclophilin D (CypD) knockout mice [135, 136] demonstrated that ANT and CypD are not the pore-forming components, implying that they can play only a regulatory role in mPTP opening [137–139]. However, inhibition of mPTP by either cyclosporine A (CsA) or genetic knockout of CypD guarantees powerful protection from reperfusion injury and heart failure [140, 141]. Recent studies have suggested that the mPiC [139] and F_1F_0-ATPase dimers may play a crucial role in mPTP formation [142, 143].

ADP is a well known mPTP inhibitor [144–146] that plays a dual role as a key substrate for ATP synthesis, thus inhibiting the channel activity of F_1F_0-ATPase dimers [143] and decreases Ca^{2+}-sensitivity by shifting ANT into "m" conformation [28, 29]. In addition, ADP may enhance Ca^{2+} sequestration in the form of Ca^{2+}-phosphate precipitates [147, 148]. Physiologically, stimulation of oxidative phosphorylation by ADP minimizes excessive ROS production and Ca^{2+} release from mitochondria. Pathologically, defects of this ADP regulatory mechanism lead to energetic failure, oxidative stress, and Ca^{2+} dysregulation, which enhance the vulnerability of cardiomyocytes to injury and death. The determination of the mechanistic aspect of cardiac protection by ADP would help in future development of a new potential therapy for oxidative stress-mediated heart diseases.

Publication IV was designed to investigate the protective effects of ADP on mPTP opening under pathophysiological conditions. The study addressed how ADP affects the Ca^{2+}-induced mPTP opening and ROS production, and how this is influenced by oxidative stress. The Ca^{2+} retention capacity (CRC) and ROS production experiments were performed on isolated mouse heart mitochondria under normal conditions and under conditions of acute (IR or tert-butyl hydroperoxide (t-BH) exposure) and chronic oxidative stress (aging and diabetes). The most notable outcome of Publication IV is the consistent effect of ADP on CRC, which relates to its concentration, even after severe oxidative stress. This may become important for mitochondrial survival in the pathological situation, where matrix ADP may increase due to Ca^{2+} overload, depolarized mitochondrial membrane potential and less efficient ATP production. The results showed that chronic oxidative stress by aging and diabetes did not affect the initial CRC or the effect of ADP. In addition, Ca^{2+}-sequestration had no effect on CRC. In control mitochondria ADP decreased both substrate and Ca^{2+}-induced increase of ROS. However, in mitochondria exposed to t-BH the effect of ADP on CRC is not the result of reduced ROS production. This suggests that significant regulation by ADP may occur via its internal binding site, which could be on F_1F_0-ATPase. Publication IV concludes that the ability of ADP to serve multiple roles as a master regulator of mitochondrial homeostasis of ATP, Ca^{2+} and ROS dynamics, makes it a unique molecule to preserve mitochondrial function under conditions of acute oxidative stress.

PHYSIOLOGICAL IMPLICATIONS OF ADP DIFFUSIONAL BARRIERS

In perspective, we propose the physiological implications of ADP diffusional barriers in cytosol and at MOM level considering the role of ADP in mPTP regulation. Cytosolic ADP diffusional barriers in permeabilized cardiomyocytes may be formed by the close SR-mitochondria associations together with cytoskeleton pro-

teins as well as by crowding of cytosolic proteins [54], hence, leading to functional coupling of ATPases and mitochondria. In vivo, such mitochondria-SR coupling is essential for providing a structural framework for bi-directional Ca^{2+}/ADP signaling that regulates mitochondrial energetics, ECC and ROS signaling, avoiding excessive mitochondrial Ca^{2+}-uptake and irreversible opening of the mPTP.

It is also considered that the diffusion restriction may be induced by the MOM. Although the exact role of VDAC in vivo remains yet unknown, it has been suggested that the limited permeability of the MOM is regulated by tubulin binding to VDAC [46, 51, 149]. As has been demonstrated, mtCK may interact with VDAC and ANT at the contact sites between MIM and MOM [150, 151] to form a microcompartment, separating mitochondrial ATP and ADP pools, and thus creating a local and efficient ADP-regenerating system. The local availability of ADP to ANT would ensure the moderate formation of ROS and the closure of the mPTP, under conditions of low permeability of the MOM to ADP.

From an alternative point of view, if such regulation of MOM via VDAC-tubulin interactions takes place, the MOM would be expected to be more permeable in the absence of a functional CK-system. However, our results in Publication III demonstrate that there was no structural changes in compartmentalization as well as in diffusion across the MOM and mitochondrial organization in GAMT-/- mice. The lack of changes in GAMT-/- mice speak in favor of SR-mitochondria interaction as a diffusion barrier. This is in agreement with the observation that mitochondria are able to provide energy for SERCA-mediated Ca^{2+} uptake with the same efficacy as CK [53]. Compromised energetics affects SERCA activity and Ca^{2+} reuptake, which may lead to mitochondrial Ca^{2+} overload. In this scenario, the protective role of ADP comes into a play. Ca^{2+} overload, combined with depolarized mitochondrial membrane potential and insufficient ATP production leads to the increase of matrix ADP concentration. Elevated level of matrix ADP can delay mPTP opening. Thereby, under conditions of disrupted energy supply or the lack of the functional CK-system, transport of ADP and Pi from SERCA to the mitochondria may enhance the mitochondrial CRC before mPTP opening is triggered [152], see also Publication IV. It thus avoids the danger of mitochondrial Ca^{2+} overload that would open the mPTP, leading to cell death.

5

CONCLUSIONS

This dissertation broadens the understanding of energetic compartmentation in cardiomyocytes and the role of ADP in the protection against mPTP opening. The main findings and results of this work are summarized below:

1) The experimental data demonstrated that cardiomyocytes from rainbow trout, which are much thinner than those of mammals, lack t-tubules and have a lower SR density, show restricted diffusion albeit to a smaller extent than in rat cardiomyocytes.
2) The analysis of the experimental data with mathematical models suggested that in the control case, the diffusion is obstructed to almost the same extent by cytosolic factors as at the MOM level.
3) Modeling results have revealed that trout cardiomyocytes lack the cytosolic PK-ATPases compartment that was found in rat cardiomyocytes. Moreover, instead of CK, results demonstrated that HK is coupled to respiration in trout. These data suggest that trout cardiomyocytes have different metabolic compartmentation and regulation compared to mammalian cardiomyocytes.
4) The quantitative analysis of morphologic and kinetic data together with mathematical modeling showed that inhibition of the CK-system by GAMT-deficiency does not cause alterations in intracellular compartmentalization and diffusion across MOM as well as mitochondrial organization in relaxed cardiomyocytes. These outcomes demonstrate that the basal cardiac function is not severely compromised in the absence of CK-facilitated energy transfer and raise questions regarding the importance of CK-system a spatial buffer at low and moderate workloads.
5) The results from trout cardiomyocytes and the lack of changes in GAMT-/- mice speak in favor of SR-mitochondria association as a diffusion barrier. This thesis considers an alternative view on diffusional restriction at the MOM level. It is possible, that in part it might be not due to the membrane itself, but due to the close association between the SR and mitochondria. The SR-mitochondria as-

sembly may restrict diffusion of molecules from the medium to mitochondria in permeabilized cardiomyocytes, whereas, in vivo, it also creates the structural basis for the energetic interaction between SERCA and mitochondria. This is essential for the optimal regulation of mitochondrial respiration, ECC, Ca^{2+} and ROS signaling, and for avoiding the mitochondrial Ca^{2+}-overload and irreversible opening of the mPTP.

6) While investigating the role of ADP in the protection from mPTP opening it was found that ADP increases the CRC in severely stressed mitochondria (IR or t-BH exposure) by the same amount as in mitochondria from control mice and its effect on CRC is related to [ADP] and not to the total concentration of adenine nucleotides. Despite the fact that ADP decreased both substrate and Ca^{2+}-induced increase of ROS production in control mitochondria, its effect on ROS is very small in t-BH-treated mitochondria. These data suggest that the mechanism with which ADP increases mitochondrial CRC is independent of its potential effect on ROS production.

7) As has been noted, under physiological conditions, ADP serves as a substrate for ATP synthesis, thus, ensuring a moderate ROS generation and the closure of mPTP. Under pathological conditions, an increase in ADP concentration can effectively delay mPTP opening so that mitochondrial membrane integrity can be preserved to maintain energy production.

REFERENCES

REFERENCES

[1] E. Barth, G. Stämmler, B. Speiser, and J. Schaper. Ultrastructural quantitation of mitochondria and myofilaments in cardiac muscle from 10 different animal species including man. *J. Mol. Cell. Cardiol.*, 24(7):669–681, 1992.

[2] R. Ventura-Clapier, A. Garnier, and V. Veksler. Energy metabolism in heart failure. *J. Physiol. (Lond.)*, 555(1):1 –13, 2004.

[3] R. S. Balaban, H. L. Kantor, L. A. Katz, and R. W. Briggs. Relation between work and phosphate metabolite in the in vivo paced mammalian heart. *Science (80-)*, 232(4754):1121–1123, 1986.

[4] L. Ligeti, M. Osbakken, B. Clark, M. Schnall, L. Bolinger, H. Subramanian, J. Leigh, and B. Chance. Cardiac transfer function relating energy metabolism to workload in different species as studied with 31p nmr. *Magn Reson Med*, 4(2):112–119, 1987.

[5] F. Heineman and R. Balaban. Phosphorus-31 nuclear magnetic resonance analysis of transient changes of canine myocardial metabolism in vivo. *J. Clin. Invest.*, 85(3):843–852, 1990.

[6] V. A. Saks, A. V. Kuznetsov, M. Vendelin, K. Guerrero, L. Kay, and E. K. Seppet. Functional coupling as a basic mechanism of feedback regulation of cardiac energy metabolism. *Mol. Cell. Biochem.*, 256-257(1):185–199, 2004.

[7] J. G. M. van Beek. Adenine nucleotide-creatine-phosphate module in myocardial metabolic system explains fast phase of dynamic regulation of oxidative phosphorylation. *Am. J. Physiol. Cell. Physiol.*, 293(3):C815–829, 2007.

[8] L. J. Reed. Regulation of mammalian pyruvate dehydrogenase complex by a phosphorylation-dephosphorylation cycle. *Curr. Top. Cell. Regul.*, 18:95–106, 1981.

[9] J. G. Mccormack, A. P. Halestrap, and R. M. Denton. Role of calcium ions in regulation of mammalian intramitochondrial metabolism. *Physiol. Rev.*, 70(2):391–425, 1990.

[10] V. A. Saks, O. Kongas, M. Vendelin, and L. Kay. Role of the creatine/phosphocreatine system in the regulation of mitochondrial respiration. *Acta Physiol. Scand.*, 168(4):635–641, 2000.

[11] S. Bose, S. French, F. Evans, F. Joubert, and R. Balaban. Metabolic network control of oxidative phosphorylation. *J. Biol. Chem.*, 278(40):39155 –39165, 2003.

[12] F. Wu, E. Zhang, J. Zhang, R. Bache, and D. Beard. Phosphate metabolite concentrations and atp hydrolysis potential in normal and ischaemic hearts. *J. Physiol. (Lond.)*, 586:4193–4208, 2008.

[13] A. V. Kuznetsov, T. Tiivel, P. Sikk, T. Kaambre, L. Kay, Z. Daneshrad, A. Rossi, L. Kadaja, N. Peet, E. Seppet, and V. A. Saks. Striking differences between the kinetics of regulation of respiration by adp in slow-twitch and fast-twitch muscles in vivo. *Eur. J. Biochem.*, 241(3):909–915, 1996.

[14] R. Ventura-Clapier, A. Kuznetsov, V. Veksler, E. Boehm, and K. Anflous. Functional coupling of creatine kinases in muscles: species and tissue specificity. *Mol. Cell. Biochem.*, 184(1-2):231–247, 1998.

[15] L. Kay, V. A. Saks, and A. Rossi. Early alteration of the control of mitochondrial function in myocardial ischemia. *J. Mol. Cell. Cardiol.*, 29(12):3399–3411, 1997.

[16] L. Kay, A. Rossi, and V. Saks. Detection of early ischemic damage by analysis of mitochondrial function in skinned fibers. *Mol. Cell. Biochem.*, 174(1-2):79–85, 1997.

[17] S. Boudina, M. Laclau, L. Tariosse, D. Daret, G. Gouverneur, S. Bonoron-Adele, V. Saks, and P. Santos. Alteration of mitochondrial function in a model of chronic ischemia in vivo in rat heart. *Am. J. Physiol. Heart Circ. Physiol.*, 282(3):H821–H831, 2002.

[18] J. Zoll, E. Ponsot, S. Doutreleau, B. Mettauer, F. Piquard, J. P. Mazzucotelli, P. Diemunsch, and B. Geny. Acute myocardial ischaemia induces specific alterations of ventricular mitochondrial function in experimental pigs. *Acta Physiol. Scand.*, 185(1):25–32, 2005.

[19] J. G. Mccormack and R. M. Denton. Mitochondrial ca2+ transport and the role of intramitochondrial ca2+ in the regulation of energy metabolism. *Dev. Neurosci.*, 15(3-5):165–173, 1993.

[20] R. Hansford. Physiological role of mitochondrial ca2+ transport. *J. Bioenerg. Biomembr.*, 26(5):495–508, 1994.

[21] R. G. Hansford and D. Zorov. Role of mitochondrial calcium transport in the control of substrate oxidation. *Mol. Cell. Biochem.*, 184(1-2):359–369, 1998.

[22] R. S. Balaban. Cardiac energy metabolism homeostasis: role of cytosolic calcium. *J. Mol. Cell. Cardiol.*, 34(10):1259–1271, 2002.

[23] P. R. Territo, S. A. French, M. C. Dunleavy, F. J. Evans, and R. S. Balaban. Calcium activation of heart mitochondrial oxidative phosphorylation: rapid kinetics of mvo2, nadh, and light scattering. *J. Biol. Chem.*, 276(4):2586–2599, 2001.

[24] S. Boncompagni, A. Rossi, M. Micaroni, G. Beznoussenko, R. Polishchuk, R. Dirksen, and F. Protasi. Mitochondria are linked to calcium stores in striated muscle by developmentally regulated tethering structures. *Mol. Biol. Cell*, 20(3):1058–1067, 2009.

[25] H. Miyata, H. S. Silverman, S. J. Sollott, E. G. Lakatta, M. D. Stern, and R. G. Hansford. Measurement of mitochondrial free ca2+ concentration in living single rat cardiac myocytes. *Am. J. Physiol.*, 261(4 Pt 2):H1123–H1134, 1991.

[26] C. Maack and B. O'rourke. Excitation-contraction coupling and mitochondrial energetics. *Basic Res. Cardiol.*, 102(5):369–392, 2007.

[27] G. Kroemer, L. Galluzzi, and C. Brenner. Mitochondrial membrane permeabilization in cell death. *Physiol. Rev.*, 87(1):99–163, 2007.

[28] R. A. Haworth and D. R. Hunter. Control of the mitochondrial permeability transition pore by high-affinity adp binding at the adp/atp translocase in permeabilized mitochondria. *J. Bioenerg. Biomembr.*, 32(1):91–96, 2000.

[29] M. Klingenberg. The adp and atp transport in mitochondria and its carrier. *BBA*, 1778(10):1978–2021, 2008.

[30] A. Hammes, S. Oberdorf-Maass, T. Rother, K. Nething, F. Gollnick, K. W. Linz, R. Meyer, K. Hu, H. Han, P. Gaudron, G. Ertl, S. Hoffmann, U. Ganten, R. Vetter, K. Schuh, C. Benkwitz, H. G. Zimmer, and L. Neyses. Overexpression of the sarcolemmal calcium pump in the myocardium of transgenic rats. *Circ. Res.*, 83(9):877–888, 1998.

[31] D. M. Bers. Ca transport during contraction and relaxation in mammalian ventricular muscle. *Basic Res. Cardiol.*, 92(S1):1–10, 1997.

[32] T. Wallimann, M. Wyss, D. Brdiczka, K. Nicolay, and H. M. Eppenberger. Intracellular compartmentation, structure and function of creatine kinase isoenzymes in tissues with high and fluctuating energy demands: the 'phosphocreatine circuit' for cellular energy homeostasis. *Biochem. J.*, 281 (Pt 1):21–40, 1992.

[33] A. Minajeva, R. Ventura-Clapier, and V. Veksler. Ca2+ uptake by cardiac sarcoplasmic reticulum atpase in situ strongly depends on bound creatine kinase. *Pflugers Arch.*, 432(5):904–912, 1996.

[34] A. M. Rossi, H. M. Eppenberger, P. Volpe, R. Cotrufo, and T. Wallimann. Muscle-type mm creatine kinase is specifically bound to sarcoplasmic reticulum and can support ca2+ uptake and regulate local atp/adp ratios. *J. Biol. Chem.*, 265(9):5258–5266, 1990.

[35] R. Grosse, E. Spitzer, V. V. Kupriyanov, V. A. Saks, and K. R. Repke. Coordinate interplay between (na+ + k+)-atpase and creatine phosphokinase optimizes (na+/k+)-antiport across the membrane of vesicles formed from the plasma membrane of cardiac muscle cell. *BBA*, 603(1):142–156, 1980.

[36] P. Dzeja, K. Vitkevicius, M. Redfield, J. Burnett, and A. Terzic. Adenylate kinase-catalyzed phosphotransfer in the myocardium: Increased contribution in heart failure. *Circ. Res.*, 84(10):1137–1143, 1999.

[37] P. Dzeja and A. Terzic. Phosphotransfer networks and cellular energetics. *J. Exp. Biol.*, 206(12):2039–2047, 2003.

[38] P. Dzeja, A. Terzic, and B. Wieringa. Phosphotransfer dynamics in skeletal muscle from creatine kinase gene-deleted mice. *Mol. Cell. Biochem.*, 256-257(1):13–27, 2004.

[39] R. Birkedal, H. Shiels, and M. Vendelin. Three-dimensional mitochondrial arrangement in ventricular myocytes: From chaos to order. *AJP: Cell Physiology*, 291(6):C1148–C1158, 2006.

[40] T. Hayashi, M. E. Martone, Z. Yu, A. Thor, M. Doi, M. J. Holst, M. H. Ellisman, and M. Hoshijima. Three-dimensional electron microscopy reveals new details of membrane systems for ca2+ signaling in the heart. *J. Cell. Sci.*, 122(7):1005, 2009.

[41] A. Illaste, M. Laasmaa, P. Peterson, and M. Vendelin. Analysis of molecular movement reveals latticelike obstructions to diffusion in heart muscle cells. *Biophys. J.*, 102(4):739–748, 2012.

[42] L. Kümmel. Ca, mg-atpase activity of permeabilised rat heart cells and its functional coupling to oxidative phosphorylation of the cells. *Cardiovasc. Res.*, 22(5):359–367, 1988.

[43] V. A. Saks, V. I. Veksler, A. V. Kuznetsov, L. Kay, P. Sikk, T. Tiivel, L. Tranqui, J. Olivares, K. Winkler, F. Wiedemann, and . Others. Permeabilized cell and skinned fiber techniques in studies of mitochondrial function in vitro. *Mol. Cell. Biochem. 184*, 1(2):81–100, 1998.

[44] V. A. Saks, Y. O. Belikova, and A. V. Kuznetsov. In vivo regulation of mitochondrial respiration in cardiomyocytes: specific restrictions for intracellular diffusion of adp. *BBA*, 1074(2):302–311, 1991.

[45] V. A. Saks, E. Vasil'eva, Y. O. Belikova, A. V. Kuznetsov, S. Lyapina, L. Petrova, and N. A. Perov. Retarded diffusion of adp in cardiomyocytes: possible role of mitochondrial outer membrane and creatine kinase in cellular regulation of oxidative phosphorylation. *BBA*, 1144(2):134–148, 1993.

[46] V. A. Saks, Z. A. Khuchua, E. V. Vasilyeva, O. Y. Belikova, and A. V. Kuznetsov. Metabolic compartmentation and substrate channelling in muscle cells. role of coupled creatine kinases in in vivo regulation of cellular respiration–a synthesis. *Mol. Cell. Biochem.*, 133-134:155–192, 1994.

[47] V. A. Saks, A. V. Kuznetsov, Z. A. Khuchua, E. V. Vasilyeva, J. O. Belikova, T. Kesvatera, and T. Tiivel. Control of cellular respiration in vivo by mitochondrial outer membrane and by creatine kinase. a new speculative hypothesis: possible involvement of mitochondrial-cytoskeleton interactions. *J. Mol. Cell. Cardiol.*, 27(1):625–645, 1995.

[48] V. Saks, Y. O. Belikova, E. Vasilyeva, A. Kuznetsov, E. Fontaine, C. Keriel, and X. Leverve. Correlation between degree of rupture of outer mitochondrial membrane and changes of kinetics of regulation of respiration by adp in permeabilized heart and liver cells [published erratum appears in biochem biophys res commun 1995 jun 26;211(3):1099]. *Biochem. Biophys. Res. Commun.*, 208(3):919–926, 1995.

[49] F. Appaix, A. Kuznetsov, Y. Usson, L. Kay, T. Andrienko, J. Olivares, T. Kaambre, P. Sikk, R. Margreiter, and V. A. Saks. Possible role of cytoskeleton in intracellular arrangement and regulation of mitochondria. *Exp. Physiol.*, 88(1):175–190, 2003.

[50] T. Anmann, R. Guzun, N. Beraud, S. Pelloux, A. V. Kuznetsov, L. Kogerman, T. Kaambre, P. Sikk, K. Paju, N. Peet, E. Seppet, C. Ojeda, Y. Tourneur, and

V. Saks. Different kinetics of the regulation of respiration in permeabilized cardiomyocytes and in hl-1 cardiac cells. importance of cell structure/organization for respiration regulation. *BBA*, 1757(12):1597–1606, 2006.

[51] T. Rostovtseva, K. Sheldon, E. Hassanzadeh, C. Monge, V. Saks, S. Bezrukov, and D. Sackett. Tubulin binding blocks mitochondrial voltage-dependent anion channel and regulates respiration. *PNAS*, 105(48):18746–18751, 2008.

[52] T. Rostovtseva and S. Bezrukov. Vdac inhibition by tubulin and its physiological implications. *Biochim. Biophys. Acta (BBA)-Biomembranes*, 1818(6):1526–1535, 2012.

[53] A. Kaasik, V. Veksler, E. Boehm, M. Novotova, A. Minajeva, and R. Ventura-Clapier. Energetic crosstalk between organelles: architectural integration of energy production and utilization. *Circ. Res.*, 89(2):153–159, 2001.

[54] H. R. Ramay and M. Vendelin. Diffusion restrictions surrounding mitochondria: A mathematical model of heart muscle fibers. *Biophys. J.*, 97(2):443–52, 2009.

[55] V. A. Saks, T. Kaambre, P. Sikk, M. Eimre, E. Orlova, K. Paju, A. Piirsoo, F. Appaix, L. Kay, V. Regitz-Zagrosek, E. Fleck, and E. Seppet. Intracellular energetic units in red muscle cells. *Biochem. J.*, 356(Pt 2):643–657, 2001.

[56] E. Seppet, T. Kaambre, P. Sikk, T. Tiivel, H. Vija, M. Tonkonogi, K. Sahlin, L. Kay, F. Appaix, U. Braun, M. Eimre, and V. Saks. Functional complexes of mitochondria with ca,mgatpases of myofibrils and sarcoplasmic reticulum in muscle cells. *BBA-Bioenerg.*, 1504(2-3):379–395, 2001.

[57] E. Seppet, M. Eimre, T. Anmann, E. Seppet, N. Peet, T. Kaambre, K. Paju, A. Piirsoo, A. Kuznetsov, M. Vendelin, F. Gellerich, S. Zierz, and V. Saks. Intracellular energetic units in healthy and diseased hearts. *Exp. Clin. Cardiol.*, 10(3):173–183, 2005.

[58] E. K. Seppet, T. Kaambre, P. Sikk, T. Tiivel, H. Vija, M. Tonkonogi, K. Sahlin, L. Kay, F. Appaix, U. Braun, M. Eimre, and V. A. Saks. Functional complexes of mitochondria with ca,mgatpases of myofibrils and sarcoplasmic reticulum in muscle cells. *BBA*, 1504(2-3):379–395, 2001.

[59] M. Vendelin, M. Eimre, E. Seppet, N. Peet, T. Andrienko, M. Lemba, J. Engelbrecht, E. Seppet, and V. Saks. Intracellular diffusion of adenosine phosphates is locally restricted in cardiac muscle. *Mol. Cell. Biochem.*, 256-257(1):229–241, 2004.

[60] O. Kongas, T. L. Yuen, M. J. Wagner, J. H. G. M. van Beek, and K. Krab. High km of oxidative phosphorylation for adp in skinned muscle fibers: where does it stem from? *AJP: Cell Physiology*, 283(3):C743–C751, 2002.

[61] N. Jepihhina, N. Beraud, M. Sepp, R. Birkedal, and M. Vendelin. Permeabilized rat cardiomyocyte response demonstrates intracellular origin of diffusion obstacles. *Biophys. J.*, 101(9):2112–2121, 2011.

[62] D. Singer. Neonatal tolerance to hypoxia: a comparative-physiological approach. *Comp. Biochem. Physiol. A Mol. Integr. Physiol.*, 123(3):221–234, 1999.

[63] J. Huang, L. Hove-Madsen, and G. Tibbits. Na+/ca2+ exchange activity in neonatal rabbit ventricular myocytes. *AJP: Cell Physiology*, 288(1):C195–C203, 2005.

[64] M. Christensen, T. Hartmund, and H. Gesser. Creatine kinase, energy-rich phosphates and energy metabolism in heart muscle of different vertebrates. *J. Comp. Physiol. [B]*, 164(2):118–123, 1994.

[65] R. Birkedal and H. Gesser. Intracellular compartmentation of cardiac fibres from rainbow trout and atlantic cod–a general design of heart cells. *BBA*, 1757(7):764–772, 2006.

[66] R. Birkedal and H. Gesser. Creatine kinase and mitochondrial respiration in hearts of trout, cod and freshwater turtle. *J. Comp. Physiol. [B]*, 173(6):493–499, 2003.

[67] R. Birkedal and H. Gesser. Effects of hibernation on mitochondrial regulation and metabolic capcities in the myocardium of painted turtle (chrysemys picta). *Comp. Biochem. Physiology A*, 139(3):285–291, 2004.

[68] M. Sepp, M. Vendelin, H. Vija, and R. Birkedal. ADP compartmentation analysis reveals coupling between pyruvate kinase and ATPases in heart muscle. *Biophys. J.*, 98(12):2785–2793, 2010.

[69] R. M. Santer. Morphology and innervation of the fish heart. *Adv. Anat. Embryol. Cell Biol.*, 89:1–102, 1985.

[70] R. M. Santer. The organization of the sarcoplasmic reticulum in teleost ventricular myocardial cells. *Cell Tissue Res.*, 151(3):395–402, 1974.

[71] M. Vornanen. L-type ca2+ current in fish cardiac myocytes: effects of thermal acclimation and beta-adrenergic stimulation. *J. Exp. Biol.*, 201(Pt 4):533–547, 1998.

[72] L. Hove-Madsen and L. Tort. L-type ca2+ current and excitation-contraction coupling in single atrial myocytes from rainbow trout. *Am. J. Physiol.*, 275(6 Pt 2):R2061–R2069, 1998.

[73] L. Hove-Madsen, A. Llach, and L. Tort. Quantification of calcium release from the sarcoplasmic reticulum in rainbow trout atrial myocytes. *Pflugers Arch.*, 438(4):545–552, 1999.

[74] L. Hove-Madsen, A. Llach, and L. Tort. Na⊕/ca(2+)-exchange activity regulates contraction and sr ca(2+) content in rainbow trout atrial myocytes. *Am. J. Physiol. Regul. Integr. Comp. Physiol.*, 279(5):R1856–R1864, 2000.

[75] L. Hove-Madsen, A. Llach, G. F. Tibbits, and L. Tort. Triggering of sarcoplasmic reticulum ca2+ release and contraction by reverse mode na+/ca2+ exchange in trout atrial myocytes. *Am. J. Physiol. Regul. Integr. Comp. Physiol.*, 284(5):R1330–R1339, 2003.

[76] L. Hove-Madsen. The influence of temperature on ryanodine sensitivity and the force-frequency relationship in the myocardium of rainbow trout. *J. Exp. Biol.*, 167:47–60, 1992.

[77] . Aho and . Vornanen. Contractile properties of atrial and ventricular myocardium of the heart of rainbow trout oncorhynchus mykiss: effects of thermal acclimation. *J. Exp. Biol.*, 202 (Pt 19):2663–2677, 1999.

[78] H. Shiels, M. Vornanen, and A. Farrell. Temperature dependence of cardiac sarcoplasmic reticulum function in rainbow trout myocytes. *J. Exp. Biology*, 205(23):3631–3639, 2002.

[79] C. Cros, L. Salle, D. E. Warren, H. A. Shiels, and F. Brette. The calcium stored in the sarcoplasmic reticulum acts as a safety mechanism in rainbow trout heart. *AJP: Regul. Integr. Comp. Physiology*, 307(12):R1493–R1501, 2014.

[80] M. Vornanen. Sarcolemmal ca influx through l-type ca channels in ventricular myocytes of a teleost fish. *Am. J. Physiol.*, 272(5 Pt 2):R1432–1440, 1997.

[81] V. A. Saks and R. Ventura-Clapier. *Cellular Bioenergetics: Role of Coupled Creatine Kinases.* Kluwer Academic Publishers, 1994.

[82] J. Ingwall and R. Weiss. Is the failing heart energy starved? *Circ. Res.*, 95(2):135 –145, 2004.

[83] U. Schlattner, M. Tokarska-Schlattner, S. Ramirez, A. Brückner, L. Kay, C. Polge, R. Epand, R. Lee, M. Lacombe, and R. Epand. Mitochondrial

kinases and their molecular interaction with cardiolipin. *Biochim. Biophys. Acta (BBA)-Biomembranes*, 1788(10):2032–2047, 2009.

[84] S. P. Bessman and P. J. Geiger. Transport of energy in muscle: the phosphorylcreatine shuttle. *Science*, 211(4481):448–452, 1981.

[85] R. A. Meyer, H. L. Sweeney, and M. J. Kushmerick. A simple analysis of the "phosphocreatine shuttle". *AJP: Cell Physiology*, 246(5):C365–C377, 1984.

[86] R. Ventura-Clapier and V. Veksler. Myocardial ischemic contracture. metabolites affect rigor tension development and stiffness. *Circ. Res.*, 74(5):920–929, 1994.

[87] S. P. Bessman and C. L. Carpenter. The creatine-creatine phosphate energy shuttle. *Annu. Rev. Biochem.*, 54:831–862, 1985.

[88] D. Beard and M. Kushmerick. Strong inference for systems biology. *PLoS Comput. Biol.*, 5(8):e1000459, 2009.

[89] R. A. Meyer, H. L. Sweeney, and M. J. Kushmerick. A simple analysis of the "phosphocreatine shuttle". *Am. J. Physiol.*, 246(5 Pt 1):C365–C377, 1984.

[90] M. Vendelin, J. Hoerter, P. Mateo, S. Soboll, B. Gillet, and J. Mazet. Modulation of energy transfer pathways between mitochondria and myofibrils by changes in performance of perfused heart. *J. Biol. Chem.*, 285(48):37240–37250, 2010.

[91] S. Neubauer, M. Horn, A. Naumann, R. Tian, K. Hu, M. Laser, J. Friedrich, P. Gaudron, K. Schnackerz, and J. Ingwall. Impairment of energy metabolism in intact residual myocardium of rat hearts with chronic myocardial infarction. *J. Clin. Invest.*, 95(3):1092–1100, 1995.

[92] Y. Ye, G. Gong, K. Ochiai, J. Liu, and J. Zhang. High-energy phosphate metabolism and creatine kinase in failing hearts: a new porcine model. *Circulation*, 103:1570–1576, 2001.

[93] R. Weiss, G. Gerstenblith, and P. Bottomley. Atp flux through creatine kinase in the normal, stressed, and failing human heart. *PNAS*, 102(3):808–813, 2005.

[94] C. Hardy, R. Weiss, P. Bottomley, and G. Gerstenblith. Altered myocardial high-energy phosphate metabolites in patients with dilated cardiomyopathy. *Am. Heart J.*, 122(3 Pt 1):795–801, 1991.

[95] M. Conway, J. Allis, R. Ouwerkerk, T. Niioka, B. Rajagopalan, and G. Radda. Detection of low phosphocreatine to atp ratio in failing hypertrophied human myocardium by 31p magnetic resonance spectroscopy. *Lancet*, 338(8773):973–976, 1991.

[96] S. Neubauer, M. Horn, M. Cramer, K. Harre, J. Newell, W. Peters, T. Pabst, G. Ertl, D. Hahn, J. Ingwall, and K. Kochsiek. Myocardial phosphocreatine-to-atp ratio is a predictor of mortality in patients with dilated cardiomyopathy. *Circulation*, 96(7):2190–2196, 1997.

[97] M. ten Hove and S. Neubauer. Mr spectroscopy in heart failure—clinical and experimental findings. *Heart Fail. Rev.*, 12(1):48–57, 2007.

[98] M. Nahrendorf, J. Streif, K. Hiller, K. Hu, P. Nordbeck, O. Ritter, D. Sosnovik, L. Bauer, S. Neubauer, P. Jakob, G. Ertl, M. Spindler, and W. Bauer. Multimodal functional cardiac mri in creatine kinase-deficient mice reveals subtle abnormalities in myocardial perfusion and mechanics. *Am. J. Physiol. Heart Circ. Physiol.*, 290(6):H2516 –H2521, 2006.

[99] E. A. Shoubridge, R. A. Challiss, D. J. Hayes, and G. K. Radda. Biochemical adaptation in the skeletal muscle of rats depleted of creatine with the substrate analogue beta-guanidinopropionic acid. *Biochem. J.*, 232(1):125–131, 1985.

[100] H. Mekhfi, J. Hoerter, C. Lauer, C. Wisnewsky, K. Schwartz, and R. Ventura-Clapier. Myocardial adaptation to creatine deficiency in rats fed with beta-guanidinopropionic acid, a creatine analogue. *Am. J. Physiol.*, 258(4 Pt 2):H1151–H1158, 1990.

[101] J. L. Zweier, W. E. Jacobus, B. Korecky, and Y. Brandejs-Barry. Bioenergetic consequences of cardiac phosphocreatine depletion induced by creatine analogue feeding. *J. Biol. Chem.*, 266(30):20296–20304, 1991.

[102] S. Neubauer, K. Hu, M. Horn, H. Remkes, K. Hoffmann, C. Schmidt, T. Schmidt, K. Schnackerz, and G. Ertl. Functional and energetic consequences of chronic myocardial creatine depletion by beta-guanidinopropionate in perfused hearts and in intact rats. *J. Mol. Cell. Cardiol.*, 31(10):1845–1855, 1999.

[103] B. Crozatier, T. Badoual, E. Boehm, P. V. Ennezat, T. Guenoun, J. Su, V. Veksler, L. Hittinger, and R. Ventura-Clapier. Role of creatine kinase in cardiac excitation-contraction coupling: studies in creatine kinase-deficient mice. *FASEB J.*, 16(7):653–660, 2002.

[104] M. Spindler, K. Meyer, H. Strömer, A. Leupold, E. Boehm, H. Wagner, and S. Neubauer. Creatine kinase-deficient hearts exhibit increased susceptibility to ischemia-reperfusion injury and impaired calcium homeostasis. *Am. J. Physiol. Heart Circ. Physiol.*, 287(3):H1039 –H1045, 2004.

[105] M. Nahrendorf, M. Spindler, K. Hu, L. Bauer, O. Ritter, P. Nordbeck, T. Quaschning, K. Hiller, J. Wallis, G. Ertl, W. Bauer, and S. Neubauer. Creatine kinase knockout mice show left ventricular hypertrophy and dilatation, but unaltered remodeling post-myocardial infarction. *Cardiovasc. Res.*, 65(2):419 –427, 2005.

[106] A. Schmidt, B. Marescau, E. A. Boehm, W. K. Renema, R. Peco, A. Das, R. Steinfeld, S. Chan, J. Wallis, M. Davidoff, K. Ullrich, R. Waldschutz, A. Heerschap, P. P. De Deyn, S. Neubauer, and D. Isbrandt. Severely altered guanidino compound levels, disturbed body weight homeostasis and impaired fertility in a mouse model of guanidinoacetate n-methyltransferase (gamt) deficiency. *Hum. Mol. Genet.*, 13(9):905–921, 2004.

[107] C. Lygate, D. Aksentijevic, D. Dawson, M. ten Hove, D. Phillips, J. de Bono, D. Medway, L. Sebag-Montefiore, I. Hunyor, K. Channon, K. Clarke, S. Zervou, H. Watkins, R. Balaban, and S. Neubauer. Living without creatine: unchanged exercise capacity and response to chronic myocardial infarction in creatine-deficient mice. *Circ. Res.*, 112(6):945–955, 2013.

[108] M. Hove, C. Lygate, A. Fischer, J. Schneider, A. E. Sang, K. Hulbert, L. Sebag-Montefiore, H. Watkins, K. Clarke, D. Isbrandt, J. Wallis, and S. Neubauer. Reduced inotropic reserve and increased susceptibility to cardiac ischemia/reperfusion injury in phosphocreatine-deficient guanidinoacetate-n-methyltransferase-knockout mice. *Circulation*, 111(19):2477–2485, 2005.

[109] J. Schneider, L. Stork, J. Bell, M. Hove, D. Isbrandt, K. Clarke, H. Watkins, C. Lygate, and S. Neubauer. Cardiac structure and function during ageing in energetically compromised guanidinoacetate n-methyltransferase (gamt)-knockout mice – a one year longitudinal mri study. *J. Cardiovasc. Magn. Reson.*, 10(1):9, 2008.

[110] E. Boehm, R. Ventura-Clapier, P. Mateo, P. Lechene, and V. Veksler. Glycolysis supports calcium uptake by the sarcoplasmic reticulum in skinned ventricular fibres of mice deficient in mitochondrial and cytosolic creatine kinase. *J. Mol. Cell. Cardiol.*, 32(6):891–902, 2000.

[111] S. P. J. Brooks and K. B. Storey. Where is the glycolytic complex? a critical evaluation of present data from muscle tissue. *FEBS Lett.*, 278(2):135–138, 1991.

[112] J. Batke. Remarks on the supramolecular organization of the glycolytic system in vivo. *FEBS Lett.*, 251(1-2):13–16, 1989.

[113] J. A. Hoerter, A. Kuznetsov, and R. Ventura-Clapier. Functional development of the creatine kinase system in perinatal rabbit heart. *Circ. Res.*, 69(3):665–676, 1991.

[114] J. A. Hoerter, R. Ventura-Clapier, and A. Kuznetsov. Compartmentation of creatine kinases during perinatal development of mammalian heart. *Mol. Cell. Biochem.*, 133-134:277–286, 1994.

[115] T. Tiivel, L. Kadaya, A. Kuznetsov, T. Kaambre, N. Peet, P. Sikk, U. Braun, R. Ventura-Clapier, V. Saks, and E. K. Seppet. Developmental changes in regulation of mitochondrial respiration by adp and creatine in rat heart in vivo. *Mol. Cell. Biochem.*, 208(1-2):119–128, 2000.

[116] C. Franzini-Armstrong and S. Boncompagni. The evolution of the mitochondria-to-calcium release units relationship in vertebrate skeletal muscles. *J. Biomed. Biotechnol.*, 2011, 2011.

[117] M. Vendelin, N. Béraud, K. Guerrero, T. Andrienko, A. Kuznetsov, J. Olivares, L. Kay, and V. Saks. Mitochondrial regular arrangement in muscle cells: A "crystal-like" pattern. *AJP: Cell Physiology*, 288(3):C757–C767, 2005.

[118] T. Anmann, M. Varikmaa, N. Timohhina, K. Tepp, I. Shevchuk, V. Chekulayev, V. Saks, and T. Kaambre. Formation of highly organized intracellular structure and energy metabolism in cardiac muscle cells during postnatal development of rat heart. *BBA-Bioenerg.*, 1837(8):1350–1361, 2014.

[119] B. Ostadal, I. Ostadalova, and N. Dhalla. Development of cardiac sensitivity to oxygen deficiency: Comparative and ontogenetic aspects. *Physiol. Rev.*, 79(3):635–659, 1999.

[120] J. Wilding, F. Joubert, C. Araujo, D. Fortin, M. Novotova, V. Veksler, and R. Ventura-Clapier. Altered energy transfer from mitochondria to sarcoplasmic reticulum after cytoarchitectural perturbations in mice hearts. *J. Physiol. (Lond.)*, 575(1):191–200, 2006.

[121] M. Crompton. The mitochondrial permeability transition pore and its role in cell death. *Biochem. J.*, 341 (Pt 2):233–249, 1999.

[122] C. P. Baines. The mitochondrial permeability transition pore and ischemia-reperfusion injury. *Basic Res. Cardiol.*, 104(2):181–188, 2009.

[123] A. P. Halestrap, K. Y. Woodfield, and C. P. Connern. Oxidative stress, thiol reagents, and membrane potential modulate the mitochondrial permeability transition by affecting nucleotide binding to the adenine nucleotide translocase. *J. Biol. Chem.*, 272(6):3346–3354, 1997.

[124] W. Wang, H. Fang, L. Groom, A. Cheng, W. Zhang, J. Liu, X. Wang, K. Li, P. Han, M. Zheng, J. Yin, W. Wang, M. Mattson, J. Y. Kao, E. Lakatta, S. Sheu, K. Ouyang, J. Chen, R. Dirksen, and H. Cheng. Superoxide flashes in single mitochondria. *Cell*, 134(2):279–290, 2008.

[125] T. Gunter and S. Sheu. Characteristics and possible functions of mitochondrial ca2+ transport mechanisms. *BBA-Bioenerg.*, 1787(11):1291–1308, 2009.

[126] P. Korge, L. Yang, J. . Yang, Y. Wang, Z. Qu, and J. N. Weiss. Protective role of transient pore openings in calcium handling by cardiac mitochondria. *J. Biol. Chem.*, 286(40):34851–34857, 2011.

[127] P. Bernardi and S. von Stockum. The permeability transition pore as a ca(2+) release channel: new answers to an old question. *Cell Calcium*, 52(1):22–27, 2012.

[128] E. Holmuhamedov, C. Ozcan, A. Jahangir, and A. Terzic. Restoration of ca2+-inhibited oxidative phosphorylation in cardiac mitochondria by mitochondrial ca2+ unloading. *Mol. Cell. Biochem.*, 220(1-2):135–140, 2001.

[129] P. Bernardi. Mitochondrial transport of cations: channels, exchangers, and permeability transition. *Physiol. Rev.*, 79(4):1127–1155, 1999.

[130] R. Rizzuto, P. Bernardi, and T. Pozzan. Mitochondria as all-round players of the calcium game. *J. Physiol. (Lond.)*, 529(1):37–47, 2000.

[131] P. Brookes, Y. Yoon, J. Robotham, M. W. Anders, and S. Sheu. Calcium, atp, and ros: a mitochondrial love-hate triangle. *Am. J. Physiol. Cell. Physiol.*, 287(4):C817 –C833, 2004.

[132] A. Rodríguez-Sinovas, Y. Abdallah, H. Piper, and D. Garcia-Dorado. Reperfusion injury as a therapeutic challenge in patients with acute myocardial infarction. *Heart Fail. Rev.*, 12(3-4):207–216, 2007.

[133] A. Halestrap. A pore way to die: the role of mitochondria in reperfusion injury and cardioprotection. *Biochem. Soc. Trans.*, 38(4):841, 2010.

[134] F. Lisa and P. Bernardi. Mitochondria and ischemia–reperfusion injury of the heart: Fixing a hole. *Cardiovasc. Res.*, 70(2):191–199, 2006.

[135] J. E. Kokoszka, K. G. Waymire, S. E. Levy, J. E. Sligh, J. Cai, D. P. Jones, G. R. Macgregor, and D. C. Wallace. The adp/atp translocator is not essential for the mitochondrial permeability transition pore. *Nature*, 427(6973):461–465, 2004.

[136] E. Basso, L. Fante, J. Fowlkes, V. Petronilli, M. Forte, and P. Bernardi. Properties of the permeability transition pore in mitochondria devoid of cyclophilin d. *J. Biol. Chem.*, 280(19):18558–18561, 2005.

[137] C. Baines, R. Kaiser, N. Purcell, N. Blair, H. Osinska, M. Hambleton, E. Brunskill, M. Sayen, R. Gottlieb, G. Dorn, J. Robbins, and J. Molkentin. Loss of cyclophilin d reveals a critical role for mitochondrial permeability transition in cell death. *Nature*, 434(7033):658–662, 2005.

[138] J. Elrod, R. Wong, S. Mishra, R. Vagnozzi, B. Sakthievel, S. Goonasekera, J. Karch, S. Gabel, J. Farber, T. Force, J. Heller Brown, E. Murphy, and J. Molkentin. Cyclophilin d controls mitochondrial pore–dependent ca2+ exchange, metabolic flexibility, and propensity for heart failure in mice. *J. Clin. Invest.*, 120(10):3680–3687, 2010.

[139] A. C. Leung, P. Varanyuwatana, and A. Halestrap. The mitochondrial phosphate carrier interacts with cyclophilin d and may play a key role in the permeability transition. *J. Biol. Chem.*, 283(39):26312 –26323, 2008.

[140] A. Halestrap, C. Connern, E. Griffiths, and P. Kerr. Cyclosporin a binding to mitochondrial cyclophilin inhibits the permeability transition pore and protects hearts from ischaemia/reperfusion injury. *Mol. Cell. Biochem.*, 174(1-2):167–172, 1997.

[141] T. Nakagawa, S. Shimizu, T. Watanabe, O. Yamaguchi, K. Otsu, H. Yamagata, H. Inohara, T. Kubo, and Y. Tsujimoto. Cyclophilin d-dependent mitochondrial permeability transition regulates some necrotic but not apoptotic cell death. *Nature*, 434(7033):652–658, 2005.

[142] V. Giorgio, E. Bisetto, M. Soriano, F. Dabbeni-Sala, E. Basso, V. Petronilli, M. Forte, P. Bernardi, and G. Lippe. Cyclophilin d modulates mitochondrial f0f1-atp synthase by interacting with the lateral stalk of the complex. *J. Biol. Chem.*, 284(49):33982–33988, 2009.

[143] V. Giorgio, S. von Stockum, M. Antoniel, A. Fabbro, F. Fogolari, M. Forte, G. Glick, V. Petronilli, M. Zoratti, I. Szabó, G. Lippe, and P. Bernardi. Dimers of mitochondrial atp synthase form the permeability transition pore. *PNAS*, 110(15):5887–5892, 2013.

[144] D. Hunter and R. Haworth. The ca2+-induced membrane transition in mitochondria. i. the protective mechanisms. *Arch. Biochem. Biophys.*, 195(2):453–459, 1979.

[145] A. Halestrap and A. Davidson. Inhibition of ca2(+)-induced large-amplitude swelling of liver and heart mitochondria by cyclosporin is probably caused by the inhibitor binding to mitochondrial-matrix peptidyl-prolyl cis-trans isomerase and preventing it interacting with the adenine nucleotide translocase. *Biochem. J.*, 268(1):153–160, 1990.

[146] S. Novgorodov, T. Gudz, D. Jung, and G. Brierley. The nonspecific inner membrane pore of liver mitochondria: modulation of cyclosporin sensitivity by adp at carboxyatractyloside-sensitive and insensitive sites. *Biochem. Biophys. Res. Commun.*, 180(1):33–38, 1991.

[147] E. Carafoli. The fateful encounter of mitochondria with calcium: how did it happen? *BBA*, 1797(6-7):595–606, 2010.

[148] C. Chinopoulos and V. Adam-Vizi. Mitochondrial ca2+ sequestration and precipitation revisited. *FEBS J.*, 277(18):3637–3651, 2010.

[149] M. Colombini. Vdac: the channel at the interface between mitochondria and the cytosol. *Mol. Cell. Biochem.*, 256-257(1-2):107–115, 2004.

[150] M. Dolder, S. Wendt, and T. Wallimann. Mitochondrial creatine kinase in contact sites: Interaction with porin and adenine nucleotide translocase, role in permeability transition and sensitivity to oxidative damage. *Neurosignals*, 10(1-2):93–111, 2001.

[151] G. Beutner, A. Rück, B. Riede, and D. Brdiczka. Complexes between porin, hexokinase, mitochondrial creatine kinase and adenylate translocator display properties of the permeability transition pore. implication for regulation of permeability transition by the kinases. *Biochim. Biophys. Acta (BBA)-Biomembranes*, 1368(1):7–18, 1998.

[152] A. Wei, T. Liu, R. Winslow, and B. O'rourke. Dynamics of matrix-free ca2+ in cardiac mitochondria: two components of ca2+ uptake and role of phosphate buffering. *J. Gen. Physiol.*, 139(6):465–478, 2012.

CURRICULUM VITAE

Curriculum Vitae

NIINA KARRO

PERSONAL INFORMATION

NAME	Niina Karro (formely Sokolova)
DATE OF BIRTH	October 26, 1981
CITIZENSHIP	Estonian
CONTACT	Email: niina@sysbio.ioc.ee

EDUCATION

2008 – 2015	**Tallinn University of Technology (TUT), Tallinn, Estonia**
SUBJECT	**PhD, Gene Technology**
THESIS	Analysis of ADP compartmentation in cardiomyocytes and its role in the protection against mitochondrial permeability transition pore opening.
SUPERVISOR	**Dr. Rikke Birkedal,** rikke@sysbio.ioc.ee , +3726204404 Senior Researcher at Laboratory of Systems Biology, Institute of Cybernetics at TUT (IoC)
2006 – 2008	**Tallinn University of Technology, Tallinn, Estonia**
SUBJECT	**MSc**, *cum laude*, **Gene Technology**
THESIS	Effect of Zn (II) Ions on Redox Equilibria of Copper Chaperone Cox17.
SUPERVISOR	**Prof. Peep Palumaa,** peep.palumaa@ttu.ee ,+3726204410 Faculty of Science, Department of Gene Technology, Chair of Genomics and Proteomics, Institute of Gene Technology.
2003 – 2006	**Tallinn University of Technology, Tallinn, Estonia**
SUBJECT	**BSc, Gene Technology**
THESIS	New Method for Expression and Purification of Monomeric and Dimeric Recombinant Human Cox17.
SUPERVISOR	**Prof. Peep Palumaa**
1999 – 2002	**Tallinn Health College, Tallinn, Estonia**
SUBJECT	**BSc, Pharmaceutical Sciences**

LANGUAGE COMPETENCE

Russian	Mother tongue
Estonian	Fluent
English	Fluent

EXPERIMENTAL EXPERIENCE AND SKILLS

- Isolation of cariomyocytes and cardiac fibers (Langendorff perfusion system), isolation of heart and skeletal muscles mitochondria.
- Oxygraphy (Oroboros Instruments, Strathkelvin Instruments).
- Spectrophotometry, fluorometry.
- Light microscopy, including conventional wide-field and fluorescence microscopy, confocal microscopy, immunocytochemistry.
- Bacterial fermentation
- Expression and purification of proteins
- SDS-PAGE electrophoresis
- High-performance liquid chromatography (HPLC): Reversed-phase chromatography, Ion-exchange

chromatography, affinity chromatography, gel filtration
• Mass Spectrometry: ESI-MS, MALDI-MS

PUBLICATIONS

• Voronova A, Kazantseva J, Tuuling M, Sokolova N, Sillard R and Palumaa P (2007). **Cox17, a copper chaperone for cytochrome c oxidase: expression, purification, and formation of mixed disulphide adducts with thiol reagents**, *Protein Expr. Purif.*, 53: 138-144.

• Sokolova N, Vendelin M, Birkedal R (2009). **Intracellular diffusion restrictions in isolated cardiomyocytes from rainbow trout**, *BMC Cell Biology*, 10:90.

• Branovets J, Sepp M, Kotlyarova S, Jepihhina N, Sokolova N, Aksentijevic D, Lygate CA, Neubauer S, Vendelin M, Birkedal R (2013). **Unchanged mitochondrial organization and compartmentation of high-energy phosphates in creatine-deficient GAMT-/- mouse hearts**, *Am J Physiol Heart Circ Physiol.,* 305(4):H506-520.

• Sokolova N, Pan S, Provazza S, Beutner G, Vendelin M, Birkedal R, Sheu SS. (2013). **Mechanisms of ADP in protecting cardiac mitochondrial injury under oxidative stress***, PLoS ONE*, 8(12).

• Sepp M, Sokolova N, Jugai S, Mandel M, Peterson P, Vendelin M. (2014). **Tight coupling of Na^+/K^+-ATPase with glycolysis demonstrated in permeabilized rat cardiomyocytes***, PLoS ONE*, 9(6).

• Bragina O, Gurjanova K, Krishtal J, Kulp M, Karro N, Tõugu V, Palumaa P. (2015). **Metallothionein 2A affects the cell respiration by suppressing the expression of mitochondrial protein cytochrome c oxidase subunit II***, Journal of Bioenergetics and Biomembranes*, 47(3), 209 - 216.

• Karro N, Sepp M, Kotlyarova S, Laasmaa M, Vendelin M, Birkedal R (2015). **Metabolic compartmentation and regulation in rainbow trout cardiomyocytes***, in preparation*.

INTERNATIONAL CONFERENCE PRESENTATIONS

2009 **53rd Biophysical Annual Meeting, Boston, USA**
POSTER Sokolova N, Birkedal R, Vendelin M
Intracellular Diffusion Restrictions in Trout Cardiomyocytes

2009 **36th International Congress of Physiological Sciences, Kyoto, Japan**
POSTER Sokolova N, Birkedal R, Vendelin M
Intracellular Diffusion Restrictions in Trout Cardiac Fibers and Cells

2009 **Annual Meeting of the Society of Experimental Biology, Glasgow, UK**
POSTER Birkedal R, Sokolova N, Laasmaa M, Vendelin M
Using Rainbow Trout Cardiomyocytes to Identify the Diffusion Restrictions Found Specifically in Oxidative Muscles

2011 **55th Biophysical Annual Meeting, Baltimore, USA**
POSTER Sokolova N, Provazza S, Pan S, Beutner G, Birkedal R, Vendelin M, Sheu S-S
Regulation of Mitochondrial Permeability Transition by ADP

POSTER Sepp M, Branovets J, Sokolova N, Kotlyarova S, Birkedal R, Vendelin M
Influence of SERCA and Actomyosin ATPase on Respiration Kinetics in Permeabilized Rat Cardiomyocytes

2011 **65th Annual Meeting of the Society of General Physiologists: Mitochondrial Physiology and Medicine, Woods Hole, USA**
POSTER Gross P, Sokolova N, Provazza S, Beutner G, Sheu S-S
Comparative Effects of Ryanodine Receptor Inhibitors on Mitochondrial Ca^{2+} Uptake Profiles in Control and Malignant Hyperthermia Mouse Heart

2012 **56th Biophysical Annual Meeting, San Diego, USA**
POSTER Sokolova N, Vendelin M, Birkedal R
Distribution of Intracellular ADP Diffusion Restrictions in Trout

Cardiomyocytes

POSTER Gross P, Sokolova N, Pan S, Beutner G, Sheu S-S
Regulation of Mitochondrial Ca^{2+} Uptake by Mitochondrial Ryanodine Receptor in Control and Malignant Hyperthermia Mouse Heart

2012 **Basic Cardiovascular Sciences 2012 Scientific Sessions, New Orleans**

POSTER O-Uchi J, Porter GA, Kang SH, Boncompagni S, Sokolova N, Gross P, Jhun BS, Beutner G, Brookes P, Blaxall BC, Dirksen RT, Protasi F, Pan S, Sheu S-S
Malignant Hyperthermia Mutation of RyR1 (Y522S) Increases Catecholamine-Induced Cardiac Arrhythmia Through Mitochondrial Injury

2013 **57th Biophysical Annual Meeting, Philadelphia, USA**

POSTER Sokolova N, Sepp M, Vendelin M, Birkedal R
Distribution of Intracellular ADP Diffusion Restriction in Trout Cardiomyocytes

POSTER Branovets J, Sepp M, Kotlyarova S, Jepihhina N, Sokolova N, Aksentijevic D, Lygate CA, Neubauer S, Vendelin M, Birkedal R
Unchanged Mitochondrial Organization and Compartmentation in Creatine Deficient GAMT-/- Mouse Heart

POSTER Kotlyarova S, Mandel M, Sokolova N, Aksentijevic D, Lygate CA, Neubauer S, Vendelin M, Birkedal R
Cardiomyocytes from Creatine-Deficient Mice Lacking L-Arginine:Glycine Amidinotransferase (AGAT) Show No Changes in Mitochondrial Organization and Cellular Compartmentation

2013 **37th International Congress of Physiological Sciences, Birmingham, UK**

POSTER Sokolova N, Sepp M, Kotlyarova S, Laasmaa M, Vendelin M, Birkedal R
Metabolic compartmentation and regulation in rainbow trout cardiomyocytes

SCHOLARSHIPS & AWARDS

- Award for the best scientific publication of a young scientist at the Institute of Cybernetics at TUT: Sokolova N, Birkedal R, Vendelin M (2009); **Intracellular diffusion restrictions in isolated cardiomyocytes from rainbow trout**; *BMC Cell Biology*,10:90.
- Young Investigators Travel Grant, 36th International Congress of Physiological Sciences, Kyoto, Japan 2009
- Grantee of Doctoral Studies and Internationalisation Programme DoRa, PhD internship at University of Rochester, Rochester, NY, USA
- Archimedes / DoRa travel awards for presenting at international conferences 2009, 2011, 2012, 2013

TEACHING AND THESES SUPERVISED

2008 – 2010 Seminars for beginning PhD students on cardiac physiology, confocal microscopy and bioenergetics.

2009 – 2013 Giving training for beginning PhD, MSc and BSc students on cell isolation, spectrophotometric and oxygraphic measurements.

2011 Co-Supervised **Aleksander Klepinin's Bachelor thesis**: "Comparative Analysis of Inhibition of Endogenous ADP Stimulated Respiration by Pyruvate Kinase (PK) and Phosphoenolpyruvate (PEP) System in Rat and Rainbow Trout Cardiomyocytes.

2013 Co-Supervised **Svetlana Kotlyarova's Master thesis**: "Cardiomyocytes from Creatine Deficient AGAT Mice Show No Changes in Mitochondrial Organization and Cellular Compartmentation".

SPECIAL COURSES

2006	Mass Spectrometry Course (ESI-MS, MALDI-MS)
2006	Basic Course on Laboratory Animal Science and Techniques: B-category competence certificate
2009	Federation of Laboratory Animal Science Associations (FELASA): C-category competence certificate

PROFESSIONAL EMPLOYMENT

2008 – Present	**Institute of Cybernetics at TUT, Tallinn, Estonia**
	Laboratory of Systems Biology
POSITION	Researcher/PhD student
2010 January – December	**University of Rochester Medical Center, Rochester, NY, USA**
	Department of Pharmacology and Physiology
POSITION	Visiting Research Scholar
2006 – 2008	**Institute of Gene Technology, Tallinn, Estonia**
	Laboratory of Proteomics
POSITION	Engineer/Researcher
2002 – 2006	**OÜ Amfora apteek**
POSITION	Head of Pharmacy
2001 – 2002	**OÜ Eluvesi apteek**
POSITION	Pharmacist

Elulookirjeldus

NIINA KARRO

ISIKUANDMED

NIMI	Naiina Karro (Sokolova)
SÜNNIAEG	26 oktoober, 1981
KODAKONDSUS	Eesti
KONTAKT	Email: niina@sysbio.ioc.ee

HARIDUSKÄIK

2008 – 2015	**Tallinna Tehnikaülikool (TTÜ), Tallinn, Eesti**
ERIALA	**PhD, Geenitehnoloogia**
LÕPUTÖÖ TEEMA	ADP kompartmentatsiooni analüüs südamelihasrakkudes ja selle roll mitokondriaalse suure läbitavusega poori avanemise eest kaitsmisel.
JUHENDAJA	**Dr. Rikke Birkedal,** rikke@sysbio.ioc.ee, +3726204404 KübI Vanemteadur, Süsteemibioloogia Labor, TTÜ Kuberneetika Instituut (KübI).
2006 – 2008	**Tallinna Tehnikaülikool, Tallinn, Eesti**
ERIALA	**MSc**, *cum laude*, **Geenitehnoloogia**
LÕPUTÖÖ TEEMA	Zn(II) ioonide mõju vase šaperooni Cox17 redokstasakaaludele.
JUHENDAJA	**Prof. Peep Palumaa,** peep.palumaa@ttu.ee ,+3726204410 Matemaatika-loodusteaduskond, Genoomika ja proteoomika õppetool, Geenitehnoloogia instituut.
2003 – 2006	**Tallinna Tehnikaülikool, Tallinn, Eesti**
ERIALA	**BSc, Geenitehnoloogia**
LÕPUTÖÖ TEEMA	Uudne metoodika rekombinantse monomeerse ja dimeerse inimese Cox17 ekspressiooniks ja puhastamiseks.
JUHENDAJA	**Prof. Peep Palumaa**
1999 – 2002	**Tallinna Tervishoiu Kõrgkool, Tallinn, Eesti**
ERIALA	**BSc, Farmaatsia ja farmakoloogia**

KEELTEOSKUS

Vene keel	emakeel
Eesti keel	kõrgtase
Inglise keel	kõrgtase

TEADUSTÖÖ KOGEMUS

2008 – …	**TTÜ Küberneetika Instituut, Tallinn, Eesti** **Süsteemibioloogia laboratoorium**
JUHENDAJA	**Dr. Rikke Birkedal** Diffusioonitakistuste uurimine südamelihasrakkudes.
2010 Jaanuar – Detsember	**PhD Internatuur Rochester'i Ülikooli Meditsiinikeskuses**
JUHENDAJA	**Prof. Shey-Shing Sheu**, shey-shing.sheu@jefferson.edu Farmakoloogia ja füsioloogia teaduskond, Rochester'i Ülikooli Meditsiinikeskus, Rochester, NY, USA; Translatsioonilise Meditsiinikeskus, Meditsiini teaduskond, Thomas Jefferson'i Ülikool, Philadelphia, USA.

ADP, Ca^{2+} ja ROS signaliseerimise rolli uurimine südame regulatsioonis füsioloogilistel ja patoloogilistel tingimustel.

2008 – 2010 **Keemilise ja Bioloogilise Füüsika Instituut, Tallinn, Eesti**
Bioenergeetika Laboratoorium
JUHENDAJA **Prof. Tuuli Käämbre,** tuuli.kaambre@kbfi.ee
Katseloomatehnika aluste, bioloogiliste eksperementaalmeetodite ning südamelihasrakkude isoleerimise õppimine.

2004 – 2008 **Geenitehnoloogia Instituut, TTÜ, Tallinn, Eesti**
Proteoomika Laboratoorium
JUHENDAJA **Prof. Peep Palumaa,** peep.palumaa@ttu.ee
Tsütokroom c vase saperooni Cox 17 struktuur ja toimemehhanismid.

PRAKTILINE KOGEMUS

- Südamelihasrakkude ja fiibrite isoleerimine (Langendorff perfusioonisüsteem), südame- ja skeletilihasrakkude mitokondrite isoleerimine.
- Oksügraafia (Oroboros Instruments, Strathkelvin Instruments).
- Spektrofotomeetria, fluoromeetria.
- Fluorestsents mikroskoopia, konfokaal mikroskoopia, immunotsütokeemia.
- Bakterite fermentatsioon
- Valkude ekspressioon ja puhastamine
- SDS-PAGE elektoforees
- Vedekikkromatograafia: affiinsus-, geelfiltratsioon, ioonvahetuskromatograafia, RP-HPLC, FPLC
- Mass Spektomeetria: ESI-MS, MALDI-MS

PUBLIKATSIOONID

- Voronova A, Kazantseva J, Tuuling M, Sokolova N, Sillard R and Palumaa P (2007). **Cox17, a copper chaperone for cytochrome c oxidase: expression, purification, and formation of mixed disulphide adducts with thiol reagents**, *Protein Expr. Purif.*, 53: 138-144.

- Sokolova N, Vendelin M, Birkedal R (2009). **Intracellular diffusion restrictions in isolated cardiomyocytes from rainbow trout**, *BMC Cell Biology*, 10:90.

- Branovets J, Sepp M, Kotlyarova S, Jepihhina N, Sokolova N, Aksentijevic D, Lygate CA, Neubauer S, Vendelin M, Birkedal R (2013). **Unchanged mitochondrial organization and compartmentation of high-energy phosphates in creatine-deficient GAMT-/- mouse hearts**, *Am J Physiol Heart Circ Physiol.,* 305(4):H506-520.

- Sokolova N, Pan S, Provazza S, Beutner G, Vendelin M, Birkedal R, Sheu SS. (2013). **Mechanisms of ADP in protecting cardiac mitochondrial injury under oxidative stress***, PLoS ONE*, 8(12).

- Sepp M, Sokolova N, Jugai S, Mandel M, Peterson P, Vendelin M. (2014). **Tight coupling of Na^+/K^+-ATPase with glycolysis demonstrated in permeabilized rat cardiomyocytes***, PLoS ONE*, 9(6).

- Bragina O, Gurjanova K, Krishtal J, Kulp M, Karro N, Tõugu V, Palumaa P. (2015). **Metallothionein 2A affects the cell respiration by suppressing the expression of mitochondrial protein cytochrome c oxidase subunit II***, Journal of Bioenergetics and Biomembranes*, 47(3), 209 - 216.

- Karro N, Sepp M, Kotlyarova S, Laasmaa M, Vendelin M, Birkedal R (2015). **Metabolic compartmentation and regulation in rainbow trout cardiomyocytes***, in preparation.*

ETTEKANDED RAHVUSVAHELISTEL KONVERENTSIDEL

2009 **53rd Biophysical Annual Meeting, Boston, USA**
POSTER Sokolova N, Birkedal R, Vendelin M
Intracellular Diffusion Restrictions in Trout Cardiomyocytes

2009 POSTER	**36th International Congress of Physiological Sciences, Kyoto, Japan** Sokolova N, Birkedal R, Vendelin M **Intracellular Diffusion Restrictions in Trout Cardiac Fibers and Cells**
2009 POSTER	**Annual Meeting of the Society of Experimental Biology, Glasgow, UK** Birkedal R, Sokolova N, Laasmaa M, Vendelin M **Using Rainbow Trout Cardiomyocytes to Identify the Diffusion Restrictions Found Specifically in Oxidative Muscles**
2011 POSTER	**55th Biophysical Annual Meeting, Baltimore, USA** Sokolova N, Provazza S, Pan S, Beutner G, Birkedal R, Vendelin M, Sheu S-S **Regulation of Mitochondrial Permeability Transition by ADP**
POSTER	Sepp M, Branovets J, Sokolova N, Kotlyarova S, Birkedal R, Vendelin M **Influence of SERCA and Actomyosin ATPase on Respiration Kinetics in Permeabilized Rat Cardiomyocytes**
2011 POSTER	**65th Annual Meeting of the Society of General Physiologists: Mitochondrial Physiology and Medicine, Woods Hole, USA** Gross P, Sokolova N, Provazza S, Beutner G, Sheu S-S **Comparative Effects of Ryanodine Receptor Inhibitors on Mitochondrial Ca^{2+} Uptake Profiles in Control and Malignant Hyperthermia Mouse Heart**
2012 POSTER	**56th Biophysical Annual Meeting, San Diego, USA** Sokolova N, Vendelin M, Birkedal R **Distribution of Intracellular ADP Diffusion Restrictions in Trout Cardiomyocytes**
POSTER	Gross P, Sokolova N, Pan S, Beutner G, Sheu S-S **Regulation of Mitochondrial Ca^{2+} Uptake by Mitochondrial Ryanodine Receptor in Control and Malignant Hyperthermia Mouse Heart**
2012 POSTER	**Basic Cardiovascular Sciences 2012 Scientific Sessions, New Orleans** O-Uchi J, Porter GA, Kang SH, Boncompagni S, Sokolova N, Gross P, Jhun BS, Beutner G, Brookes P, Blaxall BC, Dirksen RT, Protasi F, Pan S, Sheu S-S **Malignant Hyperthermia Mutation of RyR1 (Y522S) Increases Catecholamine-Induced Cardiac Arrhythmia Through Mitochondrial Injury**
2013 POSTER	**57th Biophysical Annual Meeting, Philadelphia, USA** Sokolova N, Sepp M, Vendelin M, Birkedal R **Distribution of Intracellular ADP Diffusion Restriction in Trout Cardiomyocytes**
POSTER	Branovets J, Sepp M, Kotlyarova S, Jepihhina N, Sokolova N, Aksentijevic D, Lygate CA, Neubauer S, Vendelin M, Birkedal R **Unchanged Mitochondrial Organization and Compartmentation in Creatine Deficient GAMT-/- Mouse Heart**
POSTER	Kotlyarova S, Mandel M, Sokolova N, Aksentijevic D, Lygate CA, Neubauer S, Vendelin M, Birkedal R **Cardiomyocytes from Creatine-Deficient Mice Lacking L-Arginine:Glycine Amidinotransferase (AGAT) Show No Changes in Mitochondrial Organization and Cellular Compartmentation**
2013 POSTER	**37th International Congress of Physiological Sciences, Birmingham, UK** Sokolova N, Sepp M, Kotlyarova S, Laasmaa M, Vendelin M, Birkedal R **Metabolic compartmentation and regulation in rainbow trout cardiomyocytes**

STIPENDIUMID JA AUTASUD

• TTÜ Küberneetika instituudi aasta parim teaduspublikatsioon noorte kategoorias: **Intracellular**

diffusion restrictions in isolated cardiomyocytes from rainbow trout; Sokolova N, Birkedal R, Vendelin M; *BMC Cell Biology*, 2009,10:90.

• Young Investigators Travel Grant, Füsioloogiliste teaduste XXXVI rahvusvaheline kongress, Kyoto, Jaapan, 2009

• ESF DoRa stipendium PhD internatuuri jaoks Rochesteri Ülikoolis, Rochester, NY, USA

• Archimedes / DoRa stipendiumid rahvusvahelistel konverentsidel osalemiseks 2009, 2011, 2012, 2013

ÕPETUSTEGEVUS

2008 – 2010 Alustavate doktorantide baaskursused südamefüsioloogias, bioenergeetikas ja konfokaalmikroskoopias.

2009 – 2013 Doktorantide, magistrantide ning bakalaureusetudengite koolitamine rakkude isoleerimises ning oksügraafiliste ning spektrofotomeetriliste mõõtmiste sooritamises.

2011 **Aleksander Klepinin'i bakalaureusetöö** kaasjuhendaja. "Võrdlev analüüs endogeense ADP poolt stimuleeritud rakuhingamise inhibeerimisest püruvaat kinnas (PK)-fosfoenoolpüruvaat (PEP) süsteemi poolt roti ja vikerforelli südamerakkudes".

2013 **Svetlana Kotlyarova magistritöö** kaasjuhendaja. "Kompartmentatsioon ja mitokondrite asetus kreatiini puudulikkusega AGAT hiirte südamelihasrakkudes".

TÄIENDUSÕPE

2006 Mass-Spektromeetria kursus (ESI-MS, MALDI-MS)

2006 Katseloomade tehnika kursus: B-kategooria kompetents

2009 Federation of Laboratory Animal Science Associations (FELASA): C-kategooria kompetents

TEENISTUSKÄIK

2008 – … **TTÜ Küberneetika Instituut, Tallinn, Eesti**
Süsteemibioloogia Laboratoorium
AMETIKOHT Insener/doktorant

2010 Jaanuar – Detsember **University of Rochester Medical Center, Rochester, NY, USA**
Farmakoloogia ja füsioloogia teaduskond
AMETIKOHT Külalisteadur

2006 – 2008 **Geenitehnoloogia Instituut, Tallinn, Eesti**
Proteoomika Laboratoorium
AMETIKOHT Insener/magistrant

2002 – 2006 **OÜ Amfora apteek**
AMETIKOHT Apteegi juhataja

2001 – 2002 **OÜ Eluvesi apteek**
AMETIKOHT Farmatseut

APPENDIX

PUBLICATION I

Sokolova N, Vendelin M, Birkedal R

Intracellular diffusion restrictions in isolated cardiomyocytes from rainbow trout.

BMC Cell Biology, 10:90, December 2009

BMC Cell Biology

BioMed Central

Research article

Open Access

Intracellular diffusion restrictions in isolated cardiomyocytes from rainbow trout

Niina Sokolova, Marko Vendelin and Rikke Birkedal*

Address: Laboratory of Systems Biology, Institute of Cybernetics, Tallinn University of Technology, Akadeemia 21, 12618 Tallinn, Estonia

Email: Niina Sokolova - niina@sysbio.ioc.ee; Marko Vendelin - markov@sysbio.ioc.ee; Rikke Birkedal* - rikke@sysbio.ioc.ee

* Corresponding author

Published: 17 December 2009

BMC Cell Biology 2009, **10**:90 doi:10.1186/1471-2121-10-90

Received: 17 July 2009

Accepted: 17 December 2009

This article is available from: http://www.biomedcentral.com/1471-2121/10/90

Abstract

Background: Restriction of intracellular diffusion of adenine nucleotides has been studied intensively on adult rat cardiomyocytes. However, their cause and role *in vivo* is still uncertain. Intracellular membrane structures have been suggested to play a role. We therefore chose to study cardiomyocytes from rainbow trout (*Oncorhynchus mykiss*), which are thinner and have fewer intracellular membrane structures than adult rat cardiomyocytes. Previous studies suggest that trout permeabilized cardiac fibers also have diffusion restrictions. However, results from fibers may be affected by incomplete separation of the cells. This is avoided when studying permeabilized, isolated cardiomyocytes. The aim of this study was to verify the existence of diffusion restrictions in trout cardiomyocytes by comparing ADP-kinetics of mitochondrial respiration in permeabilized fibers, permeabilized cardiomyocytes and isolated mitochondria from rainbow trout heart. Experiments were performed at 10, 15 and 20°C in the absence and presence of creatine.

Results: Trout cardiomyocytes hypercontracted in the solutions used for mammalian cardiomyocytes. We developed a new solution in which they retained their shape and showed stable steady state respiration rates throughout an experiment. The apparent ADP-affinity of permeabilized cardiomyocytes was different from that of fibers. It was higher, independent of temperature and not increased by creatine. However, it was still about ten times lower than in isolated mitochondria.

Conclusions: The differences between fibers and cardiomyocytes suggest that results from trout heart fibers were affected by incomplete separation of the cells. However, the lower ADP-affinity of cardiomyocytes compared to isolated mitochondria indicate that intracellular diffusion restrictions are still present in trout cardiomyocytes despite their lower density of intracellular membrane structures. The lack of a creatine effect indicates that trout heart lacks mitochondrial creatine kinase tightly coupled to respiration. This argues against diffusion restriction by the outer mitochondrial membrane. These results from rainbow trout cardiomyocytes resemble those from other low-performance hearts such as neonatal rat and rabbit hearts. Thus, it seems that metabolic regulation is related to cardiac performance, and it is likely that rainbow trout can be used as a model animal for further studies of the localization and role of diffusion restrictions in low-performance hearts.

Background

In permeabilized preparations of mammalian oxidative muscles such as red skeletal muscle and the heart, diffusion of ADP and phosphate from the surrounding medium to the adenine nucleotide translocase (ANT) in the inner mitochondrial membrane is restricted [1,2]. Especially the diffusion restriction of ADP in adult rat cardiomyocytes has received much attention, because the compromised energetic balance induced by ischemia-reperfusion damage is associated with diminished diffusion restrictions [3,4].

The existence of diffusion restrictions is indicated by that the apparent ADP-affinity of mitochondria *in situ* in permeabilized fibers and cardiomyocytes is much lower ($K_{M\ ADP}$~300 μM in rat fibers and cardiomyocytes) than the ADP-affinity of isolated mitochondria ($K_{M\ ADP}$ < 20 μM) [5-7]. It was first proposed that this was due to low permeability of the outer mitochondrial membrane, which is partially overcome by creatine kinase (CK) [8,9]. In addition to the outer mitochondrial membrane, some diffusion restrictions also reside in the cytosol. They lead to a preferential metabolic channeling of ADP from ATPases to mitochondria [10]. Likewise, ATP from mitochondria is channeled to the sarcoplasmic reticulum (SR) Ca^{2+}-ATPase (SERCA) and myosin ATPase [11]. This led to the hypothesis that cytosolic diffusion restrictions divide cardiomyocytes into subcellular compartments termed "intracellular energetic units" (ICEUs) [12-14]. Their confinement of ADP and ATP in small compartments with short diffusion distances enhances the functional coupling between adjacent energy producing mitochondria and energy consuming ATPases.

It is still not clear what causes the diffusion restrictions in rat cardiomyocytes. The importance of the outer mitochondrial membrane has recently regained attention in studies on isolated brain mitochondria suggesting that its permeability is regulated by tubulin [15,16]. Possible candidates for cytosolic diffusion restrictions are membrane structures such as SR and t-tubules [12,14]. But also cytoskeletal components such as tubulin have been proposed [6]. These structures are rather densely packed in adult rat cardiomyocytes. In contrast, cardiomyocytes from rainbow trout (*Oncorhynchus mykiss*) have a relatively simple morphology. They are only 2-5 μm thick [17,18], have no t-tubules and a sparsely developed SR [19]. Below the sarcolemma is a single ring of myofilaments surrounding a central core of mitochondria [18,20]. Thus, if t-tubules and SR cause diffusion restriction, we would expect diffusion restrictions to be much smaller in trout cardiomyocytes.

Previous studies on rainbow trout permeabilized cardiac fibers suggest that despite their simple morphology, they also have intracellular diffusion restrictions. As in rat permeabilized fibers, their apparent ADP-affinity is much lower than that expected for isolated mitochondria, but it is increased by the addition of creatine. Furthermore, a competitive assay with excess pyruvate kinase activity only partially inhibits mitochondrial respiration [21,22]. However, the results from permeabilized fibers may be affected by incomplete cell separation, and/or clustering of fibers on top of the stirrer during oxygraphy measurements. These are avoided with permeabilized cardiomyocytes, since the single cells disperse evenly in the oxygraphy medium. Rat permeabilized fibers and cardiomyocytes have similar ADP-kinetics [6], which reaffirm the reliability of the results. However, trout permeabilized fibers have given contradictory results, because creatine lowers the apparent $K_{M\ ADP}$ [21,23], but there does not seem to be a mitochondrial CK tightly coupled to respiration [22]. The aim of this study was to control the existence of diffusion restrictions in trout cardiomyocytes by comparing the apparent ADP-affinity in permeabilized cardiac fibers, permeabilized isolated cardiomyocytes and isolated mitochondria. An effect of temperature on diffusion restrictions in terms of apparent $K_{M\ ADP}$ was found previously on both trout and rat cardiac fibers [23,24]. This is important for the rainbow trout which lives at a temperature range of 2-23°C. Furthermore, due to the different temperature sensitivity of metabolism and diffusion speed, the effect of temperature allows us to draw conclusions about the importance of diffusion distance as one of the restricting factors. Therefore, the experiments were performed at 10, 15 and 20°C. Additionally, because CK may play an important role in facilitating ADP-diffusion across diffusion restriction barriers, the experiments were performed in both the absence and presence of creatine.

The experiments were complicated by hypercontraction of isolated trout cardiomyocytes in the R(respiration)-solution used previously for permeabilized fibers. This solution was originally developed for mammalian tissue and will be referred to as "mammalian R-solution". Therefore, we first had to develop a new "fish R-solution" for trout cardiomyocytes, in which they maintained shape and showed stable steady state respiration rates throughout each experiment. The results on cardiomyocytes were different from those on fibers suggesting that results from trout fibers were affected by incomplete separation of the cells. However, the apparent ADP-affinity of cardiomyocytes was still about an order of magnitude higher than that of isolated mitochondria. This indicates that trout cardiomyocytes still have diffusion restrictions despite their low density of intracellular membrane structures. However, in cardiomyocytes, creatine did not lower the apparent $K_{M\ ADP}$ suggesting that there is no mitochondrial creatine kinase tightly coupled to respiration to overcome diffusion restrictions.

Methods

Animals

Rainbow trout were obtained from local fish farms (Simuna Ivax OÜ, Lääne-Virumaa, and Forkala OÜ, Roosna-Alliku, Estonia). They were kept in a 1200 liter freshwater tank at 15 ± 1°C, and fed regularly with commercial fish food. They were allowed to acclimatize for at least 3 weeks before the experiments. All procedures were approved by the Estonian National Committee for Ethics in Animal Experimentation (Estonian Ministry of Agriculture). The fish was stunned by a single blow to the head followed immediately by a cut of the spine. The heart was excised and immediately transferred to ice-cold solution to minimize ischemia.

Preparation of permeabilized cardiac fibers

The excised heart was transferred to ice-cold isolation solution (see composition below). The ventricle was isolated and the spongy layer and compact layer were separated. The spongy tissue was cut into six smaller pieces, which were transferred to fresh S(skinning)-solution in a petri-dish on ice. Each piece was carefully dissected using fine tweezers (Dumont 3, Dumostar, World Precision Instruments) to separate the tissue into thin bundles of cells that were interconnected. The fibers were permeabilized by incubation for 30 min under continuous mixing in S-solution containing 50 μg/ml saponin at 4°C. After this, they were washed twice for 10 min in S-solution without saponin and stored at 4°C in S-solution until use within less than 3 hours.

Isolation of cardiomyocytes

The isolation of trout cardiomyocytes has been described previously [18]. The heart was excised with atrium and bulbus arteriosus and transferred to ice-cold isolation solution (see composition below). A cannula was inserted through the bulbus arteriosus into the ventricle and the heart was perfused in retrograde manner with isolation solution for 8-10 min to wash the heart free from blood and to lower extracellular Ca^{2+}-concentration. After washing, the heart was perfused with isolation solution containing 0.5 mg/ml trypsin, 0.75 mg/ml collagenase A and 0.75 mg/ml BSA for 18-20 min to digest the extracellular matrix and dissociate the cardiomyocytes. After digestion, the heart was taken off the cannula and cut into smaller pieces. The cardiomyocytes were suspended with a 1 ml pipette, where the tip had been cut off in order to minimize mechanical damage. The cell suspension was filtered through nylon tissue, and healthy cells were isolated by sedimentation. The isolation procedure was carried out at room temperature, and the isolated cells were kept in isolation solution at 4°C until use within at least 3 hours.

Isolation of mitochondria

Mitochondria were isolated by differential centrifugation of tissue homogenate similar to in Bouzidi et al. [25]. The heart was excised and transferred to buffer A (see composition below). The atrium and bulbus arteriosus were cut off and the ventricle was blotted dry and weighed. After one more wash in fresh buffer A it was blotted dry again and cut into smaller pieces (2 × 2 mm), which were incubated for 5 min in 2.5 ml buffer A containing 1 mg subtilisin per g ventricular muscle. At the end of incubation, 12.5 ml buffer A was added and the sample was centrifuged at 15000 g for 5 min. The resulting pellet was re-suspended in 15 ml buffer A and centrifuged at 15000 g for 5 min. The washed pellet was re-suspended in 15 ml buffer A and transferred to a glass homogenizer with a Teflon pestle. The suspension was homogenized at 500 rpm in three rounds of 1-2 seconds and centrifuged for 5 min at 1000 g. The supernatant was retained, while the pellet was re-suspended in 10 ml buffer A, homogenized at 750 rpm in three rounds of 1-2 seconds and centrifuged for 5 min at 1000 g. The two supernatants were spun at 14000 g for 10 min. Each pellet was re-suspended in 0.9 ml buffer A and centrifuged for 5 min at 2000 g. The resulting supernatants were then centrifuged for 15 min at 8000 g, and the pellets containing the mitochondria were resuspended in 0.4 ml buffer A. The isolation of mitochondria was carried out at 0-4°C, and the isolated mitochondria were kept on ice until use within 3 hours.

Recording of ADP-stimulated oxygen consumption

Oxygen consumption of the sample was recorded in an Oroboros oxygraph-2k (Oroboros Instruments, Austria), and the rate of oxygen consumption (nmol O_2 ml^{-1} min^{-1}) was calculated by software developed in our laboratory. To prepare permeabilized fibers for oxygraphy measurements, they were washed twice for 5 min in the R-solution used for oxygraphy. This was either the mammalian R-solution used previously [21-23] and composed for mammalian permeabilized fibers, or the new fish R-solution (see compositions below). These washes served to remove all adenine nucleotides, creatine and phosphocreatine that were present in the S-solution, in which the fibers were kept until use. For isolated cardiomyocytes and isolated mitochondria, which were kept in solutions without these components, a known volume of suspension was added to the oxygraph chamber with fish R-solution. Isolated cardiomyocytes were permeabilized in the oxygraph chamber by the addition of 20 μg ml^{-1}saponin to the chamber at least 4-10 min before the first recordings. This concentration of saponin was chosen on the basis of preliminary experiments, where cells were incubated with 1 mM ADP, and the increase in respiration rate was followed in time until it reached steady state. Among the different saponin-concentrations tested, we observed that 20 μg ml^{-1} led to a steady state respiration rate within 4-10 min (longer time at cold temperature) that was maintained for more than 30 min (results not shown).

Oxygen consumption was stimulated by stepwise increases in the ADP-concentration. For most experiments, 8 μM cytochrome c and 30 μM atractyloside was added at the end of the ADP-titration to test the intactness of the outer and inner mitochondrial membrane, respectively. At the end of the experiments, permeabilized fibers were taken out of the chamber to determine their dry weight, and allow for the expression of their respiration rate as nmol O_2 min^{-1} mg dw^{-1}. For isolated cardiomyocytes and isolated mitochondria, an aliquot of the suspension was frozen to later determine the protein concentration by a standard bicinchoninic acid (BCA) colorimetric assay (Thermo Scientific). Knowing the volume of suspension added to the oxygraph, respiration rate was calculated as nmol O_2 min^{-1} mg $protein^{-1}$.

Solutions

S(skinning)-solution for preparation of permeabilized fibers (originally developed by [26]) was composed of (mM): CaK_2EGTA 2.77, K_2EGTA 7.23, $MgCl_2$ 6.56, imidazole 20, taurine 20, dithiotreitol 0.5, KOH 50, MES 50, Na_2ATP 5.7, phosphocreatine 15, pH adjusted to 7.1 with KOH.

Isolation solution for isolation of cardiomyocytes [18] was composed of (mM): NaCl 100, KCl 10, KH_2PO_4 1.2, $MgSO_4$ 4, taurine 50, glucose 20, Hepes 10, pH adjusted to 6.9 with NaOH.

Buffer A for isolation of mitochondria [25] was composed of (mM): sucrose 70, mannitol 220, EDTA 1, Hepes 10, pH adjusted to 7.4 with KOH, 0.5% bovine serum albumin (BSA) added immediately before use.

Mammalian R(respiration)-solution (originally developed by [26]) was composed of (mM): CaK_2EGTA 2.77, K_2EGTA 7.23, $MgCl_2$ 1.38, imidazole 20, taurine 20, dithiotreitol 0.5, K_2HPO_4 3, KOH 90, NaOH 10, MES 100, glutamate 5, malate 2, pH adjusted to 7.1 with KOH, 0.2% BSA added immediately before use.

Fish R(respiration)-solution was composed of (mM): KCl 20, K-lactobionate 85, $MgCl_2$ 3, KH_2PO_4 5, EGTA 0.4, dithiotreitol 0.3, glutamate 5, malate 2, taurine 20, Hepes 20, pH adjusted to 7.1 with KOH, 0.2% BSA added immediately before use.

Imaging of isolated cardiomyocytes

Isolated rat cardiomyocytes were provided from other experiments in our laboratory. For transmission images, the cells were mixed in isolation solution and imaged under a Nikon Ti-U microscope with a 60×/NA 1.2 water-immersed objective. For confocal images, rat and trout cardiomyocytes were kept in Ca^{2+}-free Ringer and isolation solution, respectively, containing 30 mM BDM (2,3-butanedione monoxime). The sarcolemma and mitochondria were labeled by incubation for at least 15 min with the membrane potential sensitive dye Di-8-ANEPPS (5 μM; Invitrogen), and the mitochondrial potential sensitive dye Mitotracker Red (1 μM; Invitrogen), respectively. Three-dimensional confocal images (z-stacks) were acquired on a Zeiss LSM 510 confocal microscope with a 63×/NA 1.2 water-immersed objective. The images were deconvolved by software developed in our laboratory using the point spread function recorded at 543 nm [27].

Data and statistics

Normalized kinetic parameters such as basal respiration rate in the absence of ADP (V_0), maximal respiration rate at saturating ADP (V_{max}), acceptor control ratio (ACR = V_{max}/V_0), and the ADP-affinity in terms of the Michaelis-Menten constant ($K_{M\ ADP}$) were calculated using in-house software.

All values are presented as mean ± SEM, and statistical tests are described in the legends of the respective figures and tables.

Results

Morphology of rainbow trout compared to rat cardiomyocytes

To illustrate the size and morphology differences between trout and rat cardiomyocytes, we recorded transmission images of the two cell types together. A representative example is shown in Fig. 1A. For more detail, we recorded confocal images of cells, where the sarcolemma was labeled with the potential sensitive indicator di-8-ANEPPS (green) and mitochondria were labeled with the potential sensitive Mitotracker Red CMXRos (red). The deconvolved images and reconstructed cross sections are shown for rat and trout cardiomyocytes in Fig. 1B and 1C, respectively. These pictures illustrate that rat cardiomyocytes have several parallel rows of mitochondria that are organized as in a crystal lattice in all three dimensions [20]. This regular arrangement correlates with that of the interspersed parallel rows of myofilaments [28]. Notice also the t-tubular invaginations of the sarcolemma that extend into the center of the cell. In contrast, trout cardiomyocytes have a central core of mitochondria, which are organized rather chaotically [20]. The gap from the mitochondrial core to the sarcolemma is occupied by a single layer of myofilaments. Of note is the small diameter compared to rat cardiomyocytes and the absence of t-tubules.

Development of a new intracellular solution for trout cardiomyocytes

Recording of respiration of isolated cardiomyocytes was complicated with the use of "mammalian R-solution" used in previous studies on permeabilized trout cardiac fibers [21-23]. The mammalian R-solution was originally

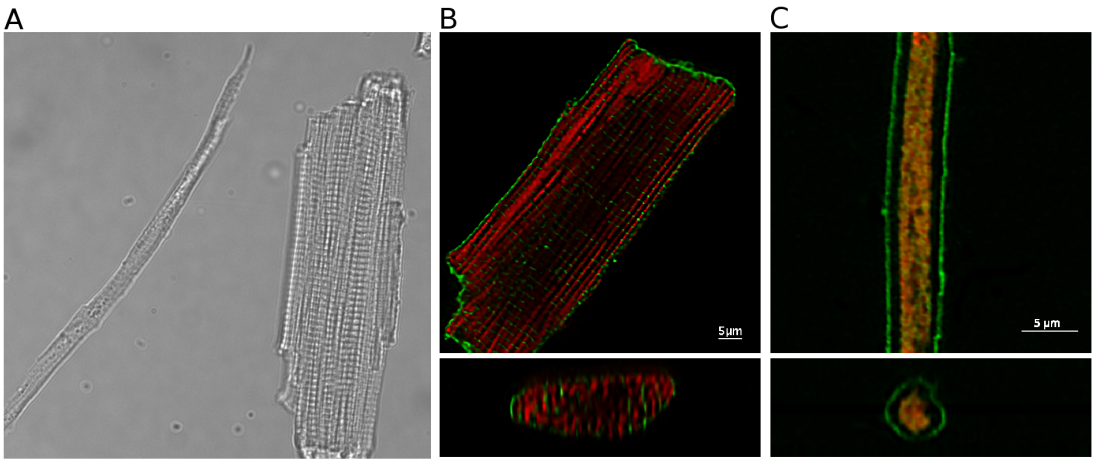

Figure 1

Comparison of trout and rat cardiomyocytes. (A) Transmission image of trout and rat cardiomyocytes next to each other in the same solution. Trout cardiomyocytes can be very long, and only half of the trout cardiomyocyte was within the camera field of view. (B, C) Deconvolved confocal images of rat cardiomyocyte (B) and trout cardiomyocyte (C) labeled with di-8-ANEPPS (green; labeling sarcolemma) and mitotracker Red CMXRos (red; labeling mitochondria). The upper image shows one image from a confocal z-stack, and lower image shows re-constructed cross section. Note different size of the scale bars.

developed for studies on mammalian tissue, but permeabilized trout fibers had an acceptable ACR in this solution (Table 1). However, when isolated trout cardiomyocytes were permeabilized in this solution, their mitochondria swelled immediately followed by hypercontraction and the formation of blebs around the hypercontracted cells. We developed a new "fish R-solution" in which isolated trout cardiomyocytes maintained their morphology and showed stable steady-state respiration rates at all concentrations of ADP (Fig. 2). Interestingly, a few preliminary experiments to test this solution showed that when rat cardiomyocytes were permeabilized in the fish R-solution, they hypercontracted and oxygen consumption was virtually absent.

The new intracellular solution for trout cardiomyocytes was developed by trial and error. An important observation in this development was that trout cardiomyocytes maintained their overall morphology in a solution with high KCl [29]. Although their mitochondria swelled due to the high chloride concentration, they did not hypercontract. Thus, this solution was used as a starting point to approach the MIR05 solution, which is recommended for permeabilized cells [30]. The composition of the final fish

Table 1: ADP-kinetics of respiration in permeabilized fibres in mammalian R-solution

Temp	Creatine	n	V_0	V_{max}	ACR	$K_{M\ ADP}$
10°C	-	5	2.28 ± 0.21	17.95 ± 2.59	7.90 ± 0.91	509 ± 57
	+	5	2.15 ± 0.25	15.88 ± 2.59	7.38 ± 0.68	252 ± 48
15°C	-	5	3.39 ± 0.45	22.17 ± 3.46	6.62 ± 0.85	399 ± 34
	+	5	3.30 ± 0.49	19.37 ± 3.69	5.82 ± 0.77	200 ± 17 *
20°C	-	5	5.48 ± 0.18	24.22 ± 1.97	4.42 ± 0.32	178 ± 32
	+	5	5.21 ± 0.45	22.71 ± 3.78	4.26 ± 0.39	129 ± 30

Respiration was stimulated by increasing concentrations of ADP, and the kinetic parameters were calculated: V_0 (nmol O_2 min^{-1} mg dw^{-1}) is the basal respiration rate before addition of ADP; V_{max} (nmol O_2 min^{-1} mg dw^{-1}) is the maximal respiration rate at saturating ADP; ACR = V_{max}/V_0; $K_{M\ ADP}$ (µM) is the ADP-concentration at which $V = V_{max}/2$. V_{max} and $K_{M\ ADP}$ were calculated by a hyperbolic fit of the data. Experiments were performed at three different temperatures in the absence and presence of creatine. Number of experiments is given in column n. At each temperature, results in the absence and presence of creatine were compared by a paired Students t-test. * denotes $P < 0.05$ significantly different in the presence of creatine. The effect of creatine at 10°C was almost significant ($P = 0.0533$). Temperature-dependency was assessed by a one-way ANOVA in the absence and presence of creatine, respectively. Temperature had a significant effect on V_0 ($P < 0.001$), ACR ($P < 0.05$) and $K_{M\ ADP}$ in the absence of creatine ($P < 0.001$).

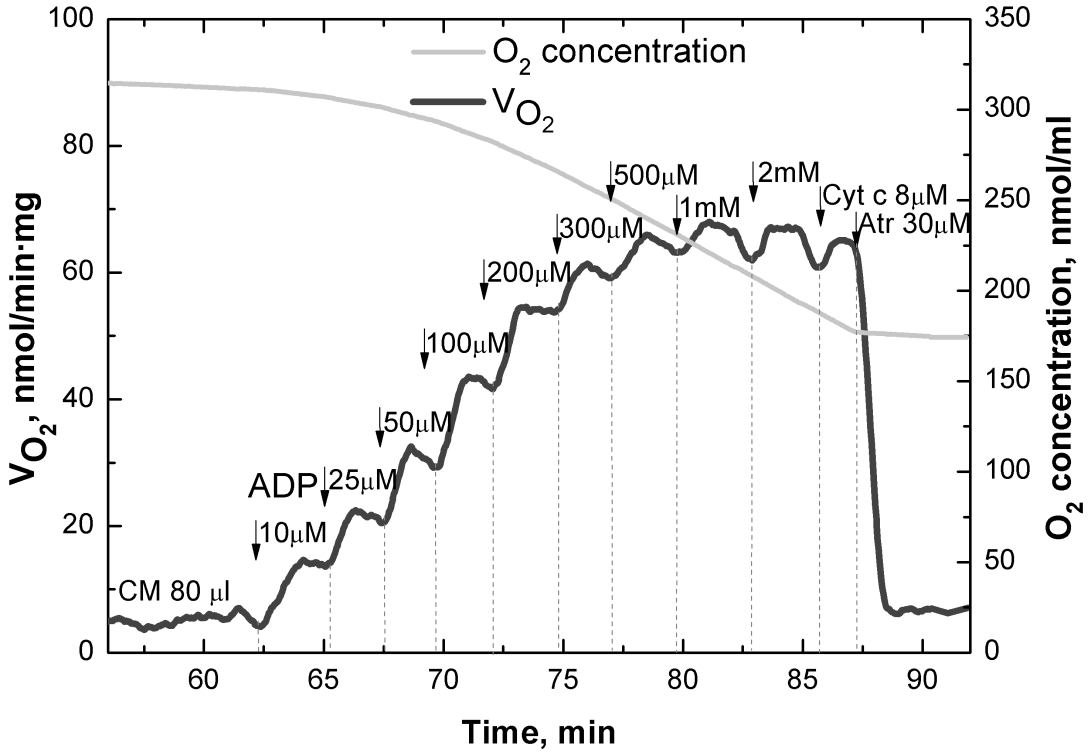

Figure 2
Example of respiration of permeabilized cardiomyocytes. Representative example recorded at 10°C in the absence of creatine showing the respiration rate of permeabilized trout cardiomyocytes (CM) during stepwise increases in ADP-concentration as indicated. Note that the respiration rate was relatively stable at each step of the ADP-titration, that cytochrome c did not increase respiration rate, and that atractyloside brought respiration rate down to the same level as the basal respiration rate before addition of ADP.

R-solution is shown in Table 2, where it is compared to the mammalian R-solution, the high KCl-solution [29] and MiR05 [30]. Compared to the MIR05 solution, the main difference is that the fish R-solution contains more K-lactobionate, 20 mM KCl and no sucrose. The concentration of K-lactobionate could be varied between 20 and 130 mM without any gross effect on the oxygraph results (not shown). We chose an intermediate concentration of 85 mM, so that total K^+-concentration was 110 mM. This is close to the concentration in the mammalian R-solution, the 108 mM in sheep purkinje cells [31], and the 118 mM in frog heart (calculated from [32] using an activity coefficient of 0.73 [33]). The presence of sucrose did not seem to affect the results, so we left it out to keep the osmolarity between that of the mammalian R-solution and MiR05 (Table 2). We speculate whether KCl was important. In some cell types, chloride transport through a mitochondrial chloride intracellular channel (mtCLIC) is believed to be important for maintaining mitochondrial membrane potential [34]. The addition of 20 mM KCl gave a total Cl^--concentration of 26 mM, which is very close to the 25 mM reported for chicken cultured cardiomyocytes [35] and calculated for frog ventricle (using an activity of 17.6 mM [36] and an activity coefficient of 0.7 as in [35]). With a physiological level of chloride, we could be sure that mitochondrial CK (if present) would not dissociate from the inner mitochondrial membrane, as it is known to happen in solutions with high KCl [37]. The 0.3 mM dithiothreitol in the fish R-solution ensures that the thiol-group of Cys-282 in the active site CK is reduced, which is crucial for CK function [38]. Ionic strength is intermediate between that of the mammalian R-solution and the MiR05 (Table 2).

Table 2: Comparison of intracellular solutions

Compound	Mammalian R-solution	KCl	MiR05	Fish R-solution
CaK_2EGTA	2.77			
K_2EGTA	7.23			
Imidazole	20			
K-MES	100			
KCl		125		20
Sucrose			110	
K-lactobionate			60	85
$MgCl_2$	1.38	3	3	3
K_2HPO_4/KH_2PO_4	3	5	10	5
Taurine	20		20	20
Dithiothreitol	0.3	0.3		0.3
EGTA		0.4	0.5	0.4
Hepes		20	20	20
Glutamate	5	5	5	5
Malate	2	2	2	2
BSA	2 mg/ml	2 mg/ml	1 mg/ml	2 mg/ml
pH	7.1	7.1	7.1	7.1
Ionic strength	142	142	95	122
Osmolarity	288	323	330	301

Composition of the mammalian R-solution, KCl-solution (Oroboros, Austria), mitomed MiR05 (Oroboros, Austria) used for mammalian cardiomyocytes and the fish R-solution developed for the present study on permeabilized trout cardiomyocytes. All units are in mM except osmolarity, which is in mOsm.

We were able to compare the ADP-kinetics of respiration in mammalian R-solution and fish R-solution in permeabilized fibers, which survived in both solutions. The results are shown in Table 1 and 3, respectively. In agreement with previous studies, the results from permeabilized fibers had two apparent $K_{M\ ADP}$ values in the absence of creatine [23], but for simplicity we show only the apparent $K_{M\ ADP}$ obtained by fitting with a single hyperbolic equation. $K_{M\ ADP}$ was higher in the fish R-solution only at 15°C in the absence of creatine ($P < 0.05$). However, the main difference was that fibers had a better performance at high temperatures in fish R-solution: V_0 was lower at 20°C ($P < 0.001$ and $P < 0.01$ in the absence and presence of creatine, respectively), and ACR was higher at both 15 and 20°C ($P < 0.05$ in the absence of creatine at both temperatures, and $P < 0.01$ and 0.001 in the presence of creatine at 15 and 20°C, respectively). The remainder of this article focuses on the oxygraphy data obtained using this fish R-solution.

ADP-kinetics of respiration in permeabilized fibers

The ADP-kinetics of respiration in permeabilized fibers is shown in Table 3 and Fig. 3. V_0, V_{max} and ACR were similar in the absence and presence of creatine at each temperature. V_0 increased with temperature, whereas V_{max} and ACR were temperature-independent. $K_{M\ ADP}$ was lowered by creatine, and this was significant at 10 and 15°C. $K_{M\ ADP}$ decreased with temperature, but the temperature-effect was only significant in the absence of creatine (Table 3).

ADP-kinetics of respiration in permeabilized cardiomyocytes

The ADP-kinetics of respiration in permeabilized isolated cardiomyocytes is shown in Table 4 and Fig. 3. V_0 was slightly higher and ACR slightly lower in the presence than in the absence of creatine at 15 and 20°C (Table 4). However, the most important result is the apparent $K_{M\ ADP}$, which is interesting to compare with that of fibers

Table 3: ADP-kinetics of respiration in permeabilized fibres in fish R-solution

Temp	Creatine	n	V_0	V_{max}	ACR	$K_{M\ ADP}$
10°C	-	6	2.34 ± 0.21	24.85 ± 3.44	10.68 ± 1.22	783 ± 160
	+	6	2.01 ± 0.19	22.6 ± 3.83	11.03 ± 1.62	376 ± 55 *
15°C	-	5	2.78 ± 0.32	29.13 ± 3.16	10.66 ± 1.01	579 ± 64
	+	5	2.51 ± 0.08	27.25 ± 2.22	10.96 ± 1.11	301 ± 42 *
20°C	-	5	3.35 ± 0.07	28.06 ± 3.37	8.40 ± 1.05	293 ± 115
	+	5	3.37 ± 0.15	30.59 ± 1.83	9.10 ± 0.52	224 ± 42

Notation and statistical tests are as in Table 1. * denotes $P < 0.05$ significantly different in the presence of creatine. Temperature had a significant effect on V_0 ($P < 0.05$ and $P < 0.001$ in the absence and presence of creatine, respectively) and $K_{M\ ADP}$ in the absence of creatine ($P < 0.05$).

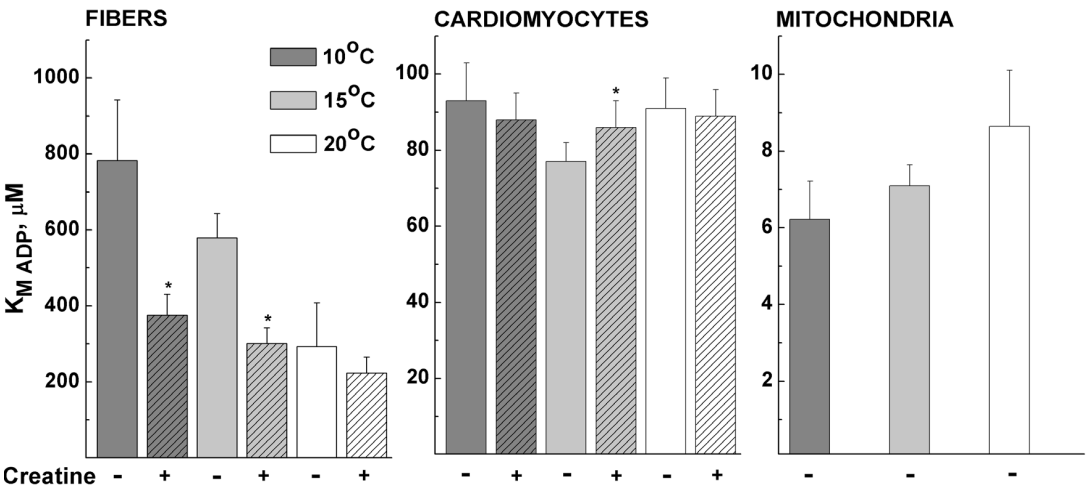

Figure 3

Apparent ADP-affinity in fibers, cardiomyocytes and mitochondria. The apparent $K_{M\ ADP}$ of permeabilized fibers, permeabilized cardiomyocytes and isolated mitochondria as obtained by fitting the data with a single hyperbolic equation. All experiments were done at 10, 15 and 20°C, and experiments on fibers and cardiomyocytes were performed in the absence and presence of creatine as indicated below the columns. Notice the different scales on the y-axes.

(compare in Fig. 3, note different scales on the y-axes). In contrast to permeabilized fibers, permeabilized cardiomyocytes had only one apparent $K_{M\ ADP}$ in the absence of creatine. This apparent $K_{M\ ADP}$ was lower than in fibers and similar at all temperatures. It was not lowered by creatine and even showed a slight increase at 15°C. The fact that creatine did not lower $K_{M\ ADP}$ was expected on the basis of a previous study [22], and suggests that trout cardiomyocytes do not have a mitochondrial CK, which is tightly coupled to respiration. The discrepancy between fibers and cardiomyocytes is discussed further below.

ADP-kinetics of respiration in isolated mitochondria

In order to make any conclusions about diffusion restrictions in trout cardiomyocytes, their apparent $K_{M\ ADP}$ should be compared with that of isolated mitochondria. The ADP-stimulated respiration kinetics of isolated mitochondria is shown in Table 5 and Fig. 3. In contrast to permeabilized cardiomyocytes, V_{max} and ACR of isolated mitochondria increased with temperature (Table 5). In another study on rainbow trout skeletal oxidative muscle, V_{max} increased but ACR decreased with assay temperature [39]. We are at present unable to explain the different temperature dependence of V_{max} and ACR in permeabilized cardiomyocytes and isolated mitochondria. The main finding is that the apparent $K_{M\ ADP}$ of isolated mitochondria was about an order of magnitude lower than that of permeabilized cardiomyocytes (compare in Fig. 3, note different scales on the y-axes).

Table 4: ADP-kinetics of respiration in permeabilized cardiomyocytes

Temp.	Creatine	n	V_0	V_{max}	ACR	$K_{M\ ADP}$
10°C	-	7	4.34 ± 0.37	52.63 ± 6.02	12.09 ± 0.67	93 ± 10
	+	7	5.40 ± 0.38 **	49.38 ± 4.70	9.11 ± 0.40 **	88 ± 7
15°C	-	8	5.79 ± 0.74	65.33 ± 5.95	12.64 ± 1.65	77 ± 5
	+	8	7.45 ± 0.55 *	63.99 ± 4.44	8.88 ± 0.78 *	86 ± 7 *
20°C	-	7	5.58 ± 1.13	63.21 ± 10.02	12.34 ± 1.08	91 ± 8
	+	7	6.04 ± 0.86	58.21 ± 9.02	9.56 ± 0.42	89 ± 7

Notation and statistical tests are as in Table 1. * and ** denote $P < 0.05$ and $P < 0.01$, respectively, significantly different in the presence of creatine.

Table 5: ADP-kinetics of respiration in isolated mitochondria

Temp.	n	V_0	V_{max}	ACR	$K_{M\ ADP}$
10°C	6	11.29 ± 2.34	46.73 ± 12.22	4.05 ± 0.28	6.22 ± 0.99
15°C	6	12.33 ± 4.89	83.18 ± 18.28	7.0 ± 0.64	7.10 ± 0.55
20°C	6	16.75 ± 2.82	131.22 ± 17.29	8.03 ± 0.51	8.65 ± 1.46

Notation and statistical tests are as in Table 1. V_{max} and ACR increased with temperature ($P < 0.01$ and $P < 0.001$, respectively).

Discussion

The main aim of this study was to verify that rainbow trout cardiomyocytes have intracellular diffusion restrictions by comparing ADP-kinetics of mitochondrial respiration in permeabilized fibers, permeabilized cardiomyocytes and isolated mitochondria. The outcomes were the following: First, isolated trout cardiomyocytes hypercontracted in solutions designed for mammalian preparations, so we had to develop a new "fish R-solution". Second, the discrepancy between fibers and cardiomyocytes suggest that previous results on trout cardiac fibers were affected by incomplete separation of the cells. Third, despite the low density of intracellular membrane structures in trout cardiomyocytes (Fig. 1), diffusion of ADP from solution to the mitochondria *in situ* is restricted. Fourth, trout cardiomyocytes seem to lack a mitochondrial CK tightly coupled to respiration. The present results on trout cardiomyocytes are very similar to those from other low-performance hearts from for example neonatal rats and rabbits [40,41].

A new intracellular solution for permeabilized trout cardiomyocytes

It was surprising that isolated cardiomyocytes hypercontracted upon permeabilization in the "mammalian R-solution" that seemed to work for fibers. Therefore, we developed a new "fish R-solution". We were able to compare these solutions on permeabilized fibers. They had a better performance in terms of a lower V_0 and higher ACR at high temperatures in the fish R-solution than in the mammalian R-solution (Tables 1 and 3, statistics are given in the Results section). In the fish R-solution, isolated cardiomyocytes maintained their morphology and showed stable steady state respiration rates throughout each experiment (Fig. 2). The addition of cytochrome c at the end of the experiment did not increase respiration rate showing that the outer mitochondrial membrane was kept intact. Atractyloside brought respiration rate down to the basal respiration rate recorded in the absence of ADP showing that the inner mitochondrial membrane was also intact (Fig. 2). Taken together, this validates our use of the fish R-solution for permeabilized trout heart preparations.

Discrepancy between fibers and cardiomyocytes

Kongas et al. suggested that the high apparent $K_{M\ ADP}$ in fibers may be due to incomplete separation of the cells, which leads to larger diffusion distances [42]. Through the window in the oxygraph chamber, we observed that fibers tend to cluster on top of the magnetic stirrer during oxygraphy measurements. This is avoided with permeabilized cardiomyocytes, where all cells are completely separated, and we observed them to be evenly distributed in the oxygraph solution. Incomplete separation of the cells is not a problem in permeabilized fibers from rat heart, which have the same apparent $K_{M\ ADP}$ as permeabilized cardiomyocytes [6,43]. However, studies on trout fibers gave paradoxical results inasmuch as creatine decreased the apparent $K_{M\ ADP}$ [21,23], although there seemed to be no mitochondrial CK tightly coupled to respiration [22].

The present experiments showed that $K_{M\ ADP}$ in trout fibers is higher than in cardiomyocytes. It depends on temperature and is lowered by creatine, but this is not the case for permeabilized cardiomyocytes. This discrepancy suggests that results from trout fibers were affected by incomplete separation of the cells. It is difficult to separate the cells more in trout heart permeabilized fibers, because the tissue is very soft and fragile compared to rat cardiac tissue. We observed that a more thorough dissection led to mechanically damaged fibers with unstable respiration rates and a low ACR.

It has been questioned whether the high apparent $K_{M\ ADP}$ in fibers could be caused by unstirred water layers immediately adjacent to the surface of the fibers or cells [42]. From the same line of thought follows whether fibers have a higher $K_{M\ ADP}$ than cardiomyocytes, because they tend to cluster and thus have thicker unstirred layers than cardiomyocytes. However, two observations from our data strongly suggest that unstirred layers are not the main cause of diffusion restriction. First, the apparent $K_{M\ ADP}$ should increase with temperature, because metabolic rate (Q_{10}~2 [44]) would be more limited by diffusion speed (Q_{10}~1.3 [45]) at higher temperatures. In contrast, we observe a decrease in $K_{M\ ADP}$ with temperature in fibers (Fig. 3A) and no effect of temperature in cardiomyocytes (Fig. 3B). Second, stimulation of cytosolic CK with creatine would also have an effect in isolated cardiomyocytes. In contrast, creatine only lowers $K_{M\ ADP}$ in fibers (Fig. 3A) and not in cardiomyocytes (Fig. 3B). Thus, neither the higher $K_{M\ ADP}$ in cardiomyocytes compared to isolated mitochondria nor the higher $K_{M\ ADP}$ in fibers compared to cardiomyocytes can be explained by unstirred layers.

One possible explanation for the higher and temperature-dependent $K_{M\ ADP}$ in fibers could be that perforated sarcolemma is still left to restrict ADP-diffusion between cells. This may become stiffer at colder temperatures and restrict ADP-diffusion more resulting in a higher $K_{M\ ADP}$. This would also explain why creatine lowers apparent $K_{M\ ADP}$ in fibers but not cardiomyocytes. Diffusion across the barriers formed by the sarcolemma in fibers is facilitated by stimulation of cytosolic CK, whereas this is not the case in permabilized cardiomyocytes. This hypothesis could be confirmed by experiments using raster image correlation spectroscopy (RICS) to study diffusion restriction. We recently used this method to determine the diffusion of fluorescent ATP in adult rat cardiomyocytes. Diffusion was anisotropic, being 2 times slower in the longitudinal direction and 3.5 times slower in the transverse direction compared to solution [46]. However, this method only gave information on the overall diffusion coefficients in cells versus solution. It needs further development before it can be used to distinguish diffusion coefficients in different cellular compartments and localize the additional diffusion barriers in fibers compared to cardiomyocytes. Although the exact cause of the discrepancy between fibers and cardiomyocytes is not completely resolved, we conclude that trout cardiac fibers, which have been used in previous studies [21-23], do not give reliable information about intracellular diffusion restrictions in trout cardiomyocytes.

ADP diffusion restrictions and role of creatine kinase in rainbow trout cardiomyocytes

The apparent $K_{M\ ADP}$ of permeabilized trout cardiomyocytes is independent of temperature and not lowered by creatine. The $K_{M\ ADP}$ is ~80-90 μM, and this is about ten times higher than of isolated mitochondria (Tables 4 and 5 and Fig. 3). Thus, diffusion of ADP from the medium to the ANT in the inner mitochondrial membrane is restricted. The present study does not give any precise information as to the cause and localization of diffusion restrictions. The magnitude of diffusion restriction in terms of $K_{M\ ADP}$ is about three times smaller in trout than in rat cardiomyocytes. Thus, t-tubules and SR may still restrict diffusion in rat cardiomyocytes. From the present experiments, we can only conclude that they are not the only cause of diffusion restriction.

Our results suggest that trout heart lacks a mitochondrial CK, because creatine does not lower the apparent $K_{M\ ADP}$ (Table 4 and Fig. 3). This is in agreement with a previous study [22]. Additionally, the positive charge of mitochondrial CK in rat heart seems to be a prerequisite for binding to the inner mitochondrial membrane [9], but preliminary experiments with isoelectric focusing suggest that trout heart does not express a positively charged CK isoform (R. Birkedal, unpublished observation). Further experiments will be required to determine whether trout heart expresses a mitochondrial CK. However, the expression of mitochondrial CK does not always correlate with functional coupling to respiration [47]. In tissues such as rat ventricle and oxidative skeletal muscle, where mitochondrial CK (Mi-CK) is tightly coupled to respiration [48], diffusion restriction by the outer mitochondrial membrane will enhance this coupling [49]. Indeed, mathematical modeling of data from rat heart suggests a moderate restriction of diffusion by the outer mitochondrial membrane and a stronger restriction of diffusion in the cytosol, probably formed by SR together with crowding of cytoplasmic proteins [50]. However, diffusion restriction by the outer mitochondrial membrane seems unfavorable in tissues that lack a tight coupling of mitochondrial CK to respiration. This is the case for adult rat atrium, which expresses Mi-CK [47,48], neonatal rat and rabbit ventricle, which do not express Mi-CK [40], and according to the present results also trout ventricle. More experiments and development of a mathematical model for trout cardiomyocytes are needed to quantify diffusion restriction by the outer mitochondrial membrane and cytosolic factors, but the present results argue against diffusion restriction by the outer mitochondrial membrane in trout cardiomyocytes.

Rainbow trout as a model animal to study diffusion restrictions in low-performance hearts

The magnitude of diffusion restriction and the importance of CK in cardiomyocytes seem to relate to metabolism and cardiac mechanical performance. Recent studies have addressed diffusion restriction and metabolic regulation in beating and non-beating HL-1 cardiomyocytes in culture derived from AT-1 mouse atrial tumor cells [51]. Both express cardiac isoforms of connexin, desmin and several ion channels [52,53], but their morphology is vastly different. The cells are flattened out against the two-dimensional surface on which they are grown. Mitochondria form a reticular network, which seems to have some relation to the sarcomeres found in beating cells [52,54]. In non-beating cells, sarcomeres are absent [53]. Their metabolic phenotype is glycolytic [55], and the apparent $K_{M\ ADP}$ is low (~50 and 25 μM for beating and non-beating cells, respectively) [54]. Indeed, the characteristics of cultured cardiomyocytes are affected by contractile activity and mechanical load [56], and it seems that for studies of intracellular diffusion restrictions, they cannot yet replace cardiomyocytes that are freshly isolated from working hearts.

Rainbow trout cardiomyocytes seem to have a phenotype that is intermediate between cultured cardiomyocytes and adult mammalian ventricular myocytes. Interestingly, they have these characteristics in common with cardiomyocytes from other low-performance hearts, e.g. neonatal

rats and rabbits. Their apparent $K_{M\ ADP}$ is close to 100 μM and they lack Mi-CK coupled to respiration [40,41]. Compared to adult mammalian cardiomyocytes, they show greater hypoxia tolerance [57] and rely more on glycolytic energy production [40,58], but less so than the cultured cells. In addition, trout and neonatal rabbit cardiomyocytes have similar morphology (compare Fig. 1 with [59,60]) and possibly also excitation-contraction coupling [61,62]. Thus, it seems that cardiomyocytes from low-performance hearts are very similar independent of species. It is likely that knowledge about the role of diffusion restrictions and CK in trout cardiomyocytes can be extrapolated to other low-performance hearts.

Conclusions

A new solution was developed for permeabilized trout cardiomyocytes. The results suggest that previous data from permeabilized trout heart fibers were affected by incomplete separation of the cells. This seems to be specific for trout cardiac fibers. The higher apparent $K_{M\ ADP}$ in fibers could be due to remains of sarcolemma between cells in a fiber bundle. However, even in permeabilized trout cardiomyocytes, which have a very small diameter and low density of intracellular membrane structures, diffusion of ADP from the surrounding medium to the ANT in the inner mitochondrial membrane is restricted. Our results exclude the hypothesis that the main cause of this restriction is unstirred layers. Trout cardiomyocytes do not have a mitochondrial CK coupled to respiration. This argues against diffusion restriction by the outer mitochondrial membrane. Whereas it may be important in rat cardiomyocytes, it is more likely that the diffusion restrictions in trout cardiomyocytes reside in the cytosol. The characteristics of rainbow trout heart are very similar to those of other low-performance hearts such as neonatal rat and rabbit hearts. Most probably, rainbow trout can be used as a model animal to study further the localization and physiological importance of intracellular diffusion restrictions in low-performance hearts in general.

List of abbreviations

ACR: acceptor control ratio (= V_{max}/V_0); ADP: adenosine diphosphate; ANT: adenine nucleotide translocase; ATP: adenosine triphosphate; BSA: bovine serum albumin; ICEU: intracellular energetic unit; $K_{M\ ADP}$: mitochondrial Michaelis Menten constant for ADP; mtCLIC: mitochondrial chloride intracellular channel; SR: sarcoplasmic reticulum; SERCA: sarco-endoplasmic reticulum Ca^{2+}-ATPase; V_0: basal respiration rate before addition of ADP; V_{max}: maximal respiration rate.

Authors' contributions

NS performed all the experimental work. MV participated in design of the study and revision of the manuscript. RB conceived, designed and coordinated the study, and drafted the manuscript. All authors have read and approved the manuscript.

Acknowledgements

We wish to thank Mervi Sepp for writing the software for analysis of oxygraphy data, and Martin Laasmaa for writing the software to deconvolve confocal images.

The research was supported by Welcome Trust Fellowship no. WT081755 MA and the Estonian Science Foundation grant no. ETF8041 (Ph.D. stipend for N. S.).

References

1. Kuznetsov AV, Tiivel T, Sikk P, Kaambre T, Kay L, Daneshrad Z, *et al.*: **Striking differences between the kinetics of regulation of respiration by ADP in slow-twitch and fast-twitch muscles in vivo.** *Eur J Biochem* 1996, **241:**909-915.
2. Scheibye-Knudsen M, Quistorff B: **Regulation of mitochondrial respiration by inorganic phosphate; comparing permeabilized muscle fibers and isolated mitochondria prepared from type-1 and type-2 rat skeletal muscle.** *Eur J Appl Physiol* 2009, **105:**279-287.
3. Kay L, Saks VA, Rossi A: **Early alteration of the control of mitochondrial function in myocardial ischemia.** *J Mol Cell Cardiol* 1997, **29:**3399-3411.
4. Kay L, Rossi A, Saks V: **Detection of early ischemic damage by analysis of mitochondrial function in skinned fibers.** *Mol Cell Biochem* 1997, **174:**79-85.
5. Saks VA, Khuchua ZA, Vasilyeva EV, Belikova OY, Kuznetsov AV: **Metabolic compartmentation and substrate channelling in muscle cells. Role of coupled creatine kinases in in vivo regulation of cellular respiration--a synthesis.** *Mol Cell Biochem* 1994, **133-134:**155-192.
6. Appaix F, Kuznetsov A, Usson Y, Kay L, Andrienko T, Olivares J, *et al.*: **Possible role of cytoskeleton in intracellular arrangement and regulation of mitochondria.** *Experimental Physiology* 2003, **88:**175-190.
7. Saks VA, Veksler VI, Kuznetsov AV, Kay L, Sikk P, Tiivel T, *et al.*: **Permeabilized cell and skinned fiber techniques in studies of mitochondrial function in vivo.** *Mol Cell Biochem* 1998, **184:**81-100.
8. Saks VA, Kuznetsov AV, Khuchua ZA, Vasilyeva EV, Belikova JO, Kesvatera T, *et al.*: **Control of cellular respiration in vivo by mitochondrial outer membrane and by creatine kinase. A new speculative hypothesis: possible involvement of mitochondrial-cytoskeleton interactions.** *J Mol Cell Cardiol* 1995, **27:**625-645.
9. Wallimann T, Wyss M, Brdiczka D, Nicolay K, Eppenberger HM: **Intracellular compartmentation, structure and function of creatine kinase isoenzymes in tissues with high and fluctuating energy demands: the 'phosphocreatine circuit' for cellular energy homeostasis.** *Biochem J* 1992, **281(Pt 1):**21-40.
10. Seppet EK, Kaambre T, Sikk P, Tiivel T, Vija H, Tonkonogi M, *et al.*: **Functional complexes of mitochondria with Ca, MgATPases of myofibrils and sarcoplasmic reticulum in muscle cells.** *Biochim Biophys Acta* 2001, **1504:**379-395.
11. Kaasik A, Veksler V, Boehm E, Novotova M, Minajeva A, Ventura-Clapier R: **Energetic crosstalk between organelles: architectural integration of energy production and utilization.** *Circ Res* 2001, **89:**153-159.
12. Saks VA, Kaambre T, Sikk P, Eimre M, Orlova E, Paju K, *et al.*: **Intracellular energetic units in red muscle cells.** *Biochem J* 2001, **356:**643-657.
13. Saks V, Kuznetsov A, Andrienko T, Usson Y, Appaix F, Guerrero K, *et al.*: **Heterogeneity of ADP Diffusion and Regulation of Respiration in Cardiac Cells.** *Biophys J* 2003, **84:**3436-3456.
14. Vendelin M, Eimre M, Seppet E, Peet N, Andrienko T, Lemba M, *et al.*: **Intracellular diffusion of adenosine phosphates is locally restricted in cardiac muscle.** *Mol Cell Biochem* 2004, **256-257:**229-241.
15. Monge C, Beraud N, Kuznetsov AV, Rostovtseva T, Sackett D, Schlattner U, *et al.*: **Regulation of respiration in brain mitochondria and synaptosomes: restrictions of ADP diffusion in situ, roles**

of tubulin, and mitochondrial creatine kinase. *Mol Cell Biochem* 2008, **318:**147-165.
16. Rostovtseva TK, Sheldon KL, Hassanzadeh E, Monge C, Saks V, Bezrukov SM, *et al.*: **Tubulin binding blocks mitochondrial voltage-dependent anion channel and regulates respiration.** *Proc Natl Acad Sci USA* 2008, **105:**18746-18751.
17. Hove-Madsen L, Tort L: **L-type Ca2+ current and excitation-contraction coupling in single atrial myocytes from rainbow trout.** *Am J Physiol* 1998, **275:**R2061-R2069.
18. Vornanen M: **L-type Ca2+ current in fish cardiac myocytes: effects of thermal acclimation and beta-adrenergic stimulation.** *J Exp Biol* 1998, **201:**533-547.
19. Santer RM: **The organization of the sarcoplasmic reticulum in teleost ventricular myocardial cells.** *Cell Tissue Res* 1974, **151:**395-402.
20. Birkedal R, Shiels HA, Vendelin M: **Three-dimensional mitochondrial arrangement in ventricular myocytes: from chaos to order.** *Am J Physiol Cell Physiol* 2006, **291:**C1148-C1158.
21. Birkedal R, Gesser H: **Regulation of mitochondrial energy production in cardiac cells of rainbow trout (Oncorhynchus mykiss).** *J Comp Physiol [B]* 2004, **174:**255-262.
22. Birkedal R, Gesser H: **Intracellular compartmentation of cardiac fibres from rainbow trout and Atlantic cod--a general design of heart cells.** *Biochim Biophys Acta* 2006, **1757:**764-772.
23. Birkedal R, Gesser H: **Creatine kinase and mitochondrial respiration in hearts of trout, cod and freshwater turtle.** *J Comp Physiol [B]* 2003, **173:**493-499.
24. Toleikis A, Majiene D, Trumbeckaite S, Dagys A, Jasaitis A: **The effect of collagenase and temperature on mitochondrial respiratory parameters in saponin-skinned cardiac fibers.** *Biosci Rep* 1996, **16:**513-519.
25. Bouzidi MF, Enjolras N, Carrier H, Vial C, Lopez-Mediavilla C, Burt-Pichat B, *et al.*: **Variations of muscle mitochondrial creatine kinase activity in mitochondrial diseases.** *Biochim Biophys Acta* 1996, **1316:**61-70.
26. Veksler VI, Kuznetsov AV, Sharov VG, Kapelko VI, Saks VA: **Mitochondrial respiratory parameters in cardiac tissue: a novel method of assessment by using saponin-skinned fibers.** *Biochim Biophys Acta* 1987, **892:**191-196.
27. Cannell MB, McMorland A, Soeller C: **Image Enhancement by Deconvolution.** In *Handbook of Biological Confocal Microscopy* Edited by: Pawley JB. New York: Springer; 2006:488-500.
28. Segretain D, Rambourg A, Clermont Y: **Three dimensional arrangement of mitochondria and endoplasmic reticulum in the heart muscle fiber of the rat.** *Anat Rec* 1981, **200:**139-151.
29. **MiPNet Protocols 2.3.C - Selected Media and Chemicals for Respirometry with Mitochondria and Permeabilized Cells** [http://www.oroboros.at/fileadmin/user_upload/OROBOROS_Handbook/2.3.C-Chemicals-Media.pdf]
30. **MiPNet Protocols 2.3.A - Mitochondrial Respiration Medium - MiR05** [http://www.oroboros.at/fileadmin/user_upload/OROBOROS_Handbook/2.3.A-Medium-MiR06.pdf]
31. Gow IF, Ellis D: **Effect of lithium on the intracellular potassium concentration in sheep heart Purkinje fibres.** *Exp Physiol* 1990, **75:**427-430.
32. Walker JL, Ladle RO: **Frog heart intracellular potassium activities measured with potassium microelectrodes.** *Am J Physiol* 1973, **225:**263-267.
33. Dick DA, McLaughlin SG: **The activities and concentrations of sodium and potassium in toad oocytes.** *J Physiol* 1969, **205:**61-78.
34. Arnould T, Mercy L, Houbion A, Vankoningsloo S, Renard P, Pascal T, *et al.*: **mtCLIC is up-regulated and maintains a mitochondrial membrane potential in mtDNA-depleted L929 cells.** *FASEB J* 2003, **17:**2145-2147.
35. Piwnica-Worms D, Jacob R, Horres CR, Lieberman M: **Transmembrane chloride flux in tissue-cultured chick heart cells.** *J Gen Physiol* 1983, **81:**731-748.
36. Ladle RO, Walker JL: **Intracellular chloride activity in frog heart.** *J Physiol* 1975, **251:**549-559.
37. Kuznetsov AV, Khuchua ZA, Vassil'eva EV, Medved'eva NV, Saks VA: **Heart mitochondrial creatine kinase revisited: the outer mitochondrial membrane is not important for coupling of phosphocreatine production to oxidative phosphorylation.** *Arch Biochem Biophys* 1989, **268:**176-190.
38. Buechter DD, Medzihradszky KF, Burlingame AL, Kenyon GL: **The active site of creatine kinase. Affinity labeling of cysteine 282 with N-(2,3-epoxypropyl)-N-amidinoglycine.** *J Biol Chem* 1992, **267:**2173-2178.
39. Guderley H, St Pierre J: **Seasonal cycles of mitochondrial ADP sensitivity and oxidative capacities in trout oxidative muscle.** *J Comp Physiol [B]* 1999, **169:**474-480.
40. Hoerter JA, Ventura-Clapier R, Kuznetsov A: **Compartmentation of creatine kinases during perinatal development of mammalian heart.** *Mol Cell Biochem* 1994, **133-134:**277-286.
41. Tiivel T, Kadaya L, Kuznetsov A, Kaambre T, Peet N, Sikk P, *et al.*: **Developmental changes in regulation of mitochondrial respiration by ADP and creatine in rat heart in vivo.** *Mol Cell Biochem* 2000, **208:**119-128.
42. Kongas O, Yuen TL, Wagner MJ, van Beek JH, Krab K: **High K(m) of oxidative phosphorylation for ADP in skinned muscle fibers: where does it stem from?** *Am J Physiol Cell Physiol* 2002, **283:**C743-C751.
43. Seppet EK, Eimre M, Andrienko T, Kaambre T, Sikk P, Kuznetsov AV, *et al.*: **Studies of mitochondrial respiration in muscle cells in situ: use and misuse of experimental evidence in mathematical modelling.** *Mol Cell Biochem* 2004, **256-257:**219-227.
44. Hill RW, Wyse GA: *Animal Physiology* 2nd edition. New York: Harper-CollinsPublishers Inc; 1989.
45. Hubley MJ, Locke BR, Moerland TS: **Reaction-diffusion analysis of the effects of temperature on high- energy phosphate dynamics in goldfish skeletal muscle.** *J Exp Biol* 1997, **200(Pt 6):**975-988.
46. Vendelin M, Birkedal R: **Anisotropic diffusion of fluorescently labeled ATP in rat cardiomyocytes determined by raster image correlation spectroscopy.** *Am J Physiol Cell Physiol* 2008, **295:**C1302-C1315.
47. Anflous K, Veksler V, Mateo P, Samson F, Saks V, Ventura-Clapier R: **Mitochondrial creatine kinase isoform expression does not correlate with its mode of action.** *Biochem J* 1997, **322(Pt 1):**73-78.
48. Ventura-Clapier R, Kuznetsov A, Veksler V, Boehm E, Anflous K: **Functional coupling of creatine kinases in muscles: species and tissue specificity.** *Mol Cell Biochem* 1998, **184:**231-247.
49. Vendelin M, Lemba M, Saks VA: **Analysis of functional coupling: mitochondrial creatine kinase and adenine nucleotide translocase.** *Biophys J* 2004, **87:**696-713.
50. Ramay HR, Vendelin M: **Diffusion restrictions surrounding mitochondria: A mathematical model of heart muscle fibers.** *Biophys J* 2009, **97:**443-52.
51. Claycomb WC, Lanson NA Jr, Stallworth BS, Egeland DB, Delcarpio JB, Bahinski A, *et al.*: **HL-1 cells: a cardiac muscle cell line that contracts and retains phenotypic characteristics of the adult cardiomyocyte.** *Proc Natl Acad Sci USA* 1998, **95:**2979-2984.
52. White SM, Constantin PE, Claycomb WC: **Cardiac physiology at the cellular level: use of cultured HL-1 cardiomyocytes for studies of cardiac muscle cell structure and function.** *Am J Physiol Heart Circ Physiol* 2004, **286:**H823-H829.
53. Pelloux S, Robillard J, Ferrera R, Bilbaut A, Ojeda C, Saks V, *et al.*: **Non-beating HL-1 cells for confocal microscopy: application to mitochondrial functions during cardiac preconditioning.** *Prog Biophys Mol Biol* 2006, **90:**270-298.
54. Anmann T, Guzun R, Beraud N, Pelloux S, Kuznetsov AV, Kogerman L, *et al.*: **Different kinetics of the regulation of respiration in permeabilized cardiomyocytes and in HL-1 cardiac cells. Importance of cell structure/organization for respiration regulation.** *Biochim Biophys Acta* 2006, **1757:**1597-1606.
55. Eimre M, Paju K, Pelloux S, Beraud N, Roosimaa M, Kadaja L, *et al.*: **Distinct organization of energy metabolism in HL-1 cardiac cell line and cardiomyocytes.** *Biochim Biophys Acta* 2008, **1777:**514-524.
56. Mitcheson JS, Hancox JC, Levi AJ: **Cultured adult cardiac myocytes: future applications, culture methods, morphological and electrophysiological properties.** *Cardiovasc Res* 1998, **39:**280-300.
57. Singer D: **Neonatal tolerance to hypoxia: a comparative-physiological approach.** *Comp Biochem Physiol A Mol Integr Physiol* 1999, **123:**221-234.
58. Christensen M, Hartmund T, Gesser H: **Creatine kinase, energy-rich phosphates and energy metabolism in heart muscle of different vertebrates.** *J Comp Physiol [B]* 1994, **164:**118-123.

59. Sedarat F, Xu L, Moore ED, Tibbits GF: **Colocalization of dihydropyridine and ryanodine receptors in neonate rabbit heart using confocal microscopy.** *Am J Physiol Heart Circ Physiol* 2000, **279:**H202-H209.
60. Dan P, Lin E, Huang J, Biln P, Tibbits GF: **Three-dimensional distribution of cardiac Na+-Ca2+ exchanger and ryanodine receptor during development.** *Biophys J* 2007, **93:**2504-2518.
61. Birkedal R, Shiels HA: **High [Na+]i in cardiomyocytes from rainbow trout.** *Am J Physiol Regul Integr Comp Physiol* 2007, **293:**R861-R866.
62. Huang J, Hove-Madsen L, Tibbits GF: **Ontogeny of Ca2+-induced Ca2+ release in rabbit ventricular myocytes.** *Am J Physiol Cell Physiol* 2008, **294:**C516-C525.

PUBLICATION II

Karro N, Sepp M, Jugai S, Laasmaa M, Vendelin M, Birkedal R

Metabolic compartmentation and regulation in rainbow trout cardiomyocytes.

Submitted, (2015)

The rules of the publisher prevent publication of the manuscript of Publication II prior to acceptance. Official committee members and opponents will be given a copy of the manuscript to enable them to carry out a judicious review of this dissertation.

PUBLICATION III

Branovets J, Sepp M, Kotlyarova S, Jepihhina N, Sokolova N, Aksentijevic D, Lygate CA, Neubauer S, Vendelin M, Birkedal R

Unchanged mitochondrial organization and compartmentation of high-energy phosphates in creatine-deficient GAMT-/- mouse hearts.

The American Journal of Physiology: Heart and Circulatory Physiology, 305(4): H506-H520, August 2013

Am J Physiol Heart Circ Physiol 305: H506–H520, 2013.
First published June 21, 2013; doi:10.1152/ajpheart.00919.2012.

Unchanged mitochondrial organization and compartmentation of high-energy phosphates in creatine-deficient GAMT$^{-/-}$ mouse hearts

Jelena Branovets,[1] Mervi Sepp,[1] Svetlana Kotlyarova,[1] Natalja Jepihhina,[1] Niina Sokolova,[1] Dunja Aksentijevic,[2] Craig A. Lygate,[2] Stefan Neubauer,[2] Marko Vendelin,[1] and Rikke Birkedal[1]

[1]*Laboratory of Systems Biology, Institute of Cybernetics, Tallinn University of Technology, Tallinn, Estonia; and* [2]*Department of Cardiovascular Medicine, Wellcome Trust Centre for Human Genetics, University of Oxford, Oxford, United Kingdom*

Submitted 12 December 2012; accepted in final form 6 June 2013

Branovets J, Sepp M, Kotlyarova S, Jepihhina N, Sokolova N, Aksentijevic D, Lygate CA, Neubauer S, Vendelin M, Birkedal R. Unchanged mitochondrial organization and compartmentation of high-energy phosphates in creatine-deficient GAMT$^{-/-}$ mouse hearts. *Am J Physiol Heart Circ Physiol* 305: H506–H520, 2013. First published June 21, 2013; doi:10.1152/ajpheart.00919.2012.—Disruption of the creatine kinase (CK) system in hearts of CK-deficient mice leads to changes in the ultrastructure and regulation of mitochondrial respiration. We expected to see similar changes in creatine-deficient mice, which lack the enzyme guanidinoacetate methyltransferase (GAMT) to produce creatine. The aim of this study was to characterize the changes in cardiomyocyte mitochondrial organization, regulation of respiration, and intracellular compartmentation associated with GAMT deficiency. Three-dimensional mitochondrial organization was assessed by confocal microscopy. On populations of permeabilized cardiomyocytes, we recorded ADP and ATP kinetics of respiration, competition between mitochondria and pyruvate kinase for ADP produced by ATPases, ADP kinetics of endogenous pyruvate kinase, and ATP kinetics of ATPases. These data were analyzed by mathematical models to estimate intracellular compartmentation. Quantitative analysis of morphological and kinetic data as well as derived model fits showed no difference between GAMT-deficient and wild-type mice. We conclude that inactivation of the CK system by GAMT deficiency does not alter mitochondrial organization and intracellular compartmentation in relaxed cardiomyocytes. Thus, our results suggest that the healthy heart is able to preserve cardiac function at a basal level in the absence of CK-facilitated energy transfer without compromising intracellular organization and the regulation of mitochondrial energy homeostasis. This raises questions on the importance of the CK system as a spatial energy buffer in unstressed cardiomyocytes.

creatine kinase shuttle; mitochondrial positioning; confocal imaging; intracellular diffusion barriers; respiration and ATPase kinetics; guanidinoacetate methyltransferase

CREATINE KINASE (CK) plays an important role as an energy buffer in several cell types, including heart, skeletal muscle, and brain. It catalyzes the phosphotransfer between creatine (Cr) and ATP. The importance of CK is highlighted by its strong regulation of local ATP concentration as shown by studies of sarcolemmal ATP-sensitive K^+ channels (1) and rigor formation in permeabilized fibers (55, 57). After induction of ischemia, contraction correlates with the phosphocreatine (PCr) level (14), and, after heart failure, the PCr-to-ATP ratio in the heart is a strong predictor of patient mortality (20). Additionally, a recent study (15) has shown that overexpression of cytosolic CK improves cardiac contractile function and viability after induced heart failure.

Cr deficiency inhibits the CK system. It may occur due to deficiency of the enzymes that synthesize Cr [L-arginine:glycine amidinotransferase (AGAT) and guanidinoacetate methyltransferase (GAMT)] or the Cr transporter (CrT or SLC6A8), which imports Cr across the sarcolemma. All three cases of Cr deficiency have been found in humans (8, 43), and all have been reproduced in mouse models (AGAT$^{-/-}$, GAMT$^{-/-}$, and CrT$^{-/-}$ mice). The GAMT$^{-/-}$ model is the most studied to date.

Considering the presumed importance of CK in the heart, it is remarkable that the baseline cardiac function of GAMT$^{-/-}$ mice is so little affected by the lack of a functional CK system. For example, ejection fraction is normal and only LV systolic pressure is slightly lower in GAMT$^{-/-}$ mice (19, 42). Furthermore, when the maximal exercise capacity and response to chronic myocardial infarction was compared in GAMT$^{-/-}$ and wild-type (WT) mice, no significant difference was observed (30). It is only under acute stress conditions that functional deficits are observed in both GAMT$^{-/-}$ and CK$^{-/-}$ hearts, e.g., reduced inotropic reserve and impaired recovery from ischemia-reperfusion injury (10, 19, 47). The near-normal basal cardiac performance in GAMT$^{-/-}$ mice could be due to extensive compensatory changes not identified in Ref. 30, similar to those described in the hearts of CK$^{-/-}$ mice, where the CK system is disabled by the lack of both cytosolic and mitochondrial muscle-specific CK isoforms. CK$^{-/-}$ hearts show only minor changes in performance (35), explained in part by cytoarchitectural changes that facilitate direct cross-talk between mitochondria and ATPases (23). Direct cross-talk between organelles is possible due to intracellular diffusion restrictions (60), as evidenced by a low apparent ADP affinity of mitochondrial respiration in permeabilized cardiomyocytes (27), which leads to the coupling of endogenous ATPases to mitochondria or glycolysis (44, 45) as well as anisotropy in diffusion (21, 51). In CK$^{-/-}$ mice, in the absence of Cr, the apparent ADP affinity of mitochondrial respiration was higher than in control experiments with WT mice (23). This suggests a reduction of the overall diffusion restriction between mitochondria and the surrounding solution (36). However, diffusion was sufficiently restricted for sarco(endo)plasmic reticulum Ca^{2+}-ATPase (SERCA) and myosin ATPase to preferentially use ATP generated in mitochondria as efficiently as in WT mice (23).

The aim of this study was to determine whether the hearts of GAMT$^{-/-}$ mice exhibit similar compensatory changes as those observed in the hearts of CK$^{-/-}$ mice. We used three approaches that we have previously applied to rat cardiomyo-

Address for reprint requests and other correspondence: M. Vendelin, Laboratory of Systems Biology, Institute of Cybernetics, Tallinn Univ. of Technology, Akadeemia 21, Tallinn 12618, Estonia (e-mail: markov@ioc.ee).

  ISSN 0363-6135.

cytes. Using confocal microscopy, we quantified the three-dimensional (3-D) relative position of mitochondrial centers (as in Ref. 4). This allowed us to detect whether mitochondrial positioning is different in GAMT$^{-/-}$ mice. On permeabilized cardiomyocytes, we recorded a full set of kinetic data to analyze the intracellular compartmentation of ADP/ATP using mathematical models. In rat cardiomyocytes, we discovered a strong functional coupling between pyruvate kinase (PK) and a fraction of ATPases (45). Because the activity of other phosphotransfer systems increases in CK$^{-/-}$ mice (34) and because failing hearts experiencing a loss of CK (2), we speculated whether the coupling between PK and ATPases is upregulated in GAMT$^{-/-}$ mice. Finally, we used fluorescence microscopy to record changes in NADH and flavoprotein (Fp) autofluorescence when permeabilized cardiomyocytes were exposed to increasing doses of ADP (as in Ref. 22). This would test whether the ADP kinetics of respiration, as recorded on a population level, also occurred on the single cell level.

MATERIALS AND METHODS

Animal procedures were approved by the Estonian National Committee for Ethics in Animal Experimentation (Estonian Ministry of Agriculture).

Animals. We received GAMT$^{-/-}$ mice and WT littermates, which had been bred at The Wellcome Trust Centre for Human Genetics (Oxford, UK). Mice had been backcrossed on to a C57Bl/6J background for at least eight generations. Animals were kept in our local animal facility in cages with free access to water and food (vegetable-based, Cr-free chow, R70 from Lactamin). Mice of different genotypes were housed separately to prevent GAMT$^{-/-}$ mice from taking up Cr via coprophagia of feces from WT littermates (41).

Cardiomyocytes were successfully isolated from eight GAMT$^{-/-}$ mice (4 females and 4 males) and nine WT mice (5 females and 4 males) of similar age (female WT: 46.9 ± 4.9 wk and female GAMT$^{-/-}$: 45 ± 4.3 wk; male WT: 45.6 ± 1.5 wk and male GAMT$^{-/-}$: 45.9 ± 1.4 wk).

Genotyping. Knockout and WT mice were genotyped by PCR. Briefly, genomic DNA was extracted from tissue samples by SDS/proteinase K digestion followed by isopropanol precipitation. PCR amplification of the DNA fragments was performed using the following specific primers: 5′-CAGGCTCCCACCCACTTGA-3′, 5′-AGGCCTACCCGCTTCCATTG-3′, 5′-CCTCAGGCTCCCACCCACTTG-3′, and 5′-GGTCTCCCAACGCTCCATCACT-3′. PCRs were carried out in a 25-μl volume containing 1× PCR buffer (Bioline Immobuffer), 0.5 mM dNTP mixture (Fermentas), 2 mM $MgCl_2$ (Bioline), 0.5–0.7 pmol of each primer (TAG Copenhagen), 5% DMSO (Sigma), 0.6 M betaine (Sigma), 0.06 U/μl IMMOLASE DNA polymerase (Bioline), and 5 μl template DNA. After the initial denaturation step at 94°C for 5 min, nine cycles of PCR were carried out as follows: denaturation at 94°C for 60 s, annealing at 60°C for 60 s, and extension at 72°C for 30 s. In each cycle, the temperature was decreased by 0.5°C in each consequent annealing step. This was followed by 34 cycles of the following PCR: denaturation at 94°C for 60 s, annealing at 55°C for 60 s, and extension at 72°C for 30 s. This was done in a thermal cycler (Bio-Rad DNA Engine Peltier Thermal Cycler). PCR products were electrophoresed on a 1% agarose gel with ethidium bromide in 1× Tris-borate-EDTA. Amplification of a single 265-bp product or a 427-bp PCR product corresponded to WT GAMT (GAMT$^{+/+}$) or homozygous GAMT knockout (GAMT$^{-/-}$) genotype, respectively. Simultaneous amplification of a 265- and 427-bp fragments corresponded to a heterozygous GAMT (GAMT$^{+/-}$) genotype.

Total Cr content. The total Cr content was measured enzymatically from mouse hindlimb skeletal muscle. The metabolite extraction from tissue samples was done as follows. A 50- to 100-mg piece of tissue was homogenized in 2 ml of 0.6 M perchloric acid with 2 mM EDTA. Water was added to provide a total volume of 10 ml, and the suspension was centrifuged at 10,000 *g* for 10 min at 4°C. The supernatant was neutralized with KOH, the precipitated salt was removed by centrifugation, and total Cr levels were assayed immediately from the resulting extract (pH 7.0–7.2) via coupled enzymatic reactions using a spectrofluorophotometer. The enzymatic reaction was performed in 500 μl of 100 mmol/l potassium phosphate buffer (pH 7.5) containing 5 mmol/l $MgCl_2$, 16 kU/l CK, 8 mmol/l ADP, 16 kU/l hexokinase, 4 mM glucose, 40 kU/l creatinase, 20 kU/l sarcosine oxidase, 4 kU/l horseradish peroxidase, 10 μmol/l Amplex red, and 6–40 μl tissue extract. This mixture ensured that Cr and PCr were degraded by creatinase, which led to the production of H_2O_2 (which was later determined fluorescently using Amplex red conversion to resorufin). The blank mixture was identical except for the omission of creatinase. The reaction mixture was incubated for 30 min at room temperature. H_2O_2 was determined spectrofluorometrically in 2 ml of 100 mmol/l phosphate buffer containing 5 mmol/l $MgCl_2$. Fluorescence measurements were performed using 4-ml plastic cuvettes (four-faced transparent cuvettes, Deltalab, Rubí, Spain) in an RF-5301 PC spectrofluorometer (Shimadzu Scientific Instruments, Kyoto, Japan). The temperature was maintained at 25°C (Julabo F12-ED, JULABO Labortechnik). First, background fluorescence of the buffer without enzymes was measured, and 1 μl of 5 mM Amplex red and 5 μl of 100 U/ml horseradish peroxidase were then added to measure the contribution of Amplex red to fluorescence intensity. Finally, the fluorescence of the diluted reaction mixture was measured. At the end of each experiment, a calibration signal was generated with five additions of 1 μl of 0.1 mM H_2O_2, each leading to a concentration increase of 50 nM. Measured fluorescence intensities (emission/excitation = 585/570 nm) were fitted assuming a linear relationship between fluorescence and the resorufin concentration in the cuvette, with the offset determined by the background fluorescence of the buffer. The fit was performed by minimizing the least-square difference between calculated and measured fluorescence through variation of the gain (fluorescence-to-resorufin concentration ratio), total Cr content, and resorufin contamination of Amplex red solution (proportional to the Amplex red concentration). Cr concentrations were expressed as nanomoles per milligram wet weight tissue. All measurements were repeated with three different dilutions, and a paired *t*-test between recordings with and without creatinase (sample vs. blank) was used to determine whether the total Cr content was identifiable by the method (a significance level of $P < 0.05$ was used).

Isolation of cardiomyocytes. Isolation of cardiomyocytes was carried out as previously described (45). Briefly, the heart was excised and immediately transferred to ice-cold wash solution (see composition below). It was cannulated via the aorta on a Langendorff perfusion system, which was thermostatted to 38.5°C (Julabo ED, JULABO Labortechnik). The heart was first perfused with wash solution at a constant pressure of 80 cmH_2O for at least 5 min. The flow rate under these conditions was 3.68 ± 1.68 ml/min (n = 17). After the heart was washed free of blood, the perfusion was switched to a digestion solution containing an additional 0.25 mg/ml collagenase P (Roche) and 3 mg/ml BSA. Perfusion was also switched to a constant flow of 1 ml/min until the pressure had decreased to 10–15% of the initial pressure at 80 cmH_2O and the heart was soft. After perfusion, the ventricles were isolated. They were cut into four pieces, which were incubated further in the digestion solution at 38.5°C with gentle shaking until the tissue started falling apart. Cells were further dissociated with a 5-ml pipette. Sedimentation solution (5 ml) was added before the cells were filtered into a glass tube. As a result, the cell suspension was a mix of isolated cardiomyocytes from the left and right ventricles. Cells were washed by sedimentation. First, extracellular Ca^{2+} was gradually increased to 1 mM to ensure Ca^{2+} tolerance of the cells (Ca^{2+} from a stock of 1 M $CaCl_2$ was added to the sedimentation solution). After this, extracellular Ca^{2+} was washed out again by washing the cells three times with 10 ml sedimentation solution.

Mitochondrial imaging. Freshly isolated cells kept in sedimentation solution were loaded with 1 μM TMRE (T-669, Molecular Probes, Life Technologies) for at least 15 min. A small fraction of the cells was added to 200 μl sedimentation solution in the chamber of a flexiPERM micro 12 reusable silicone cell culture chamber (Greiner Bio-One) attached to a coverslip. Confocal images were acquired on a Zeiss LSM 510 Duo built around an inverted Axio Observer Z1 microscope (Carl Zeiss) with a ×63/1.2 numerical aperture (NA) water-immersion objective. The signal was acquired via a high-voltage single photomultiplier tube using 8-bit mode; the pinhole was set to one Airy disk. TMRE was excited with a 543-nm laser, and emission was recorded through a 575-nm long-pass filter. These experiments were carried out at room temperature.

Estimating the relative positioning of mitochondrial centers. Mitochondrial positioning was quantified by statistical analysis of the relative distances between neighboring mitochondrial centers, as in Ref. 4. In short, the following procedure was used. Each stack of confocal images was blurred by a 3-D Gaussian blur with a SD of 0.3 μm in all directions. The position of all mitochondrial centers was determined by finding local fluorescence maxima of the blurred 3-D stack of images. Subsarcolemmal mitochondria and mitochondria around the nucleus (perinuclear mitochondria) were filtered out as judged by the eye. A space around each mitochondrial center was divided into 14 sectors: 2 sectors in the *y*-direction along the myofibril, 2 sectors in the *x*-direction across the myofibril in the image plane, 2 sectors in the *z*-direction across the myofibril perpendicular to the image plane, 4 diagonal sectors in the *xy*-direction, and 4 diagonal sectors in the *yz*-direction (Fig. 1). For each mitochondrial center, we found the closest neighboring mitochondrial center in each of these sectors, as shown in Fig. 1. Finally, the relative position of these neighboring mitochondrial centers was analyzed by finding the probability density function and cumulative probability distribution, as in Ref. 4.

For statistical analysis, we found for each cell separately the cumulative distribution function for the nearest neighboring mitochondria in each direction. The averaged results of the distance at 25%, 50%, and 75% of the distribution function for R and R_{XZ} (notation from Fig. 5) were compared for WT and GAMT$^{-/-}$ cardiomyocytes, as detailed in the RESULTS.

Respirometer recordings. Respirometer recordings were used to determine *1*) the respiration kinetics of permeabilized cells stimulated by stepwise increases in ADP or ATP and *2*) the inhibition of ATP-stimulated respiration by a competitive assay consisting of phosphoenol pyruvate (PEP; 5 mM) and PK (20 IU/ml). For this, we used a Strathkelvin RC 650 respirometer equipped with six 1302 O_2 electrodes connected via a 929 Oxygen System interface (all from Strathkelvin Instruments) to a computer. The respirometer was thermostatted to 25°C (Julabo F12-ED, JULABO Labortechnik). The O_2 tension in each chamber was recorded by the software provided by Strathkelvin and our homemade software, which immediately calculated the rate of O_2 consumption as well. The latter is open-source software and is freely available at http://code.google.com/p/iocbio/wiki/IOCBioStrathKelvin.

For recordings of ADP kinetics, a 15- to 20-μl cell suspension was added to the respiration chamber containing 2 ml Cr and PCr-free respiration solution (see composition below). Cells were allowed at least 5 min to permeabilize before the steady-state basal respiration rate (V_0) was recorded. ADP was added to the respirometer chamber using a Hamilton syringe (801RN, Hamilton Bonaduz). The ADP concentration was increased in steps, and the respiration rate was allowed to reach steady state for at least 2 min before the addition of more ADP. Recordings of ATP kinetics were carried out in a similar way except that a 30- to 50-μl cell suspension was added to the chamber and ATP was added instead of ADP. To record how a competitive ADP-trapping assay consisting of PEP and PK competes with mitochondria for the consumption of ADP from ATPases, a 30- to 60-μl cell suspension was added to the respirometer chamber. After recording V_0, 2 mM ATP was added to stimulate ATPases. Initially, this endogenously produced ADP was exclusively consumed by the mitochondria and stimulated respiration ($V_{2\ mM\ ATP}$). The addition of 5 mM PEP (no. P-7002, Sigma-Aldrich) activated endogenous PK to compete with mitochondria for the consumption of ADP and the lowered respiration rate (V_{PEP}). Further addition of 20 U/ml exogenous PK (no.

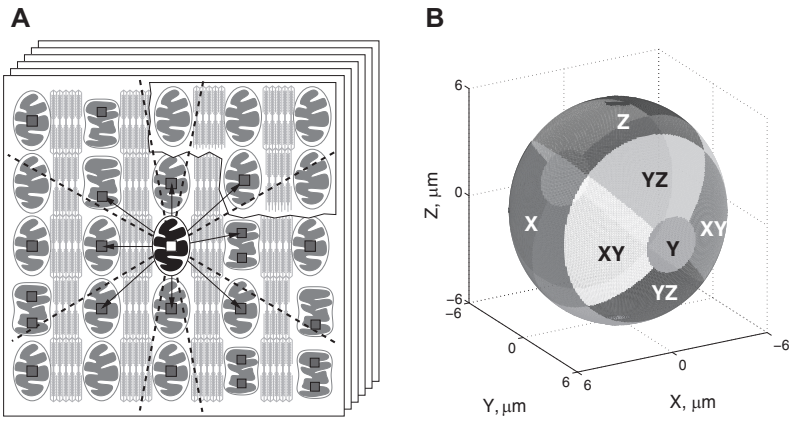

Fig. 1. Method used to analyze distribution of mitochondria in cardiomyocytes, taken from Ref. 4. *A*: first, a series of *Z*-stack confocal images of mitochondria in nonpermeabilized cardiomyocytes was acquired (scheme). Second, the local fluorescence maxima (small squares) were found. As indicated in the scheme, the maxima were not always on the same image in the stack. Note that sometimes two fluorescence maxima seem to be found per mitochondrion (as shown in *A*). Next, the closest neighbors were found for each mitochondrion, one per sector (the projections of the sector borders in two dimensions are shown by the dashed lines). In this scheme, the mitochondrion, in which neighbors are sought, is highlighted, and the closest neighbors to this mitochondrion are indicated by arrows. Note that the closest mitochondria in some sectors are not always from the same image in the stack. The relative coordinates of the closest neighbors, i.e., the coordinates relative to the highlighted mitochondria, were stored and further analyzed. *B*: division of three-dimensional space into the sectors, with sectors shown by the different levels of gray. The mitochondrion for which neighbors are sought is positioned at the origin of coordinate system. Here, the coordinate *y*-axis corresponds to the fiber orientation. The sector names are shown in the scheme.

10109045001, Roche), lowered the respiration rate ($V_{PEP + PK}$) even more.

Spectrophotometer recordings. ATP kinetics of ATPases and ADP kinetics of endogenous PK were recorded using an Evolution 600 spectrophotometer (Thermo Fisher Scientific) equipped with a Peltier water-cooled cell changer (SPE 8 W, Thermo Fisher Scientific) to maintain temperature at 25°C. ADP production by ATPases in permeabilized cardiomyocytes was recorded in 2 ml respiration solution using a coupled assay consisting of 5 mM PEP (no. P-7002, Sigma-Aldrich), 0.3 mM NADH (no. 10128015001, Roche), 7.2 U/ml LDH (no. 61311, Sigma-Aldrich), and 20 U/ml PK (no. 10109045001, Roche). To avoid ADP consumption by mitochondria, respiration was inhibited by 5 mM NaCN (no. 205222, Sigma-Aldrich) and 10 μM oligomycin (no. 75351, Sigma-Aldrich). The basal ATPase rate was first recorded in the absence of ATP and then at increasing concentrations of ATP. Rates were recorded for 3 min after each addition, and steady state was verified for each step. NADH was replenished as needed to keep absorbance between 1.7 and 0.7 (the linear range of NADH consumption as verified by preliminary experiments; data not shown). The ADP kinetics of endogenous PK were recorded using the same coupled assay (where only 5 mM NaCN, 10 μM oligomycin, 5 mM PEP, 0.3 mM NADH, and 7.2 U/ml LDH were added), and PK activity was recorded at increasing ADP concentrations.

For normalization, the protein content was measured with a Nanodrop 2000 (Thermo Fisher Scientific).

Mathematical model. For a detailed description of the model, see Ref. 45. In brief, models of different complexity were considered (Fig. 2). All models included three separate compartments: extracellular solution, cytoplasm, and intermembrane space (IMS). *Models 3* and *4* also included a fourth compartment (*compartment 4*) with PK and ATPase to describe coupling between glycolysis and ATPases, as described in Ref. 45. The processes considered in the models were diffusion between compartments restricted by diffusion barriers, the reactions of ATPases, oxidative phosphorylation, and the reactions of endogenous PK. The models containing two groups of ATPases (2, 3, and 4) were also considered in a simplified form (2s, 3s, and 4s) with both groups of ATPases having the same affinities for ATP and ADP.

For simplicity, ATP synthesis in mitochondria was described by the simple phenomenological Michaelis-Menten-type equation involving the concentrations of ATP and ADP only in the IMS, as shown in Fig. 2. Note that this approach is possible due to high concentrations of P_i, oxygen, and substrates, as used in our experiments. This simplification allowed us to simulate diffusion and reactions in the intracellular compartments only (cytoplasm, IMS, and *compartment 4*) and thus allowed us to ignore the details of the reactions involved in the respiratory chain. The same approach has been applied by us earlier and used to estimate the compartmentation of ATPases and intracellular diffusion restrictions in two dimensions (52), three dimensions (36), and simplified multicompartment (45) analysis of the intracellular environment.

To compare the models, the goodness of fit was evaluated using Akaike information criteria (AIC), corrected AIC (AIC_c), and Bayesian information criteria (BIC), which were calculated for each model. For all three criteria, the best-fitting model is the one with the minimum criterion value. Those criteria take into account the goodness of fit and number of parameters in the model. Using AIC_c and BIC, a larger number of parameters is penalized more than in AIC. Multiple goodness criteria were used to ensure that the conclusions would not depend on the selection of one particular criterion.

In addition, models were compared by an *F*-test for nested models, which allows comparison of *models 1* and *2* with *model 3* as well as *models 1* and *2* with *model 4*. The *F*-test takes the number of parameters into account so that statistical significance indicates that the more complicated model fits the data better irrespective of the number of parameters.

Next, the *F*-test was used to evaluate confidence intervals for each of the fitted model parameters. Confidence intervals were calculated using an *F*-test and show the range where the fit is worse than an optimal fit but with a *P* value larger than 0.05 (in terms of extra sum of squares), as in Ref. 45.

Finally, to test whether the data recorded in WT and GAMT$^{-/-}$ cardiomyocytes were significantly different from each other, the data were fit either separately for different types of cardiomyocytes or by fitting both sets with the same model parameters (pooled data set). The *F*-test was applied to test whether an increased number of parameters induced by fitting the experiments separately was justified or whether the better fits were due to chance. For this test, a fit of pooled data by a single set of model parameters can be considered as a simplified version of fitting the data separately using two sets of model parameters: one for WT cardiomyocytes and one for GAMT$^{-/-}$ cardiomyocytes.

For a detailed model description, numeric methods, and statistical analysis, see Ref. 45.

Recordings of NADH and Fp autofluorescence. Recordings of NADH and Fp autofluoresence were performed as described in Ref. 22. In brief, microscope experiments were performed on an inverted Nikon Eclipse Ti-U microscope (Nikon, Tokyo, Japan; objective CFI Super Plan Fluor ELWD ×20/0.45 NA) equipped with two tiers of motorized filter turrets for simultaneous acquisition of transmission and fluorescence images. For images of NADH and Fp autofluorescence, respectively, light from a Prior Lumen 200 with a 200-W metal halide lamp with extended wavelength (Prior Scientific, Cambridge, UK) was passed via an optical fiber into the upper filter turret. For NADH recordings, the light was passed through a 340/26-nm excita-

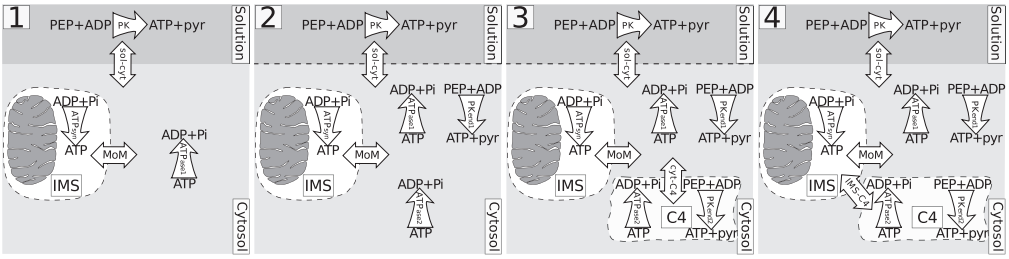

Fig. 2. Schematic diagrams of *models 1–4*. Compartments are indicated by dashed lines, reactions by single-headed curved arrows, and exchange between compartments by double-headed straight arrows. All models have compartments representing the solution, cytosol, and mitochondrial intermembane space (IMS). *Models 3* and *4* include a fourth compartment (C4). The reactions considered are mitochondrial ATP synthesis in the mitochondrial matrix leading to the conversion of ADP to ATP in the mitochondrial IMS (ATP_{syn}), ATP consumption by ATPases (ATPase1 and ATPase2), and ATP synthesis by endogenous pyruvate kinase (PK; PKend1 and PKend2) and exogenous PK. The following exchanges between compartments were calculated: solution and cytosol (sol-cyt), IMS and cytosol through the outer mitochondrial membrane (MoM), cytosol and C4 (cyt-C4), and IMS and C4 (IMS-C4). PEP, phosphoenol pyruvate.

tion filter onto a 400-nm long-pass dichroic mirror, which deflected the light onto the specimen. Light emitted from the specimen passed back through the upper filter cube to a 510 XR dichroic in the lower filter cube and reflected through a 460/80-nm emission filter to an Andor Ixon EMCCD camera (Andor Technologies, Belfast, UK). For Fp recordings, the light was passed through a 465/30-nm excitation filter onto a 510-nm dichroic mirror, which deflected the light onto the specimen. Light emitted from the specimen passed back through the upper filter cube to a 560 XR dichroic in the lower filter cube and reflected through a 525/50-nm emission filter. All filters were purchased from AHF Analysentechnik. For each filter, the first number describes the mode wavelength and the second number describes the total bandwidth at half-maximum transparency (half-minimum optical density). This means that a 340/26-nm filter mainly passes light between 327 and 356 nm. Filter specifications, including plots of their optical density at different wavelengths, can be found on the suppliers website (http://www.ahf.de). Transmission images together with images of NADH or Fp autofluorescence were acquired every 30 s. To reduce photobleaching, a Uniblitz shutter (VCM-D1, Vincent Associates, Rochester, NY) timed the light exposure with the acquisition.

Immediately before each experiment, a new batch of cells was permeabilized for 5 min with gentle mixing in an Eppendorf tube with respiration solution containing 25 μg/ml saponin and 50 μM ADP. A fraction of the permeabilized cells was put into a diamond-shaped fast-exchange chamber (15 × 6 mm, RC-24N, Warner Instruments, Harvard Apparatus, March-Hugstetten, Germany) on the microscope. Cells were allowed to sediment for 5–10 min before the superfusion was started with respiration solution containing different concentrations of ADP. Only cells located in the middle of the chamber were used for measurements. According to the manufacturer, the geometry of the chamber provided laminar flow of solutions during experiments at the used flow rate of ≈0.5 ml/min and was laminar in our conditions, as confirmed by mathematical model of the flow (22). The ADP concentration was increased stepwise from 50 to 100, 300, 500, 1,000, and 2,000 μM, and cells were superfused for at least 4.5 min at each step.

Fluorescence signal intensity from microscope single cell experiments was analyzed using ImageJ software. Both regions containing each cell and background regions were selected, and corresponding average fluorescence signal intensities were determined with the ImageJ plug-in "measure stack." Background fluorescence was then subtracted from cell fluorescence, and the data were plotted on a timescale. From the latter plot, average fluorescence was found for each condition to which the cell was exposed (ADP concentration, uncoupling or block of oxidative phosphorylation). To enable comparison between cells, signals were normalized to maximum and minimum fluorescence recorded under fully reduced (respiration inhibited with oligomycin and cyanide) or oxidized (mitochondria uncoupled with FCCP) conditions.

Solutions. The wash solution consisted of (in mM) 117 NaCl (no. 71379, Sigma-Aldrich), 5.7 KCl (no. P-5405, Sigma-Aldrich), 1.5 KH_2PO_4 (no. P-0662, Sigma-Aldrich), 4.4 $NaHCO_3$ (no. S-6014, Sigma-Aldrich), 1.7 $MgCl_2$ (no. 63068, Sigma-Aldrich), 21 HEPES (no. H-3375, Sigma-Aldrich), 20 taurine (no. 86329, Sigma-Aldrich), and 11.7 glucose (no. 158968, Sigma-Aldrich). pH was adjusted to 7.4 with NaOH.

For the collagenase solution, 0.25 mg/ml collagenase P (no. 11213873001, Roche) and 3 mg/ml BSA (no. 10775835001, Roche) was added to 40 ml of the wash solution.

For the sedimentation solution, 2 mM pyruvate (no. P-2256, Sigma-Aldrich), 10 μM leupeptin (no. 11034626001, Roche), 2 μM soybean trypsin inhibitor (no. 93619, Sigma-Aldrich), and 3 mg/ml BSA (no. 10775835001, Roche) were added to 60 ml of the wash solution.

The respiration solution contained (in mM) 110 sucrose (no. S-1888, Sigma-Aldrich), 60 K-lactobionic acid (no. L-2398, Sigma-Aldrich), 3 KH_2PO_4 (no. P-0662, Sigma-Aldrich), 3 $MgCl_2$ (no. 63068, Sigma-Aldrich), 20 HEPES (no. H-3375, Sigma-Aldrich), 20 taurine (no. 86329, Sigma-Aldrich), 0.5 EGTA (no. 71379, Sigma-Aldrich), 0.5 DTT (no. D-0632, Sigma-Aldrich), 2 malate (no. M-6413, Sigma-Aldrich), and 5 glutamate (no. 49449, Sigma-Aldrich). pH was adjusted to 7.1 with KOH. Immediately before use, 5 mg/ml BSA (no. 10775835001, Roche) and 20 μg/ml saponin (no. 47036, Sigma-Aldrich) were added.

The ADP stock solution contained 200 mM ADP (no. A-2754, Sigma-Aldrich) and 60 mM $MgCl_2$ (no. 63068, Sigma-Aldrich). pH was adjusted to 7.1 with KOH.

The ATP stock solution contained (in mM) 200 ATP (no. 10127531001, Roche), 200 Mg-acetate (no. M-5661, Sigma-Aldrich), and 20 HEPES (no. H-3375, Sigma-Aldrich). pH was adjusted to 7.1 with KOH.

Concentrations of the uncoupler and respiration blockers were as follows: FCCP (10 μM, no. Asc-081, Ascent Scientific), oligomycin A (10 μM, no. 579-13-5, Tebu-bio), and sodium cyanide (5 mM, no. 205222, Sigma-Aldrich).

Statistics. Raw data were analyzed using homemade software. Values are given as means ± SD.

RESULTS

Characteristics of WT and GAMT$^{-/-}$ mice. Genotypes of the mice were confirmed by PCR. The results are shown in Fig. 3.

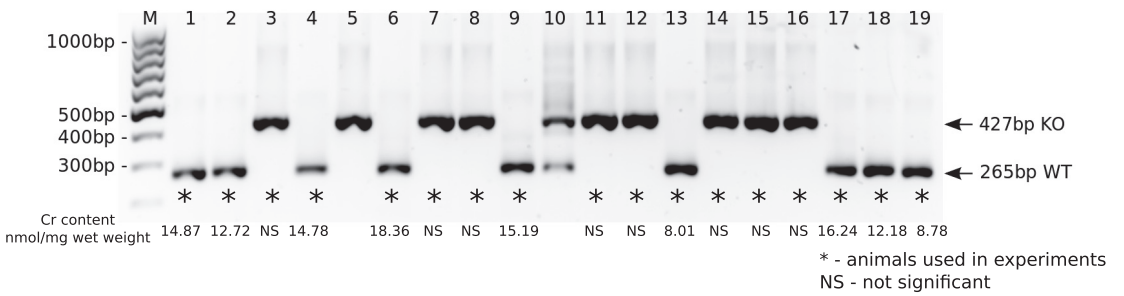

Fig. 3. Genotyping of guanidinoacetate methyltransferase (GAMT)-deficient (GAMT$^{-/-}$) mice by PCR. After PCR amplification, samples were analyzed on 1% agarose gel stained with ethidium bromide along with a DNA ladder (*lane M*: GeneRuler 100-bp DNA Ladder). The 265- and 427-bp-long PCR products corresponded to wild-type (WT) GAMT (GAMT$^{+/+}$) or homozygous GAMT knockout (GAMT$^{-/-}$ KO) genotypes, respectively. *Animals that were used in experiments. Total skeletal muscle creatine (Cr) content (expressed as nmol/mg wet wt) is shown under each mouse used in the experiments, respectively. The levels of Cr in GAMT$^{-/-}$ mice were statistically not significant (NS).

GAMT$^{-/-}$ mice had a lower body weight than their WT littermates [female WT: 24.2 ± 3.8 g vs. female GAMT$^{-/-}$: 17.5 ± 2.6 g ($P < 0.05$); male WT: 34.5 ± 5.3 g vs. male GAMT$^{-/-}$: 23.0 ± 2.7 g ($P < 0.01$)]. In female mice, tibial length was also shorter in GAMT$^{-/-}$ than WT mice [female WT: 21.8 ± 0.2 mm vs. female GAMT$^{-/-}$: 21.1 ± 0.6 mm ($P < 0.05$); male WT: 22.6 ± 0.6 mm vs. male GAMT$^{-/-}$: 21.7 ± 0.8 mm ($P = 0.1330$)]. This is in agreement with previous observations (19, 41).

Total Cr content was measured enzymatically in GAMT$^{-/-}$ and WT mice used in the experiments. Skeletal muscle Cr content was 13.46 ± 3.40 nmol/mg wet wt in WT control mice ($n = 9$) and undetectable in GAMT$^{-/-}$ mice ($n = 8$) (Fig. 3). This was confirmed statistically with a paired *t*-test showing no significant difference in the Cr content between the GAMT$^{-/-}$ sample and the corresponding blank ($P > 0.05$) and a significant difference between the WT sample and the corresponding blank ($P < 0.05$).

Mitochondrial positioning. Visual inspection of the confocal images showed similar mitochondrial distribution in GAMT$^{-/-}$ and WT cardiomyocytes. This was confirmed by quantitative analysis of the relative positioning of the mitochondrial centers (Figs. 4 and 5). Figure 4 shows the probability densities of the closest mitochondrial centers found in the different sectors. There was no difference between GAMT$^{-/-}$ and WT cardiomyocytes. Figure 5 shows plots of the cumulative distribution functions. The graphs for WT and GAMT$^{-/-}$ cardiomyocytes were overlapping or were very close in all directions (Fig. 5).

For statistical analysis, we found the averaged distances R and R_{XZ} (notation from Fig. 5) at 25%, 50%, and 75% of the cumulative distribution function (Table 1). There was no significant

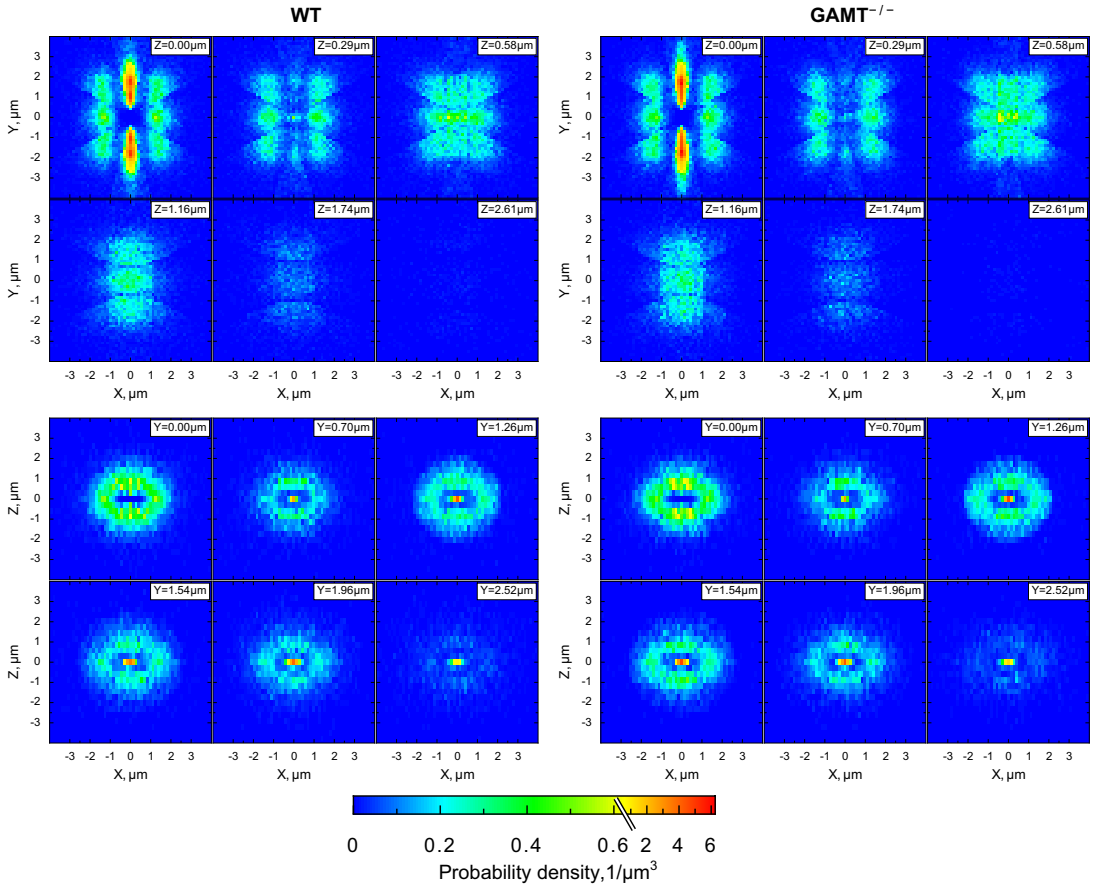

Fig. 4. Probability density of the closest mitochondrial centers in each of the directions in WT (*left*) and GAMT$^{-/-}$ (*right*) cardiomyocytes. A total of 24,588 (WT) and 23,405 (GAMT$^{-/-}$) mitochondria from 6 cells were analyzed. Each mitochondrial center was considered to be in the origin (0, 0). The space around was divided into 14 sectors, and the distribution of the closest mitochondrial centers in each sector was analyzed. Results from sectors with the same direction were pooled. Here, and in the following analysis, the *y*-direction was taken along the myofibrills and *x*- and *z*-directions were transversal directions at and perpendicular to the image planes, respectively. The *xy*- and *yz*-directions were diagonal directions. Two-dimensional probability density is shown at different planes perpendicular to the *z*-axis (*XY*-planes; *top*) or the *y*-axis (*XZ*-planes; *bottom*) at different distances from the origin as indicated at the *top right* corner of each plane. Note how similar the mitochondrial distributions were in GAMT$^{-/-}$ and WT cardiomyocytes.

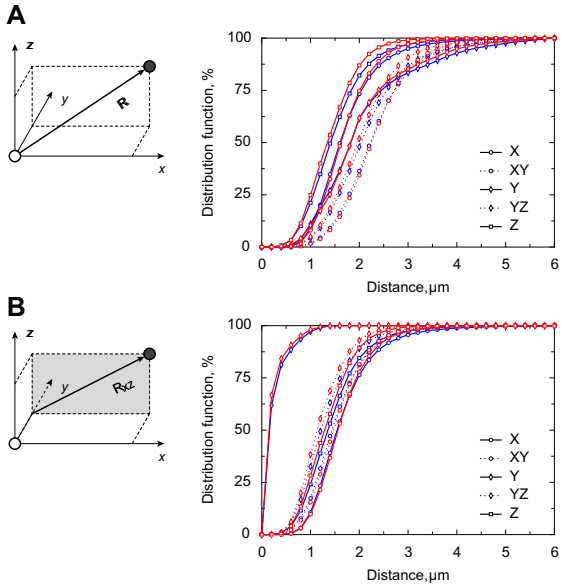

Fig. 5. Cumulative distribution function of the distance between centers of neighboring mitochondria in different directions. The distribution functions for the following distances were calculated: distance (R) from the origin to the nearest mitochondrion in each direction (A) and distance (R_{XZ}) from the y-axis through the origin to the nearest mitochondrion in each direction (B). The differences in the corresponding distances are highlighted on the schemes shown in A and B, *left*. If the rows of mitochondria were parallel, R_{XZ} would be the same in the X- and XY-directions and Z- and YZ-directions. Indeed, their distribution functions were very close. For parallel rows, R_{XZ} in the Y-sector would be 0. Note in both A and B that the distribution functions for the WT (blue) and GAMT$^{-/-}$ (red) groups were either overlapping or very close to each other.

difference in the distances between WT and GAMT$^{-/-}$ cardiomyocytes as analyzed with mixed-design ANOVA. In this statistical test, the between-subject variables were mouse genotypes (2 levels: WT or GAMT$^{-/-}$) and the within-subject variables were directions for R and R_{XZ} (5 directions for each, 10 levels in total) and percentile points (3 levels). On the basis of ANOVA, we concluded that there was no significant main effect of genotype, $P = 0.28$. No significant differences in the distances were found when we compared the distances obtained at all directions and all percentile points for WT and GAMT$^{-/-}$ cardiomyocytes using Welch's t-test and correcting for multiple comparisons using the Šidák correction.

From this analysis, we conclude that the distances between mitochondrial centers in WT and GAMT$^{-/-}$ cardiomyocytes were not significantly different. Furthermore, we did not observe any compensation in mitochondrial positioning to the lack of a functional CK shuttle in GAMT$^{-/-}$ cardiomyocytes.

Kinetic recordings. In the respirometer, we recorded the kinetics of ADP- and ATP-stimulated respiration in permeabilized cardiomyocytes. ADP directly stimulates respiration, whereas ATP is first hydrolyzed by ATPases to ADP, which diffuses to the mitochondria and stimulates respiration (Fig. 6, A and B). In addition, we recorded how ATP-stimulated respiration is affected by a competitive ADP-trapping system consisting of PEP activating endogenous PK and PEP activating additional 20 U/ml exogenous PK (Table 2). The respiration data were complemented by spectrophotometric recordings of the kinetics of ATP-stimulated ATPase activity and ADP-stimulated endogenous PK activity using a coupled assay (Fig. 6, C and D).

Analysis of kinetic data by mathematical models. The experimental data were fitted by several mathematical models with different levels of compartmentation (Fig. 2). The model fits were compared with the measurements shown in Fig. 6 and Table 2. To analyze the data obtained from WT and GAMT$^{-/-}$ mouse cardiomyocytes, we first fitted the data separately. The data were then pooled together and fitted (parameters shown in Table 3). As expected, the fit was better when the models were allowed to fit the WT and GAMT$^{-/-}$ data separately (quantified by sum of squares in least-squares fitting). However, according to the extra sum-of-squares F-test (F-test), the increased number of parameters induced by fitting the experiments separately was not justified, and the better fits were due to chance (depending on the model, P was from 0.37 to 0.99). From this, we concluded that the kinetic recordings in WT and GAMT$^{-/-}$ mouse cardiomyocytes were not significantly different and that the two cases could be described by a single set of a model parameters.

Table 1. *Distances at 25%, 50%, and 75% of the distribution function for R_{XYZ} and R_{XZ}*

	25%		50%		75%	
Direction	WT	GAMT$^{-/-}$	WT	GAMT$^{-/-}$	WT	GAMT$^{-/-}$
R_{XYZ}						
X	1.28 ± 0.04	1.31 ± 0.08	1.61 ± 0.04	1.64 ± 0.07	2.07 ± 0.09	2.06 ± 0.09
XY	1.81 ± 0.08	1.88 ± 0.12	2.25 ± 0.07	2.29 ± 0.11	2.76 ± 0.10	2.78 ± 0.13
Y	1.35 ± 0.15	1.39 ± 0.18	1.83 ± 0.08	1.82 ± 0.09	2.56 ± 0.29	2.39 ± 0.15
YZ	1.61 ± 0.08	1.57 ± 0.10	2.08 ± 0.11	2.01 ± 0.11	2.65 ± 0.23	2.48 ± 0.11
Z	1.07 ± 0.05	0.99 ± 0.08	1.43 ± 0.08	1.35 ± 0.08	1.89 ± 0.19	1.75 ± 0.08
R_{XZ}						
X	1.23 ± 0.03	1.27 ± 0.08	1.55 ± 0.04	1.58 ± 0.07	2.00 ± 0.09	2.00 ± 0.10
XY	1.12 ± 0.03	1.17 ± 0.07	1.45 ± 0.02	1.50 ± 0.08	1.88 ± 0.05	1.90 ± 0.10
Y	0.08 ± 0.01	0.07 ± 0.02	0.16 ± 0.03	0.12 ± 0.04	0.32 ± 0.09	0.24 ± 0.06
YZ	0.92 ± 0.04	0.86 ± 0.07	1.23 ± 0.05	1.14 ± 0.08	1.68 ± 0.15	1.54 ± 0.10
Z	1.03 ± 0.05	0.95 ± 0.08	1.38 ± 0.08	1.29 ± 0.08	1.82 ± 0.20	1.68 ± 0.09

Values (in μm) are means ± SD; $n = 6$ wild-type (WT) cardiomyocytes and 6 guanidinoacetate methyltransferase (GAMT)-deficient (GAMT$^{-/-}$) cardiomyocytes. R_{XYZ}, distance from the origin to the nearest mitochondrion; R_{XZ}, distance from the y-axis through the origin to the nearest mitochondrion.

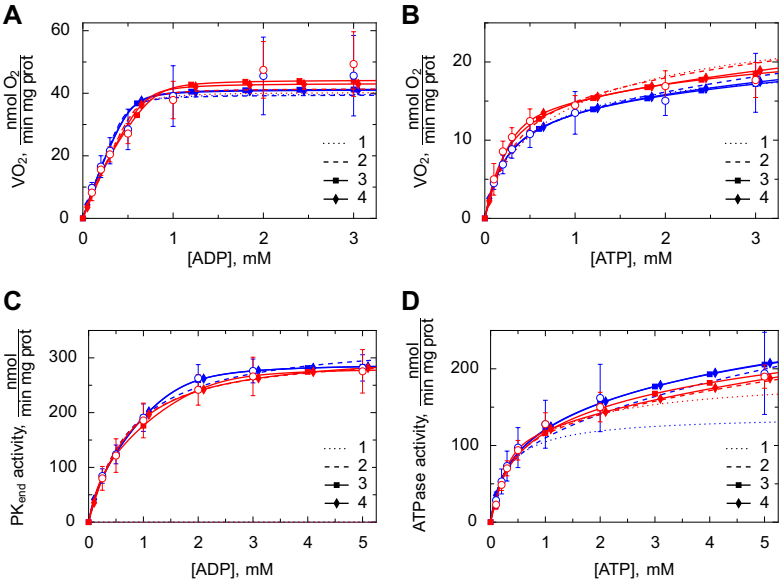

Fig. 6. Kinetic analysis of permeabilized cardiomyocytes from WT (blue) and GAMT$^{-/-}$ (red) mice. Measurements were performed in respiration solution containing 2 mM malate and 5 mM glutamate to support ADP-stimulated respiration. The experimental results are shown as means ± SD (open circles). These were compared with the solutions from *models 1–4*. Fits from simplified *model 2s*, *3s*, and *4s* were excluded for simplicity. *A*: respiration rate as a function of the ADP concentration added to the respirometer chamber (n = 6 and 5 for WT and GAMT$^{-/-}$ cardiomyocytes, respectively). *B*: respiration rate as a function of ATP (n = 7 and 5 for WT and GAMT$^{-/-}$ cardiomyocytes, respectively). *C*: endogenous PK activity as a function of ADP in the spectrophotometer cuvette (n = 8 and 7 for WT and GAMT$^{-/-}$ cardiomyocytes, respectively). *D*: ATPase activity as a function of ATP in the spectrophotometer cuvette (n = 9 and 7 for WT and GAMT$^{-/-}$ cardiomyocytes, respectively). Note that the fits from *models 3* and *4* were either very close or overlapping in all cases. Vo_2, O_2 consumption.

As previously found for rat cardiomyocytes (45), the fits obtained by *models 1*, *2*, and *2s* were considerably worse than the fits with the other models, as shown by statistical analysis using an F-test of the nested models (Table 4). However, when information criteria were used, only *model 1* was considerably worse than the other models (AIC_c and BIC). By comparing the results from multiple goodness-of-fit criteria, we can conclude that solutions of all models, except for *model 1*, can be considered reasonable. The main difference between *model 2* and *models 3*, *3s*, *4*, and *4s* is the introduction of a coupling between a part of endogenous PK and ATPases. Thus, while the *F*-test strongly suggests that a part of endogenous PK is coupled to ATPases ($P < 0.05$), the information criteria analysis was not conclusive, and further studies are needed. In addition, considerable diffusion restriction was identified at the level of the mitochondrial outer membrane and at the level of intracellular diffusion restrictions separating mitochondria from the surrounding solution.

As explained above, when analyzing the model parameters obtained by fitting the data, we have to consider the pooled case only (Table 3). In the models, all reaction rates were simulated using Michaelis-Menten kinetics with the apparent kinetic constants V_{max} and K_m. ATPases were considered to be inhibited competitively by ADP (where $K_{iATPase}$ is the apparent inhibition constant). The diffusion restrictions are described via exchange coefficients between the compartments (where $C_{compartment\ 1\text{-}compartment\ 2}$ is the exchange coefficient between *compartment 1* and *compartment 2*). Table 3 shows the parameters used for each model. According to our simulation results using the pooled data set, the diffusion restrictions that separate the surrounding solution from mitochondria were similar to the diffusion restrictions

Table 2. *$V_{2\ mM\ ATP}$, V_{PEP}, and $V_{PEP\ +\ PK}$ for experimental data and the various models*

		Models						
	Experimental Data	*1*	*2*	*2s*	*3*	*3s*	*4*	*4s*
WT								
$V_{2\ mM\ ATP}$	14.48 ± 4.24	15.98	16.14	16.72	15.71	15.33	15.79	15.51
V_{PEP}	11.15 ± 3.73	17.23	11.45	11.73	8.88	11.15	9.1	11.53
$V_{PK\ +\ PEP}$	4.84 ± 2.02	5.53	4.42	5.68	6.5	6.87	6.15	6.43
GAMT$^{-/-}$								
$V_{2\ mM\ ATP}$	14.07 ± 3.02	18.12	17.97	19.08	17.14	16.58	17.14	17
V_{PEP}	10.86 ± 2.53	19.69	12.36	12.82	9.81	11.29	11.52	13.07
$V_{PK\ +\ PEP}$	5.21 ± 2.18	8.16	7.16	7.62	9.22	9.9	6.46	10.43
Pooled								
$V_{2\ mM\ ATP}$	14.30 ± 3.64	17.66	17.31	18.4	16.6	16.04	16.5	16.55
V_{PEP}	11.02 ± 3.16	19.06	12.06	12.69	9.19	11.07	11.26	12.25
$V_{PK\ +\ PEP}$	5.00 ± 2.03	7.13	6.04	7.07	8.4	8.95	5.61	9.01

Values are in nmol·min^{-1}·mg protein^{-1}; n = 8 WT cardiomyocytes, 7 GAMT$^{-/-}$ cardiomyocytes, and 15 pooled cardiomyocytes. Experimental data were compared with simulation results obtained by *models 1–4* and their simplified versions (*models 2s*, *3s*, and *4s*). $V_{2\ mM\ ATP}$, ATP-stimulated respiration rate; V_{PEP}, inhibition of ATP-stimulated respiration rate by endogenous pyruvate kinase (PK); $V_{PEP\ +\ PK}$, inhibition of ATP-stimulated respiration rate by endogenous PK; PEP, phosphoenol pyruvate.

Table 3. *Model parameters found by fitting the pooled data obtained from WT and GAMT$^{-/-}$ cardiomyocytes*

	Models						
	1	*2 s*	*2*	*3 s*	*3*	*4 s*	*4*
$V_{maxATPsyn}$, nmol·min^{-1}·mg protein^{-1}							
Optimal value	233	248	243	257	262	255	254
Confidence intervals	62–720	174–335	172–330	191–332	193–344	182–338	190–327
$C_{sol\text{-}cyt}$, nmol·mM^{-1}·min^{-1}·mg protein^{-1}							
Optimal value	1,461	1,017	1,295	409	299	493	1,234
Confidence intervals	175 to >10^5	562–2031	606–3,062	249–651	199–426	273–893	635–2,464
C_{MoM}, nmol·mM^{-1}·min^{-1}·mg protein^{-1}							
Optimal value	646	676	612	1,132	2,362	950	517
Confidence intervals	222–2,231	530–875	481–791	786–1,788	1,264–7,394	662–1,479	425–635
$C_{IMS\text{-}C4}$, nmol·mM^{-1}·min^{-1}·mg protein^{-1}							
Optimal value						8.39	366
Confidence intervals						1.72–16	261–544
$C_{cyto\text{-}C4}$, nmol·mM^{-1}·min^{-1}·mg protein^{-1}							
Optimal value				0.005	156		
Confidence intervals				0.003–0.009	81–343		
$V_{maxATPase1}$, nmol·min^{-1}·mg protein^{-1}							
Optimal value	181	177	614	119	89	105	742
Confidence intervals	90–298	156–198	322–954	108–130	79–99	93–117	474–1,045
$K_{mATPase1}$, Mm							
Optimal value	0.21	0.271	10	0.235	0.201	0.201	10
Confidence intervals	0.06–0.834	0.206–0.358	≥10	0.187–0.294	0.147–0.276	0.143–0.279	6.91 to >10
$K_{iATPase1}$, mM							
Optimal value	0.051	0.102	0.05	9.62	10	10	0.051
Confidence intervals	0.05 to >10	0.056–0.228	0.05 to >10	0.208 to >10	≥10	0.229 to >10	0.05–0.09
$V_{maxATPase2}$, nmol·min^{-1}·mg protein^{-1}							
Optimal value			107	119	278	127	95
Confidence intervals			92–122	75–169	186–391	42–4,500	82–108
$K_{mATPase2}$, mM							
Optimal value			0.194		3.77		0.051
Confidence intervals			0.131–0.286		2.47–6.26		0.05–0.1
$K_{iATPase2}$, mM							
Optimal value			10		0.053		10
Confidence intervals			0.142 to >10		0.05–0.147		0.166 to >10
$V_{maxPKend1}$, nmol·min^{-1}·mg protein^{-1}							
Optimal value		322	327	235	68	284	327
Confidence intervals		282–362	287–368	204–267	42–94	244–325	293–361
$K_{mPKend1}$, mM							
Optimal value		0.546	0.621	0.33	0.05	0.596	0.616
Confidence intervals		0.366–0.809	0.424–0.904	0.208–0.502	0.05–0.112	0.414–0.852	0.448–0.845
$V_{maxPKend2}$, nmol·min^{-1}·mg protein^{-1}							
Optimal value				356	217	47	0.118
Confidence intervals				111–7199	180–258	23–72	0.053–29

induced by mitochondrial outer membrane. This is clear from a comparison of the exchange coefficients $C_{sol\text{-}cyt}$ and C_{mom} for all the models that provided reasonable fits (Table 3). Namely, while for some models (*models 2*, *2s*, and *4*) the diffusion restriction induced by the mitochondrial outer membrane was larger than the one separating the surrounding solution from mitochondria, the opposite was true for the other models (*models 3*, *3s*, and *4s*). However, we should note that for all models, with the exception of *model 3*, those diffusion restrictions were of the same order of magnitude, suggesting that they are similar. Note that the description of ATPases and endogenous PK interaction in *compartment 4* is a phenomenological one and that all the model parameters obtained for this compartment, including the exchange coefficient, are phenomenological coefficients and may not represent the interaction between ATPases and PK in a mechanistic way (as discussed in Ref. 45). As such, the obtained low exchange coefficient for *compartment 4* is a part of a general description of coupling between PK and ATPases and cannot be compared directly with the other exchange coefficients found by the model.

Autofluorescence of single, permeabilized cardiomyocytes during ADP titration. To verify that diffusion restrictions were not due to clumping of the cells, we recorded NADH and Fp autofluorescence responses to the change in ADP at the single cell level (Fig. 7). The mainly mitochondrial origin of NADH and Fp fluorescence signals allowed us to relate fluorescence to the state of oxidative phosphorylation. NADH and Fp signals decreased and increased, respectively, as the concentration of ADP in the surrounding solution was increased (Fig. 7). We compared the normalized NADH and Fp fluorescence at each ADP concentration and found no statistically significant difference between cardiomyocytes from WT and GAMT$^{-/-}$ mice (P from 0.09 to 0.95 by Welch's t-test; Fig. 7, *C* and *D*).

Table 4. *Statistical analysis of the fits*

				F-Tests					
	AIC	AIC_c	BIC	*Model 2s*	*Model 2*	*Model 3s*	*Model 3*	*Model 4s*	*Model 4*
WT cardiomyocytes									
Model 1	98.39	102.2	590.48	<0.0001	<0.0001	<0.0001	<0.0001	<0.0001	<0.0001
Model 2s	−23.1	−15.9	34.47		0.124	<0.05	<0.05	<0.05	<0.05
Model 2	−26.13	−10.61	42.56				<0.05		<0.05
Model 3s	−32.68	−17.15	41.44				0.113		
Model 3	−36.58	−12.32	47.13						
Model 4s	−30.43	−14.9	41.8						<0.05
Model 4	−37.7	−13.44	47.0						
GAMT$^{-/-}$ cardiomyocytes									
Model 1	77.59	81.41	298.61	<0.0001	<0.0001	<0.0001	<0.0001	<0.0001	<0.0001
Model 2s	7.75	14.95	48.76		0.139	<0.01	<0.01	<0.05	<0.001
Model 2	5.14	20.67	53.25				<0.01		<0.001
Model 3s	−11.33	4.2	46.23				0.583		
Model 3	−9.28	14.98	52.37						
Model 4s	0.55	16.08	50.88						<0.01
Model 4	−16.84	7.43	50.4						
Pooled WT and *GAMT*$^{-/-}$ cardiomyocytes									
Model 1	167.94	169.59	877.59	<0.0001	<0.0001	<0.0001	<0.0001	<0.0001	<0.0001
Model 2s	−15.07	−12.13	66.43		<0.01	<0.0001	<0.0001	<0.001	<0.0001
Model 2	−27.04	−21.3	69.56				<0.0001		<0.0001
Model 3s	−47.47	−41.73	62.17				0.052		
Model 3	−51.09	−42.82	68.14						
Model 4s	−33.13	−27.4	67.08						<0.0001
Model 4	−54.96	−46.68	67.15						

Fits were analyzed by calculating Akaike information criteria (AIC), corrected AIC (AIC_c), and Bayesian information criteria (BIC). For all three criteria, the best-fitting model was the one with the minimum criterion value. Note that for AIC_c and BIC, a larger number of parameters is penalized more than in AIC. *F*-tests of the nested models are shown, with the simpler model (rows) compared with the nested, more complicated model (columns). The analysis was performed for fits of the data recorded from WT and GAMT$^{-/-}$ mouse cardiomyocytes separately as well as for pooled data.

Because no statistically significant difference was found when we performed multiple comparisons separately, no additional correction for multiple tests or ANOVA analysis was required to check whether the difference in autofluorescence between cardiomyocytes from WT and GAMT$^{-/-}$ mice was significant. Thus, on the basis of our results, diffusion from the solution to the mitochondrial inner membrane is restricted to the same extent.

DISCUSSION

The present study shows that inactivation of the CK system by GAMT deficiency due to lack of Cr is not associated with any changes in cardiomyocyte mitochondrial organization or stimulated respiration or its regulation by exogenous and endogenous ADP-supply. In addition, according to our modeling results, there was no change in intracellular compartmentation when cells were in a relaxed state. This indicates that inactivation of the CK system by GAMT deficiency does not induce cytoarchitectural changes.

The CK system is considered an important temporal and spatial energy buffer in the heart. In all muscle types, CK is present near sites of ATP consumption and sites of ATP production. In white, glycolytic skeletal muscle, CK is present near the myofibrillar I-band and functionally coupled to glycolytic enzymes (26). In oxidative skeletal muscle and the heart, mitochondrial CK is bound to the outer side of the inner mitochondrial membrane (25) and functionally coupled to respiration (59). Cytosolic CK is localized at the myofibrillar M-band, which is favorable for the regeneration of ATP for myosin ATPase (58). Also, it is bound near and functionally coupled to SERCA (33), sarcolemmal ATP-sensitive K^+ channels (9), and Na^+-K^+-ATPase (13). The "spatial energy buffer" or "energy transport" function of CK has mainly been ascribed to tissues such as the heart, where a relatively large fraction of the CK activity is of mitochondrial origin (56, 59). Mitochondrial CK activity is tissue specific and relates to oxidative capacity (56). This relationship can also be observed during cardiac maturation (12, 16). Facilitation of ADP/ATP transport may seem particularly important in oxidative muscles, where ADP/ATP diffusion is restricted (28, 40, 56) and mitochondrial energy production, although more efficient than glycolysis, is more distant and physically separated from ATPases by the mitochondrial membranes. In terms of energy transport, the CK system provides a parallel energy circuit between sites of production and consumption. PCr and Cr are smaller molecules than ATP and ADP and thus diffuse faster (32). Another advantage is that they are present in higher concentrations, allowing the build up of larger gradients of Cr than ADP. For example, whereas the Cr concentration is in the order of 10 mM, the ADP concentration is ~50 μM. Since diffusion is driven by the absolute difference in concentration, the same gradient for ADP would require 10 mM/50 μM = 20 × larger relative difference in concentration than for Cr.

The importance of CK has been the subject of debate for a long time, with sometimes vague hypotheses used to define the role of CK, precluding testing of the hypotheses using a strong inference approach (3). An alternative view has been proposed that the high transport via PCr and Cr is simply a consequence of the CK reaction being close to equilibrium (32). After making some assumptions on the relative concentrations of ATP, ADP, PCr, and Cr, it has been shown that CK is expected to facilitate energy transfer, leading to most of the energy

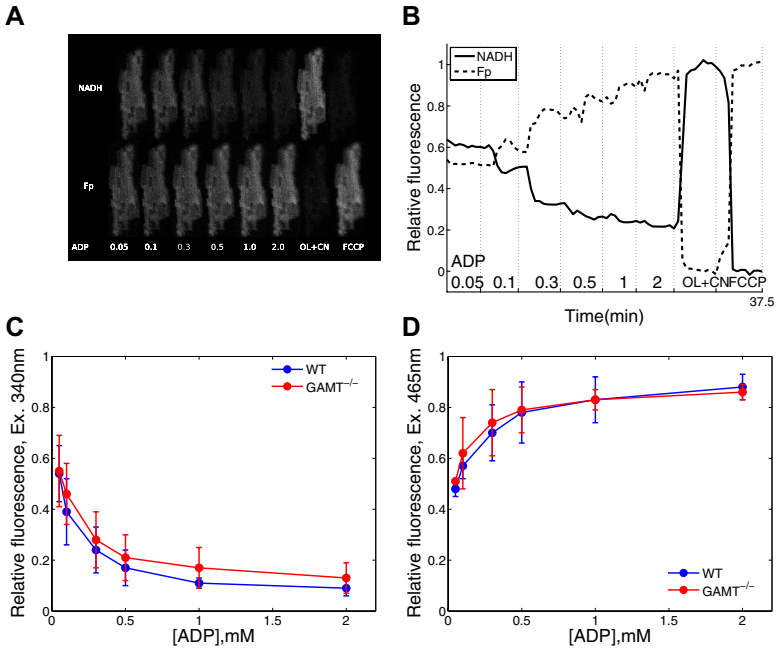

Fig. 7. Autofluorescence response of a permeabilized cardiomyocytes to changes in solution. *A*: representative example of NADH and flavoprotein (Fp) fluorescence from a GAMT$^{-/-}$ cardiomyocyte exposed to different concentrations of ADP, oligomycin and NaCN (OL + CN), and FCCP, as indicated at the *bottom*. *B*: normalized integrated fluorescence of the cardiomyocyte shown in *A*. *C* and *D*: comparison of NADH (*C*) and Fp (*D*) autofluorescence responses in permeabilized cardiomyocytes from WT (blue; $n = 6$) and GAMT$^{-/-}$ (red; $n = 6$) cardiomyocytes to the changes in exogenous ADP.

transfer to occur through PCr and Cr diffusion. In addition, for small diffusion distances, such as in cardiac muscle, the absence of an active CK system should not have any significant functional consequences (32). The latter was demonstrated assuming that there are no significant diffusion restrictions on the diffusion path of molecules between ATPases and mitochondria. Recently, on the basis of analysis of raster image correlation spectroscopy recordings, we (21) suggested that rat cardiomyocytes are split into smaller compartments with lattice-like barriers. The location of the barriers and the intracellular structures forming them are still unknown and would have different physiological consequences depending on whether the barriers are between ATPases and mitochondria or not. The lack of adaptation to inactive CK reported by us is in agreement with the mechanism of CK operation suggested by Meyer et al. (32) in their analysis.

If we assume the importance of the CK system as an additional energy transport system in the heart, it seems intuitive that disruption of this shuttle by genetic knockout of cytosolic and mitochondrial CK would lead to changes in the ultrastructure and regulation of mitochondrial respiration. In cardiomyocytes from CK$^{-/-}$ mice, rows of myofilaments were split into thinner myofilaments by mitochondria wedging into the branching points, as if to compensate for a lack of energy transfer by diminishing intracellular diffusion distances (23). In addition, permeabilized fibers from CK$^{-/-}$ mice have a higher ADP affinity of respiration than WT control mice, indicating smaller intracellular diffusion restrictions imposed on the molecules (23). Such changes in morphology and ADP affinity were consistent with the viewpoint that CK regulates the local ATP-to-ADP ratio and "compensatory mechanisms should be operating in CK$^{-/-}$ mouse heart to overcome diffusion limitation and to preserve cardiac function at least at moderate levels of activity" (23). It was therefore surprising to find no difference between cardiomyocytes from GAMT$^{-/-}$ and their WT littermates. Both had parallel rows of mitochondria with the same distances between mitochondrial centers (Figs. 4 and 5 and Table 1). In permeabilized cardiomyocytes, ADP sensitivity was similar at the population level (Fig. 6) as well as at the single cell level (Fig. 7). Finally, intracellular compartmentation, as assessed by kinetic measurements and mathematical modeling, was found to be the same in both WT and GAMT$^{-/-}$ cardiomyocytes. These findings are in agreement with and extend the observations of a recent study (30) that failed to identify any adaptational changes when left ventricular proteomes, adenylate kinase activity, or mitochondrial respiration were compared.

The difference between our results and those from CK$^{-/-}$ mice might be explained by differences in the genetic background (CK$^{-/-}$ mice on a mixed C57BL/6 and S129 background were compared with WT C57BL/6 mice) and genetic drift. This has been shown to play a role in a study (31) of mice deficient in mitochondrial CK (Mt-CK$^{-/-}$ mice). In the present study, we compared GAMT$^{-/-}$ mice with their WT littermates. Alternatively, the different outcomes may be the result of different genetic modifications. Indeed, CK is a structural as well as catalytic protein. Muscle-type CK is an integral part of the myofibrillar M-band (17, 18, 49), where it serves as an efficient ATP-regenerating system for myosin ATPase located on both sides of the M-band (58). Mt-CK in the mitochondria seems to play a structural role in addition to ADP regeneration. It has been suggested that the octameric form induces the formation of contact sites between the inner and outer mitochondrial membranes (46), where it is involved in lipid transfer

between the two membranes (11). In another study (29), the structural role of Mt-CK has been demonstrated by finding that it stabilizes specific contact sites between inner and outer mitochondrial membranes. It must be noted that these findings are not from cardiac muscle. It remains to be verified whether the lack of Mt-CK in cardiac muscle affects mitochondrial organization. However, an increase citrate synthase activity does suggest an increased mitochondrial volume in cardiac muscle of Mt-CK$^{-/-}$ mice (31). As CK is expressed to the same extent in GAMT$^{-/-}$ mice as in WT mice (19), these other roles of (especially) Mt-CK are preserved in GAMT$^{-/-}$ mice, and our results reflect only the catalytic role of CK.

It is tempting to speculate that guanidinoacetate (GA) may be used by CK in a similar manner as Cr. Indeed, although GAMT$^{-/-}$ mice have undetectable levels of total Cr, as shown in Fig. 3, they have a considerable amount of phosphorylated (p-)GA. In the heart, the p-GA concentration in a GAMT$^{-/-}$ mouse is ~2/3 of the PCr concentration in a WT mouse (19). However, phosphotransfer from ATP to p-GA was undetectable in GAMT$^{-/-}$ mice (29), and it has been shown that the reactivity of muscle-type CK with GA is ~100 times smaller than with Cr (5). This reactivity is sufficient to dephosphorylate p-GA at the induction of ischemia (24) or cyanide inhibition of oxidative phosphorylation (5). However, for energy transfer between mitochondria and ATPases, Mt-CK must convert ATP into PCr or its analog. When ATP-stimulated respiration on isolated mitochondria or on permeabilized fibers was analyzed, Mt-CK reactivity in the presence of GA was negligible and ADP synthesis from GA and ATP was not able to stimulate respiration (5). Taking into account the inability of Mt-CK to react with GA as well as undetectable levels of total Cr, the contribution of the CK shuttle to energy transfer is expected to be negligible in GAMT$^{-/-}$ cardiomyocytes. Thus, in contrast to the suggestion cited above from Ref. 23, the present results suggest that disruption of CK shuttle does not necessarily lead to compensatory changes in mitochondrial arrangement and intracellular compartmentation.

Applied methods and study limitations. In this study, we used confocal microscopy to estimate the intracellular mitochondrial positioning in WT and GAMT$^{-/-}$ cardiomyocytes. The analysis was based on a method that we have previously applied on rat and trout cardiomyocytes (4, 50). Compared with traditional electron microscopy, there are several differences that ought to be considered when interpreting the data obtained by our method. Analysis of confocal images allowed us to use live cells. Thus, there are no histological artifacts that may be introduced by the fixation and dehydration of cells during their preparation for electron microscopy (38). In addition, the distances between the centers of mitochondria estimated by our method can be analyzed in three dimensions (Fig. 1) with an estimation based on a large number of mitochondria. In this study, >20,000 mitochondria were analyzed for each of the genotypes. Collecting a similar amount of data using electron microscopy is possible but would probably not be feasible when time and monetary costs are considered. Taking into account that most of the SDs of the percentile points shown in Table 1 are below 100 nm, the method can be considered precise and should be able to identify subtle changes in mitochondrial positioning. Note that those deviations include variability between cells as well. Such precision can be attributed to sub-Airy disk accuracy in finding centers of the objects in optical microscopy. However, in contrast to electron microscopy, confocal microscopy images do not allow us to determine relative distances between the borders of the objects, such as the distance between membranes of neighboring mitochondria, due to the limits induced by diffraction. As a result, in our study, such distances cannot be analyzed accurately and have not been reported. A further consideration is the isolation procedure, which is of great importance in obtaining a high yield of viable cardiomyocytes with unaltered morphological characteristics. The dissociation of a heart into a single cell suspension involves several critical factors such as excision and cannulation for perfusion, collagenase quality and activity, the length of enzyme digestion, and the Ca^{2+} concentration in the perfusion solution. To control for these variables, we used several criteria to check the quality of the isolation procedure, for example, contraction of cardiomyocytes upon electrical field stimulation, indicating that cells are Ca^{2+} tolerant, and checking for the prevalence of rod-shaped cells with clear striations and well-delineated membranes. However, even with those tests, we cannot exclude a possibility that there are some morphological changes introduced during the isolation procedure that may influence the analysis of mitochondrial positioning.

It is important to keep in mind the limitations of this study. For the functional assays, we studied cardiomyocytes with the sarcolemma permeabilized by saponin. Because the surrounding solution contained low free Ca^{2+}, cells were kept in a resting state. We stimulated mitochondrial respiration and endogenous PK and ATPases by adding ADP or ATP to the solution outside the cells. Thus, these compounds had to cross an unstirred layer around the cells (22) as well as the intracellular diffusion obstacles, which partition cardiomyocytes into smaller compartments (21, 23, 45), before reaching the mitochondria. In contrast, in intact, working cells, there is a circuit of ADP/ATP between adjacent ATPases and mitochondria significantly reducing the diffusion distances and obstacles that influence the energy transfer if compared with the permeabilized cardiomyocyte experiments. In addition, the level of intracellular compartmentation induced by diffusion restrictions is not known in working heart muscle cells. While an analysis of raster image correlation spectroscopy measurements on relaxed rat cardiomyocytes suggested lattice-like intracellular diffusion barriers separating the cardiomyocytes into smaller compartments (21), it is not clear whether such compartmentation persists in the contracting cell. Mitochondrial respiration was stimulated to the maximal rate by very high concentrations of ADP in the presence of a high concentration of P_i, which is also an important regulator of mitochondrial respiration (7, 39, 61). Thus, the changes induced by GAMT deficiency have not been probed in the same conditions as in vivo experiments. However, on the basis of our analysis, we can conclude that the mitochondrial organization and intracellular compartmentation, as observed in our experiments, are unchanged in GAMT$^{-/-}$ mice.

Disruption of the CK system may be compensated for by other mechanisms that were not measured in this study. For example, upregulation of alternative phosphotransfer systems, such as adenylate kinase, has been observed in CK$^{-/-}$ mice (34), and upregulation of other glycolytic enzymes is observed after heart failure (2). Upregulation of these alternative phosphotransfer systems may serve to compensate for both the

temporal and spatial buffer functions of the CK system. However, the change after heart failure may also simply reflect a change of phenotype induced by reverting to a fetal gene expression (37). Metabolically, this includes an upregulation of glycolytic enzymes and a downregulation of mitochondrial enzymes (48, 54). Clearly, further studies are needed to determine how disruption of the CK system by GAMT deficiency affects the cardiac phenotype.

Our kinetic recordings, such as mitochondrial respiration and ATPase activities, were performed in the absence of Cr in solution. This was done to determine whether intracellular compartmentation and mitochondrial respiration capacity changed during adaptation of the cells to Cr deficiency in GAMT$^{-/-}$ mice. As we have previously demonstrated (45), this information can be obtained using kinetic recordings without Cr. Thus, while we know on the basis of earlier studies that the total Cr content is too low to be determined in GAMT$^{-/-}$ mice leading to inactivation of the CK shuttle system in GAMT$^{-/-}$ mice, the kinetic properties of CK isoforms, their distribution, and coupling to mitochondrial respiration is not known and cannot be predicted on the basis of our measurements.

Physiological implications. The lack of compensatory changes in GAMT$^{-/-}$ mice prompts a careful consideration of the role of the CK system in cardiomyocytes. At the whole heart level, both CK$^{-/-}$ and GAMT$^{-/-}$ mice show almost no changes in basal contractile performance (6, 42), but they fail to perform at inotropically stimulated high workload and are more susceptible to ischemia-reperfusion injury (10, 19, 47). Clearly, the CK system is indispensable when the heart is exposed to a severe energetic challenge. But how important is it as an energy transport system? It is well established that a significant fraction of energy transport occurs via the CK system in the heart, and this is severely diminished in the failing heart (20). However, Meyer et al. (32) suggested that CK-facilitated energy transfer is merely a consequence of the existence of the CK system and is not required for cardiac function, if the diffusion distances are taken into account. Its main role is to buffer temporal fluctuations in the ADP-to-ATP ratio during situations, when energy demand is higher than energy production (32). A recent analysis of ^{31}P NMR data suggested that the contribution of the CK shuttle to overall energy transfer between mitochondria and ATPases can depend on the workload and could reduce with an increase in workload or in pathological conditions (53). While our results are by no means conclusive, they raise questions regarding the importance of CK as an energy transport system at low and moderate workloads.

In conclusion, our results suggest that the healthy heart is able to preserve cardiac function at a basal level in the absence of CK-facilitated energy transfer without compromising intracellular organization and the regulation of mitochondrial energy homeostasis.

ACKNOWLEDGMENTS

The authors acknowledge Prof. Dirk Isbrandt (University of Hamburg, Hamburg, Germany) for generating the strain of GAMT-deficient mice as well as Merle Mandel and Adele Puusalu (Institute of Cybernetics, Tallinn University of Technology, Tallinn, Estonia) for technical assistance.

GRANTS

This work was funded by The Wellcome Trust Fellowship WT081755MA, the European Union through the European Regional Development Fund, Estonian Science Foundation Grant ETF8041 (PhD stipends for J. Branovets, N. Jepihhina, and N. Sokolova), and British Heart Foundation Grant RG/10/002/28187.

DISCLOSURES

No conflicts of interest, financial or otherwise, are declared by the author(s).

AUTHOR CONTRIBUTIONS

Author contributions: J.B., S.K., N.J., N.S., and D.A. performed experiments; J.B., M.S., S.K., N.J., and M.V. analyzed data; J.B., M.S., M.V., and R.B. interpreted results of experiments; J.B., M.S., and M.V. prepared figures; C.A.L., S.N., M.V., and R.B. conception and design of research; C.A.L., S.N., M.V., and R.B. edited and revised manuscript; C.A.L., S.N., M.V., and R.B. approved final version of manuscript; R.B. drafted manuscript.

REFERENCES

1. **Abraham MR, Selivanov VA, Hodgson DM, Pucar D, Zingman LV, Wieringa B, Dzeja PP, Alekseev AE, Terzic A.** Coupling of cell energetics with membrane metabolic sensing. *J Biol Chem* 277: 24427–24434, 2002.
2. **Aksentijević D, Lygate CA, Makinen K, Zervou S, Sebag-Montefiore L, Medway D, Barnes H, Schneider JE, Neubauer S.** High-energy phosphotransfer in the failing mouse heart: role of adenylate kinase and glycolytic enzymes. *Eur J Heart Fail* 12: 1282–1289, 2010.
3. **Beard DA, Kushmerick MJ.** Strong Inference for Systems Biology. *PLoS Comput Biol* 5: e1000459, 2009.
4. **Birkedal R, Shiels HA, Vendelin M.** Three-dimensional mitochondrial arrangement in ventricular myocytes: from chaos to order. *Am J Physiol Cell Physiol* 291: C1148–C1158, 2006.
5. **Boehm EA, Radda GK, Tomlin H, Clark JF.** The utilisation of creatine and its analogues by cytosolic and mitochondrial creatine kinase. *Biochim Biophys Acta* 1274: 119–128, 1996.
6. **Bonz AW, Kniesch S, Hofmann U, Küllmer S, Bauer L, Wagner H, Ertl G, Spindler M.** Functional properties and $[Ca^{2+}]_i$ metabolism of creatine kinase–KO mice myocardium. *Biochem Biophys Res Commun* 298: 163–168, 2002.
7. **Bose S, French S, Evans FJ, Joubert F, Balaban RS.** Metabolic network control of oxidative phosphorylation. *J Biol Chem* 278: 39155–39165, 2003.
8. **Braissant O, Henry H, Béard E, Uldry J.** Creatine deficiency syndromes and the importance of creatine synthesis in the brain. *Amino Acids* 40: 1315–1324, 2011.
9. **Crawford RM, Ranki HJ, Botting CH, Budas GR, Jovanovic A.** Creatine kinase is physically associated with the cardiac ATP-sensitive K^+ channel in vivo. *FASEB J* 16: 102–104, 2002.
10. **Crozatier B, Badoual T, Boehm E, Ennezat PV, Guenoun T, Su J, Veksler V, Hittinger L, Ventura-Clapier R.** Role of creatine kinase in cardiac excitation-contraction coupling: studies in creatine kinase-deficient mice. *FASEB J* 16: 653–660, 2002.
11. **Epand RF, Schlattner U, Wallimann T, Lacombe ML, Epand RM.** novel lipid transfer property of two mitochondrial proteins that bridge the inner and outer membranes. *Biophys J* 92: 126–137, 2007.
12. **Fischer A, ten Hove M, Sebag-Montefiore L, Wagner H, Clarke K, Watkins H, Lygate CA, Neubauer S.** Changes in creatine transporter function during cardiac maturation in the rat. *BMC Dev Biol* 10: 70, 2010.
13. **Grosse R, Spitzer E, Kupriyanov VV, Saks VA, Repke KR.** Coordinate interplay between (Na^+ + K^+)-ATPase and creatine phosphokinase optimizes (Na^+/K^+)-antiport across the membrane of vesicles formed from the plasma membrane of cardiac muscle cell. *Biochim Biophys Acta* 603: 142–156, 1980.
14. **Gudbjarnason S, Mathes P, Ravens KG.** Functional compartmentation of ATP and creatine phosphate in heart muscle. *J Mol Cell Cardiol* 1: 325–339, 1970.
15. **Gupta A, Akki A, Wang Y, Leppo MK, Chacko VP, Foster DB, Caceres V, Shi S, Kirk JA, Su J, Lai S, Paolocci N, Steenbergen C, Gerstenblith G, Weiss RG.** Creatine kinase-mediated improvement of function in failing mouse hearts provides causal evidence the failing heart is energy starved. *J Clin Invest* 122: 291–302, 2012.

16. **Hoerter JA, Ventura-Clapier R, Kuznetsov A.** Compartmentation of creatine kinases during perinatal development of mammalian heart. *Mol Cell Biochem* 133–134: 277–286, 1994.
17. **Hornemann T, Kempa S, Himmel M, Hayeß K, Fürst DO, Wallimann T.** Muscle-type creatine kinase interacts with central domains of the M-band proteins myomesin and M-protein. *J Mol Biol* 332: 877–887, 2003.
18. **Hornemann T, Stolz M, Wallimann T.** Isoenzyme-specific interaction of muscle-type creatine kinase with the sarcomeric M-line is mediated by NH_2-terminal lysine charge-clamps. *J Cell Biol* 149: 1225–1234, 2000.
19. **Hove ten M, Lygate CA, Fischer A, Schneider JE, Sang AE, Hulbert K, Sebag-Montefiore L, Watkins H, Clarke K, Isbrandt D, Wallis J, Neubauer S.** Reduced inotropic reserve and increased susceptibility to cardiac ischemia/reperfusion injury in phosphocreatine-deficient guanidinoacetate-*N*-methyltransferase-knockout mice. *Circulation* 111: 2477–2485, 2005.
20. **Ten Hove M, Neubauer S.** MR spectroscopy in heart failure-clinical and experimental findings. *Heart Fail Rev* 12: 48–57, 2007.
21. **Illaste A, Laasmaa M, Peterson P, Vendelin M.** Analysis of molecular movement reveals latticelike obstructions to diffusion in heart muscle cells. *Biophys J* 102: 739–748, 2012.
22. **Jepihhina N, Beraud N, Sepp M, Birkedal R, Vendelin M.** Permeabilized rat cardiomyocyte response demonstrates intracellular origin of diffusion obstacles. *Biophys J* 101: 2112–2121, 2011.
23. **Kaasik A, Veksler V, Boehm E, Novotova M, Minajeva A, Ventura-Clapier R.** Energetic crosstalk between organelles: architectural integration of energy production and utilization. *Circ Res* 89: 153–159, 2001.
24. **Kan HE, Renema WKJ, Isbrandt D, Heerschap A.** Phosphorylated guanidinoacetate partly compensates for the lack of phosphocreatine in skeletal muscle of mice lacking guanidinoacetate methyltransferase. *J Physiol* 560: 219–229, 2004.
25. **Karo J, Peterson P, Vendelin M.** Molecular dynamics simulations of creatine kinase and adenine nucleotide translocase in mitochondrial membrane patch. *J Biol Chem* 287: 7467–7476, 2012.
26. **Kraft T, Hornemann T, Stolz M, Nier V, Wallimann T.** Coupling of creatine kinase to glycolytic enzymes at the sarcomeric I-band of skeletal muscle: a biochemical study in situ. *J Muscle Res Cell Motil* 21: 691–703, 2000.
27. **Kümmel L.** Ca, Mg-ATPase activity of permeabilised rat heart cells and its functional coupling to oxidative phosphorylation of the cells. *Cardiovasc Res* 22: 359–367, 1988.
28. **Kuznetsov AV, Tiivel T, Sikk P, Kaambre T, Kay L, Daneshrad Z, Rossi A, Kadaja L, Peet N, Seppet E, Saks VA.** Striking differences between the kinetics of regulation of respiration by ADP in slow-twitch and fast-twitch muscles in vivo. *Eur J Biochem* 241: 909–915, 1996.
29. **Lenz H, Schmidt M, Welge V, Kueper T, Schlattner U, Wallimann T, Elsässer HP, Wittern KP, Wenck H, Staeb F, Blatt T.** Inhibition of cytosolic and mitochondrial creatine kinase by siRNA in HaCaT- and HeLaS3-cells affects cell viability and mitochondrial morphology. *Mol Cell Biochem* 306: 153–162, 2007.
30. **Lygate CA, Aksentijevic D, Dawson D, ten Hove M, Phillips D, de Bono JP, Medway DJ, Sebag-Montefiore L, Hunyor I, Channon KM, Clarke K, Zervou S, Watkins H, Balaban RS, Neubauer S.** Living without creatine: unchanged exercise capacity and response to chronic myocardial infarction in creatine-deficient mice. *Circ Res* 112: 945–955, 2013.
31. **Lygate CA, Hunyor I, Medway D, de Bono JP, Dawson D, Wallis J, Sebag-Montefiore L, Neubauer S.** Cardiac phenotype of mitochondrial creatine kinase knockout mice is modified on a pure C57BL/6 genetic background. *J Mol Cell Cardiol* 46: 93–99, 2009.
32. **Meyer RA, Sweeney HL, Kushmerick MJ.** A simple analysis of the "phosphocreatine shuttle". *Am J Physiol Cell Physiol* 246: C365–C377, 1984.
33. **Minajeva A, Ventura-Clapier R, Veksler V.** Ca^{2+} uptake by cardiac sarcoplasmic reticulum ATPase in situ strongly depends on bound creatine kinase. *Pflügers Arch* 432: 904–912, 1996.
34. **Momken I, Lechêne P, Koulmann N, Fortin D, Mateo P, Doan BT, Hoerter J, Bigard X, Veksler V, Ventura-Clapier R.** Impaired voluntary running capacity of creatine kinase-deficient mice. *J Physiol* 565: 951–964, 2005.
35. **Nahrendorf M, Streif JU, Hiller KH, Hu K, Nordbeck P, Ritter O, Sosnovik D, Bauer L, Neubauer S, Jakob PM, Ertl G, Spindler M, Bauer WR.** Multimodal functional cardiac MRI in creatine kinase-deficient mice reveals subtle abnormalities in myocardial perfusion and mechanics. *Am J Physiol Heart Circ Physiol* 290: H2516–H2521, 2006.
36. **Ramay HR, Vendelin M.** Diffusion restrictions surrounding mitochondria: a mathematical model of heart muscle fibers. *Biophys J* 97: 443–452, 2009.
37. **Razeghi P, Young ME, Alcorn JL, Moravec CS, Frazier OH, Taegtmeyer H.** Metabolic gene expression in fetal and failing human heart. *Circulation* 104: 2923–2931, 2001.
38. **Roy RR, Pierotti DJ, Edgerton VR.** Skeletal muscle fiber cross-sectional area: effects of freezing procedures. *Acta Anat (Basel)* 155: 131–135, 1996.
39. **Saks VA, Kongas O, Vendelin M, Kay L.** Role of the creatine/phosphocreatine system in the regulation of mitochondrial respiration. *Acta Physiol Scand* 168: 635–641, 2000.
40. **Saks V, Kuznetsov A, Andrienko T, Usson Y, Appaix F, Guerrero K, Kaambre T, Sikk P, Lemba M, Vendelin M.** Heterogeneity of ADP diffusion and regulation of respiration in cardiac cells. *Biophys J* 84: 3436–3456, 2003.
41. **Schmidt A, Marescau B, Boehm EA, Renema WK, Peco R, Das A, Steinfeld R, Chan S, Wallis J, Davidoff M, Ullrich K, Waldschutz R, Heerschap A, De Deyn PP, Neubauer S, Isbrandt D.** Severely altered guanidino compound levels, disturbed body weight homeostasis and impaired fertility in a mouse model of guanidinoacetate *N*-methyltransferase (GAMT) deficiency. *Hum Mol Genet* 13: 905–921, 2004.
42. **Schneider JE, Stork LA, Bell JT, Hove ten M, Isbrandt D, Clarke K, Watkins H, Lygate CA, Neubauer S.** Cardiac structure and function during ageing in energetically compromised guanidinoacetate *N*-methyltransferase (GAMT)-knockout mice–a one year longitudinal MRI study. *J Cardiovasc Magn Reson* 10: 9, 2008.
43. **Schulze A.** Creatine deficiency syndromes. *Mol Cell Biochem* 244: 143–150, 2003.
44. **Seppet EK, Kaambre T, Sikk P, Tiivel T, Vija H, Tonkonogi M, Sahlin K, Kay L, Appaix F, Braun U, Eimre M, Saks VA.** Functional complexes of mitochondria with Ca,MgATPases of myofibrils and sarcoplasmic reticulum in muscle cells. *Biochim Biophys Acta* 1504: 379–395, 2001.
45. **Sepp M, Vendelin M, Vija H, Birkedal R.** ADP compartmentation analysis reveals coupling between pyruvate kinase and ATPases in heart muscle. *Biophys J* 98: 2785–2793, 2010.
46. **Speer O, Bäck N, Buerklen T, Brdiczka D, Koretsky A, Wallimann T, Eriksson O.** Octameric mitochondrial creatine kinase induces and stabilizes contact sites between the inner and outer membrane. *Biochem J* 385: 445, 2005.
47. **Spindler M, Meyer K, Strömer H, Leupold A, Boehm E, Wagner H, Neubauer S.** Creatine kinase-deficient hearts exhibit increased susceptibility to ischemia-reperfusion injury and impaired calcium homeostasis. *Am J Physiol Heart Circ Physiol* 287: H1039–H1045, 2004.
48. **Taegtmeyer H, Wilson CR, Razeghi P, Sharma S.** Metabolic energetics and genetics in the heart. *Ann NY Acad Sci* 1047: 208–218, 2005.
49. **Turner DC, Wallimann T, Eppenberger HM.** A protein that binds specifically to the M-line of skeletal muscle is identified as the muscle form of creatine kinase. *Proc Natl Acad Sci USA* 70: 702–705, 1973.
50. **Vendelin M, Béraud N, Guerrero K, Andrienko T, Kuznetsov AV, Olivares J, Kay L, Saks VA.** Mitochondrial regular arrangement in muscle cells: a "crystal-like" pattern. *Am J Physiol Cell Physiol* 288: C757–C767, 2005.
51. **Vendelin M, Birkedal R.** Anisotropic diffusion of fluorescently labeled ATP in rat cardiomyocytes determined by raster image correlation spectroscopy. *Am J Physiol Cell Physiol* 295: C1302–C1315, 2008.
52. **Vendelin M, Eimre M, Seppet E, Peet N, Andrienko T, Lemba M, Engelbrecht J, Seppet EK, Saks VA.** Intracellular diffusion of adenosine phosphates is locally restricted in cardiac muscle. *Mol Cell Biochem* 256–257: 229–241, 2004.
53. **Vendelin M, Hoerter JA, Mateo P, Soboll S, Gillet B, Mazet JL.** Modulation of energy transfer pathways between mitochondria and myofibrils by changes in performance of perfused heart. *J Biol Chem* 285: 37240–37250, 2010.
54. **Ventura-Clapier R, Garnier A, Veksler V.** Energy metabolism in heart failure. *J Physiol* 555: 1–13, 2004.
55. **Ventura-Clapier R, Kuznetsov AV, d' Albis A, Deursen van J, Wieringa B, Veksler VI.** Muscle creatine kinase-deficient mice. I. Alterations in myofibrillar function. *J Biol Chem* 270: 19914–19920, 1995.

56. **Ventura-Clapier R, Kuznetsov A, Veksler V, Boehm E, Anflous K.** Functional coupling of creatine kinases in muscles: species and tissue specificity. *Mol Cell Biochem* 184: 231–247, 1998.
57. **Ventura-Clapier R, Mekhfi H, Vassort G.** Role of creatine kinase in force development in chemically skinned rat cardiac muscle. *J Gen Physiol* 89: 815–837, 1987.
58. **Wallimann T, Schlosser T, Eppenberger HM.** Function of M-line-bound creatine kinase as intramyofibrillar ATP regenerator at the receiving end of the phosphorylcreatine shuttle in muscle. *J Biol Chem* 259: 5238–5246, 1984.
59. **Wallimann T, Wyss M, Brdiczka D, Nicolay K, Eppenberger H.** Intracellular compartmentation, structure and function of creatine kinase isoenzymes in tissues with high and fluctuating energy demands: the "phosphocreatine circuit" for cellular energy homeostasis. *Biochem J* 281: 21–40, 1992.
60. **Weiss JN, Korge P.** The cytoplasm: no longer a well-mixed bag. *Circ Res* 89: 108–110, 2001.
61. **Wu F, Zhang EY, Zhang J, Bache RJ, Beard DA.** Phosphate metabolite concentrations and ATP hydrolysis potential in normal and ischaemic hearts. *J Physiol* 586: 4193–4208, 2008.

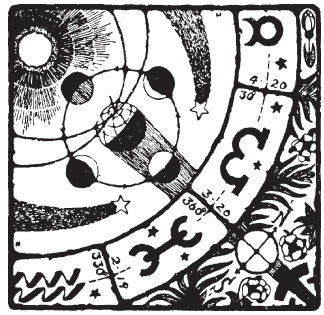

PUBLICATION IV

Sokolova N, Pan S, Provazza S, Beutner G, Vendelin M, Birkedal R and Sheu SS

ADP protects cardiac mitochondria under severe oxidative stress.

PLoS One, 8(12):e83214, December 2013

OPEN ACCESS Freely available online

PLOS ONE

ADP Protects Cardiac Mitochondria under Severe Oxidative Stress

Niina Sokolova[1], Shi Pan[3], Sarah Provazza[2], Gisela Beutner[2], Marko Vendelin[1], Rikke Birkedal[1*], Shey-Shing Sheu[2,3*]

1 Institute of Cybernetics, Tallinn University of Technology, Tallinn, Estonia, **2** Department of Pharmacology and Physiology, University of Rochester, Rochester, New York, United States of America, **3** Center for Translational Medicine, Thomas Jefferson University, Philadelphia, Pennsylvania, United States of America

Abstract

ADP is not only a key substrate for ATP generation, but also a potent inhibitor of mitochondrial permeability transition pore (mPTP). In this study, we assessed how oxidative stress affects the potency of ADP as an mPTP inhibitor and whether its reduction of reactive oxygen species (ROS) production might be involved. We determined quantitatively the effects of ADP on mitochondrial Ca^{2+} retention capacity (CRC) until the induction of mPTP in normal and stressed isolated cardiac mitochondria. We used two models of chronic oxidative stress (old and diabetic mice) and two models of acute oxidative stress (ischemia reperfusion (IR) and tert-butyl hydroperoxide (t-BH)). In control mitochondria, the CRC was 344 ± 32 nmol/mg protein. 500 µmol/L ADP increased CRC to 774 ± 65 nmol/mg protein. This effect of ADP seemed to relate to its concentration as 50 µmol/L had a significantly smaller effect. Also, oligomycin, which inhibits the conversion of ADP to ATP by F_0F_1ATPase, significantly increased the effect of 50 µmol/L ADP. Chronic oxidative stress did not affect CRC or the effect of 500 µmol/L ADP. After IR or t-BH exposure, CRC was drastically reduced to 1 ± 0.2 and 32 ± 4 nmol/mg protein, respectively. Surprisingly, ADP increased the CRC to 447 ± 105 and 514 ± 103 nmol/mg protein in IR and t-BH, respectively. Thus, it increased CRC by the same amount as in control. In control mitochondria, ADP decreased both substrate and Ca^{2+}-induced increase of ROS. However, in t-BH mitochondria the effect of ADP on ROS was relatively small. We conclude that ADP potently restores CRC capacity in severely stressed mitochondria. This effect is most likely not related to a reduction in ROS production. As the effect of ADP relates to its concentration, increased ADP as occurs in the pathophysiological situation may protect mitochondrial integrity and function.

Citation: Sokolova N, Pan S, Provazza S, Beutner G, Vendelin M, et al. (2013) ADP Protects Cardiac Mitochondria under Severe Oxidative Stress. PLoS ONE 8(12): e83214. doi:10.1371/journal.pone.0083214

Editor: Salvatore V Pizzo, Duke University Medical Center, United States of America

Received May 15, 2013; **Accepted** October 31, 2013; **Published** December 13, 2013

Funding: NS was supported by Estonian Science Foundation grant no. ETF8041, Wellcome Trust grant no. 081755 and a travel grant (Estonian Science foundation Dora programme activity 6) from the Archimedes Foundation. S. Provazza was supported by HL-33333 and an ARRA supplement award. GB and SSS were supported by NIH grant RO1HL-033333, RO1HL-093671, and R21HL-110371. MV and RB were supported by Wellcome Trust grant no. 081755. The funders had no role in study design, data collection and analysis, decision to publish, or preparation of the manuscript.

Competing interests: The authors have declared that no competing interests exist.

* E-mail: shey-shing.sheu@jefferson.edu (SSS); rikke@sysbio.ioc.ee (RB)

Introduction

Ca^{2+} and ADP are the two major regulators of mitochondrial energy metabolism that function in coordination to keep the balance between the energy demand and supply. In cardiac muscle cells, during the excitation-contraction coupling, Ca^{2+} enters mitochondria to stimulate Krebs' cycle. As such, the nicotinamide adenine dinucleotide redox potential and ATP synthesis required for cardiac workload are maintained [1]. Concomitantly, ADP generated by ATPases and kinases enters the mitochondrial matrix via the adenine nucleotide translocase (ANT) and stimulates ATP-production by F_1F_0-ATPase [2,3]. Therefore, both Ca^{2+} and ADP have a positive impact on ATP generation under physiological conditions.

Ca^{2+} and ADP are also major modulators of mPTP [4–7]. But here, they function oppositely. Physiologically, the mPTP may open briefly, functioning as a mitochondrial Ca^{2+}-release channel [8]. Pathologically, mitochondrial Ca^{2+}-overload triggers irreversible opening of mPTP, which is a major cause of cell death. ADP, on the contrary, is a potent inhibitor of mPTP [6,7].

The molecular identity of mPTP is still unsolved. Two hypotheses exist regarding the pore-forming component. Both involve cyclophilin D (CypD) and ADP as regulators. CypD is a peptidyl-prolyl cis-trans isomerase, which binds to several proteins including ANT, the mitochondrial phosphate carrier (mPiC) and F_1F_0 ATPase, and increases mPTP Ca^{2+}-sensitivity [9]. Irrespective of its exact site of action, it was shown that cyclosporine A (CsA) binding to CypD inhibits mPTP opening

by unmasking an inhibitory P_i-binding site [10]. Some suggest that mPiC is the pore-forming component and mainly regulated by CypD and ANT [11]. ANT in the "c" (cytosol) or "m" (matrix) conformation increases or decreases mPTP Ca^{2+}-sensitivity, respectively. ADP decreases Ca^{2+}-sensitivity, because its binding shifts ANT to the "m" conformation [12]. Others suggest that dimers of F_1F_0-ATPase are responsible for the formation of mPTP [13]. CypD also binds and inhibits F_1F_0-ATPase activity [14], and ADP is a potent inhibitor of the channel activity of F_0F_1-ATPase dimers [13].

Until today, little is known about the effect of ADP on mPTP in diseased mitochondria, which experience increased oxidative stress, Ca^{2+}-load, and energy deficiency. ADP-binding to ANT is reduced by oxidative stress [15], which might reduce the inhibiting effect of ADP on mPTP. In this paper, we wanted to address the potency of ADP as an mPTP inhibitor in diseased mitochondria with the hope to obtain clues about its mechanism of action. As noted above, ADP may exert its function by binding to either ANT or the F_0F_1-ATPase. But ADP may also enhance Ca^{2+}-sequestration in the form of Ca^{2+}-phosphate precipitates [16,17]. Furthermore, it may be speculated that part of the ADP-effect on Ca^{2+}-uptake capacity is due to its reduction of ROS production [18]. Indeed, as the substrate of F_1F_0-ATPase, which uses the electrochemical energy stored in the proton gradient to produce ATP, ADP should reduce ROS production.

In this study, we assessed at the level of isolated mitochondria from mouse hearts how chronic and acute oxidative stress affects the effect of ADP on CRC and ROS production. As models of long-term oxidative stress, we used old mice and diabetic mice. As models of acute oxidative stress, we used IR and exposure to a low dose of t-BH.

Methods

Ethics Statement

All procedures were in accordance with the NIH Guide for the Care and Use of Laboratory Animals and were approved by an Institutional Animal Care and Use Committee (University Committee on Animal Resources (UCAR) protocol 2010–030).

Animals and models of disease and oxidative stress

Control mice: 6-8 weeks old male C57BL6 mice (n=64). Aging: 12-15-month old male C57BL6 mice (n=8). Diabetes: To induce type I diabetes, 5 weeks old male C57BL6 mice (n=12) were injected intraperitoneally with 150 mg/kg streptozotocin dissolved in 0.1 mol/L sodium citrate buffer, pH 4, prepared within 5 min of administration. Mice were given drinking water supplemented with 7.5 % sucrose for 2.5 days to avoid severe hyperglycemia. After 5 weeks the mice were diabetic and used for experiments. Exposure to t-BH: Mitochondria from 6-8 weeks old C57BL6 male mice (n=44) were exposed to 5 µmol/L t-BH for 10 min before recording Ca^{2+}-uptake or ROS production. Ischemia-reperfusion injury: Male C57BL6 mice, 6-8 weeks old (n=20) were anesthetized with freshly prepared Avertin (2,2,2-tribromoethanol, 0.5 mg/kg injected intraperitoneally). Isolated hearts were retrogradely perfused in Langendorff mode under constant flow (4 ml/min) with Krebs–Henseleit buffer as in [19]. After 10 min of equilibration, hearts were subjected to 15 min of global ischemia followed by 60 min of reperfusion.

Unless otherwise stated, the mice were euthanized by CO_2 inhalation and sacrificed by cervical dislocation.

Isolation of heart mitochondria

Mitochondria from 2-4 mouse hearts were isolated using the protocol of Rehncrona et al with modifications [20]. The minced heart tissue was subjected to protease treatment: it was incubated with 5 mg nagarse dissolved in 10 ml medium A for 8 minutes at room temperature while gently stirring. The protease reaction was stopped by adding 1 ml of 0.2 mg/ml of bovine serum albumin dissolved in medium A. The tissue was then homogenized with a Potter-Elvehjem homogenizer, and mitochondria were isolated by differential centrifugation. The final mitochondrial pellet was suspended in isolation medium B.

For mitochondrial ROS generation measurements, mitochondria were Ca^{2+} depleted to minimize possible signalling of Ca^{2+} on ROS generation [21]. This procedure consisted of 15 min incubation at room temperature in Ca^{2+}-depletion buffer. The mitochondria were subsequently washed several times in a Ca^{2+}-depletion buffer without NaCl, EGTA and succinate. The isolated mitochondria were kept on ice and used within 4 hours. Protein concentration was determined by the Lowry method using BSA as a standard.

Ca^{2+} uptake measurements with arsenazo III

Ca^{2+} uptake was measured with arsenazo III at room temperature as a difference in absorbance at 662 nm and the background at 692 nm using Beckman Coulter DU 800 UV-Vis spectrophotometer (Beckman Coulter Inc., Brae, CA). Isolated mitochondria (~1 mg/ml of mitochondrial protein) were added to 1 ml Ca^{2+}-uptake buffer. The absorbance change upon Ca^{2+} addition was determined every 15 sec and followed for 30-70 min. Varying amounts of free Ca^{2+} were added every 2 minutes. Free Ca^{2+} concentrations were calculated using the MaxChelator program (http://www.stanford.edu/~cpatton/maxc.html).

Measurement of mitochondrial ROS production

Mitochondrial superoxide production was determined indirectly by coupling the dismutation of superoxide to H_2O_2. H_2O_2 was detected fluorimetrically using Amplex red (10-acetyl-3,7-dihydroxyphenoxazine), which reacts with H_2O_2 in a 1:1 stochiometry in the presence of horseradish peroxidase (HRP), producing highly fluorescent resorufin. For these experiments, mitochondria (~0.5 mg/ml of mitochondrial protein) were added to 2 ml ROS buffer. Fluorescence was recorded at room temperature using a Cary Eclipse fluorescence spectrophotometer (Varian Inc., Walnut Creek, CA). The excitation wavelength was 563 nm and the emitted fluorescence was detected at 587 nm. A calibration signal was generated with known amounts of H_2O_2 at the end of each experiment.

Measurement of mitochondrial oxygen consumption

Mitochondrial oxygen consumption was measured at room temperature using a Clark-type oxygen electrode from Hansatech (PP Systems, Boston MA).The measurements were carried out in 1 ml of respiration medium. The basal rate of respiration (State 2) was initiated by the addition of 5 mmol/L glutamate and 5 mmol/L malate as substrates. Maximal respiration rate (State 3) was measured in the presence of 1 mmol/L ADP. Respiration rates were expressed as nmol O_2 min^{-1} mg mitochondrial $protein^{-1}$. The respiratory control index (RCI) was calculated as RCI = State3/State2. At the end of each experiment, 8 µmol/L cytochrome c and 30 µmol/L atractyloside were added to test the intactness of the outer and inner mitochondrial membrane, respectively.

Solutions

Krebs–Henseleit buffer for Langendorff perfusion and IR (in mmol/L): 118 NaCl, 4.7 KCl, 1.2 $MgSO_4$, 24 $NaHCO_3$, 1.2 KH_2PO_4, 2.5 $CaCl_2$, 11 D-glucose.

For isolation of mitochondria, medium A contained (in mmol/L): 225 mannitol, 70 sucrose, 1 EGTA and 10 HEPES, pH 7.2. Medium B contained (in mmol/L): 225 mannitol, 70 sucrose, and 10 HEPES, pH 7.2.

Ca2+-depletion buffer contained (in mmol/L): 195 mannitol, 25 sucrose, 40 HEPES, 10 NaCl, 1 EGTA, 5 succinate, pH 7.2

For recording mitochondrial CRC, the Ca^{2+}-uptake buffer contained (in mmol/L): 120 KCl, 70 mannitol, 25 sucrose, 5 KH_2PO_4, 0.5 EGTA, 10 HEPES, pH 7.2 in the presence of 5 mmol/L malate and 5 mmol/L glutamate as substrates and 100 µmol/L arsenazo III.

For recording ROS production, the ROS buffer contained (in mmol/L): 120 KCl, 70 mannitol, 25 sucrose, 5 KH_2PO_4, 0.5 EGTA, 10 HEPES, pH 7.2, 10 µmol/L Amplex® red, 1 U/ml type II HRP, and 80 U/ml Cu/Zn superoxide dismutase.

For respiration experiments, respiration medium contained (in mmol/L): 120 KCl, 70 mannitol, 25 sucrose, 5 KH_2PO_4, 3 $MgCl_2$, 0.5 EGTA, 20 HEPES, pH 7.2.

Statistical analysis

All values are expressed as mean ± SEM. Data were analysed by a nonparametric Mann–Whitney U test. Differences were considered significant at $P < 0.05$.

Results

RCI of mitochondrial preparations

The quality of the mitochondrial preparations was controlled by recording their respiration rate in the presence of substrates alone, State 2, and after addition of 1 mmol/L ADP, State 3. RCI was calculated as State 3/State 2. These values are shown in Table 1. RCI in control mice was 7.6 ± 0.2, n=10. The respiratory parameters were not different in diabetic mice. Old mice had a lower State 2 (8.6 ± 0.8, P = 0.057, n=7) and State 3 (61.3 ± 6.7, P = 0.028, n=7), but RCI was the same as in control (7.0 ± 0.4, P = 0.222, n=7). This may be attributed to a fraction of the mitochondria having already undergone mPTP. However, their CRC was the same as in control (see below).

Table 1. Respiration of isolated mouse heart mitochondria from control mice and different models of chronic and acute oxidative stress.

	n	State 2	State 3	RCI
Control	10	13.1 ± 1.4	100.8 ± 12.0	7.6 ± 0.2
Aging	7	8.6 ± 0.8	61.3 ± 6.7*	7.0 ± 0.4
Diabetes	3	14.1 ± 2.8	83.8 ± 11.3	6.2 ± 0.9
IR	4	9.3 ± 1.1	48.8 ± 6.4	5.3 ± 0.6**
t-BH	3	9.3 ± 1.4	64.1 ± 8.6	6.9 ± 0.4

Basal respiration rate in the absence of ADP (State 2), respiration rate in the presence of 1mmol/L ADP (State 3), and respiration control index (RCI = State 3/ State 2). Respiration rates are expressed as nmol O_2 min^{-1} mg mitochondrial $protein^{-1}$. Number of experiments is given in column n. Results were compared by a nonparametric Mann–Whitney U test. * and ** denote $P < 0.05$ and $P < 0.01$, respectively, compared to control.

doi: 10.1371/journal.pone.0083214.t001

The low concentration of t-BH (5 µmol/L for 10 min) does not affect glutamate and malate-dependent respiration [22], and this was confirmed in our recordings, where State 2 and 3 and RCI was not significantly different from control. RCI was significantly lower after IR (5.3 ± 0.6, P = 0.009, n=4), consistent with an inhibition of electron transport chain activities after severe stress.

The protective effect of ADP is specific to [ADP]

The inhibition of mPTP by ADP has been widely reported including the seminal studies by Haworth and Hunter [23–25], in which the mPTP phenomenon was discovered. When adding ADP to the solution with isolated mitochondria in the presence of substrates, the majority will be converted into ATP. After a short period of time, an equilibrium between [ADP] and [ATP] will be reached. Oligomycin inhibits the conversion of ADP into ATP by F_1F_0-ATPase. Thus, [ADP] will be higher in the presence of oligomycin. We addressed the question whether the total amount of adenine nucleotides ([ADP] + [ATP]) or [ADP] specifically is important for the inhibition of mPTP. Figures 1A and B show representative traces of Ca^{2+}-uptake recordings. Figure 1C summarizes the mitochondrial Ca^{2+}-uptake capacity under various conditions as indicated below each column. Ca^{2+}-uptake capacity for control and 500 µmol/L ADP was 344 ± 32 nmol/mg protein and 774 ± 65 nmol/mg protein, respectively, confirming that ADP inhibited mPTP potently. 1 mmol/L ATP and 10 mmol/L creatine, which stimulate mitochondrial creatine kinase to generate ADP, had a similar effect as 500 µmol/L ADP on Ca^{2+}-uptake capacity (P = 0.432). A smaller dose of ADP, 50 µmol/L, had a significantly smaller effect increasing CRC to only 458 ± 30 nmol/mg protein (Figure 1C) (P = 0.003 compared to 500 µmol/L ADP; P = 0.013 compared to 1 mmol/L ATP and creatine). Inhibition of the F_1F_0-ATPase with 5 µmol/L oligomycin had a negative effect on Ca^{2+}-uptake capacity, which decreased to approximately 62% of control (P = 0.016, Figure 1C). However, in the presence of oligomycin, 50 µmol/L ADP had a significantly larger effect on CRC, which increased from 213 ±

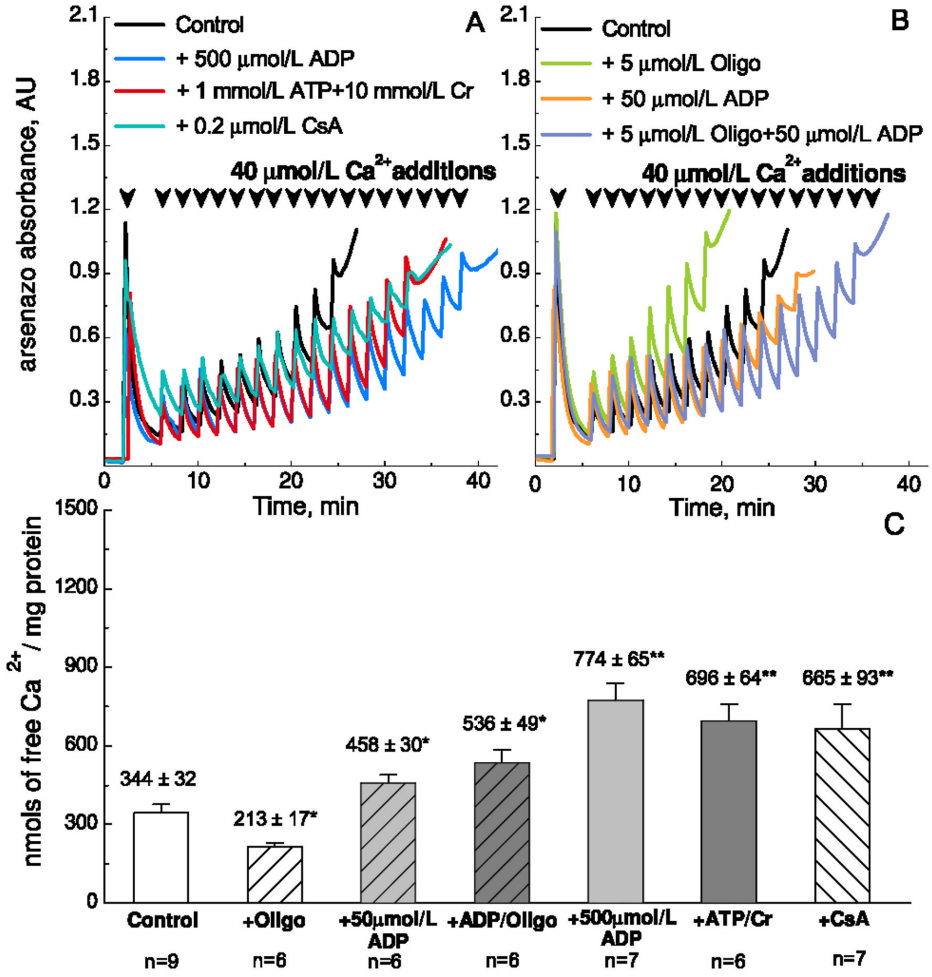

Figure 1. Ca^{2+}-uptake capacity of isolated heart mitochondria from control mice. A-B. Representative raw traces of the Ca^{2+}-uptake experiments. Mitochondria were incubated with Arsenazo III to follow extramitochondrial Ca^{2+} spectrophotometrically. Consecutive pulses leading to an increase of 40 µmol/L free Ca^{2+} were added as indicated by arrow heads. The CRC was defined as the concentration at which the mitochondria failed to accumulate more Ca^{2+} and mPTP opened to release all Ca^{2+} so far accumulated by the mitochondria. A. Traces are shown with mitochondria from control mice, 6-8 weeks old, under control conditions (no additions; black), in the presence of 500 µmol/L ADP (blue), 1 mmol/L ATP and 10 mmol/L creatine (Cr) (red), and 0.2 µmol/L cyclosporine A (CsA) (turquoise). B. Representative raw traces of the Ca^{2+}-uptake experiments in the presence of 5 µmol/L oligomycin (green), 50 µmol/L ADP (orange), 5 µmol/L oligomycin and 50 µmol/L ADP (violet). C. Column diagrams of the averaged results under the conditions indicated below. The amount of Ca^{2+} was normalized to the mitochondrial content (mg protein). All values are mean ± SEM. * and ** denote significant difference $P < 0.05$, and $P<0.01$, respectively, between treatment and control. The number of experiments is indicated below.

doi: 10.1371/journal.pone.0083214.g001

17 nmol/mg protein to 536 ± 49 nmol/mg protein. Thus, [ADP] is the most important inhibitor of mPTP.

ADP recovers mitochondrial Ca^{2+}-uptake capacity after acute oxidative stress

Figure 2 shows the CRC in the different models of oxidative stress. Ca^{2+} was added consecutively to isolated mitochondria until they reached their maximum uptake capacity, where mPTP opened to release all Ca^{2+}, causing an increase in extramitochondrial Ca^{2+} as monitored by Arsenazo III absorbance. Control mitochondria were able to sequester up to 10 pulses of 40 µmol/L free Ca^{2+} with a mean value of 344 ± 32 nmol/mg protein (Figure 1A and Figure 1C). We were surprised to find that chronic oxidative stress did not affect the initial CRC or the effect of ADP (Figure 2C-D). In contrast, acute oxidative stress had an adverse effect on mitochondrial CRC by facilitating mPTP opening. After IR or t-BH exposure, the first addition of 40 µmol/L Ca^{2+} was able to trigger mPTP opening (Figure 2B, red trace). Therefore, 0.2 µmol/L and 5 µmol/L Ca^{2+} additions were used for assessing mitochondrial CRC after IR and t-BH treatments, respectively (Figure 2B). The CRC was dramatically decreased to 1 ± 0.2 nmol/mg protein (IR) and 32 ± 4 nmol/mg protein (t-BH) (Figure 2E-F).

CsA is a well-known inhibitor of CypD and protects against ischemia-reperfusion damage at a concentration of 0.2 µmol/L [26]. Indeed, this concentration of CsA increased CRC in all models (Figure 2). 500 µmol/L ADP had a similar effect and restored CRC to 447 ± 105 nmol/mg protein after IR and to 514 ± 103 nmol/mg protein after t-BH exposure, respectively (Figure 2E-F). The recovered CRC was not significantly different from that of control mice in the absence of ADP ($P = 0.109$ for t-BH and $P = 0.689$ for IR, respectively, Figure 2E-F). Thus, ADP is a potent inhibitor of mPTP – also in mitochondria, which have been exposed to severe oxidative stress.

Similar effect of ADP irrespective of initial Ca^{2+}-uptake capacity

Figure 3 is a column diagram showing the effect of ADP – i.e. how much does ADP increase CRC. It illustrates, as noted above, that 50 µmol/L ADP increased CRC much more, when F_1F_0-ATPase was inhibited by oligomycin ($P = 0.008$). But what is in our opinion more remarkable, is the fact that although CRC was drastically lowered by acute oxidative stress (IR and t-BH) to the extent that mitochondrial Ca^{2+}-buffering was almost absent (Figure 2E-F), ADP exerted a similar effect as in mitochondria from control mice. In control as well as all model of oxidative stress, 500 µmol/L ADP increased CRC by 360-460 nmol/mg protein (Figure 3).

In mitochondria from control mice, the increase in Ca^{2+}-uptake capacity induced by 50 µmol/L ADP in the absence and presence of oligomycin, and 500 µmol/L ADP alone and in the presence of cyclosporine A (CsA) are shown as indicated. In models of chronic and acute oxidative stress, the increase induced by 500 µmol/L ADP is shown as indicated below the columns. The increase induced by 500 µmol/L ADP is remarkably consistent in control and the different models of oxidative stress.

ADP attenuates ROS generation in control, but not after exposure to t-BH

In addition to Ca^{2+}, ROS are also potent activators of mPTP. To determine whether ADP-mediated ROS decrease contributes to the inhibition of mPTP, we measured ROS production in the preparations. Amplex Red was used to record ROS production with three consecutive steps: 1) mitochondria alone, 2) after addition of substrates (glutamate and malate), and 3) after the addition of one pulse of a submaximal Ca^{2+}-concentration to trigger partial opening of mPTP. The data on ROS production in old and diabetic mice and after IR did not give any new information. Therefore, we show only the results from control and after t-BH exposure. Figure 4A shows original traces of recordings from control mice and the results are summarized in Figure 4C. As expected, ROS production increased upon addition of substrates, as indicated by the increase in the slope of Amplex Red fluorescence trace. Addition of 250 µmol/L Ca^{2+} increased ROS production further (Figure 4A and C, control). ADP or ATP and creatine, which stimulate F_1F_0-ATPase to utilize the proton gradient, both significantly abolished the substrate- and Ca^{2+}-induced increase in ROS generation (Figure 4C). CsA abolished mostly the Ca^{2+}-induced increase in ROS generation, but the net effects were significantly smaller than those of ADP (Figure 4C, $P = 0.003$ and $P = 0.002$ for substrate- and Ca^{2+}-induced increase in ROS generation, respectively).

In mitochondria exposed to t-BH, ROS-production was much higher than in control (Figure 4B and D). Neither Ca^{2+} nor ADP and CsA had a profound effect on ROS-production. This implies that the ADP-induced increase in mitochondrial Ca^{2+}-uptake capacity is not related to a decrease in ROS-production in mitochondria treated with t-BH.

Discussion

The most notable results from this study are that 1) ADP increases CRC after IR and t-BH exposure to an extent that is remarkably similar to that in control, and 2) the effect of ADP on CRC in mitochondria exposed to t-BH is not the result of a decreased ROS-production.

Inhibition of mPTP relates to the concentration of ADP

The main mechanism through which ADP decreases mitochondrial Ca^{2+}-sensitivity has been attributed to the binding of ADP to ANT, which stabilizes the transporter in the m-state and prevents pore opening [27]. It was demonstrated that ANT is not a pore-forming component of the mPTP, as mPTP opening is still triggered in mice lacking ANT1 and ANT2 [28]. However, the regulating role of ANT cannot be disputed, as inhibition of ANT in different conformations by bongkrekic acid or atractyloside has opposite effects on mitochondrial Ca^{2+}-sensitivity [4]. Haworth and Hunter proposed that ADP exerts its effect by binding to an internal site as well as to ANT [23]. Recent studies suggest that either the mitochondrial phosphate carrier or F_1F_0-ATPase could be one of the key components for mPTP [13,14,29,30]. Both cases include a role for ADP [13,29]. In the latter case, ADP affects mPTP via direct binding to F_0F_1-

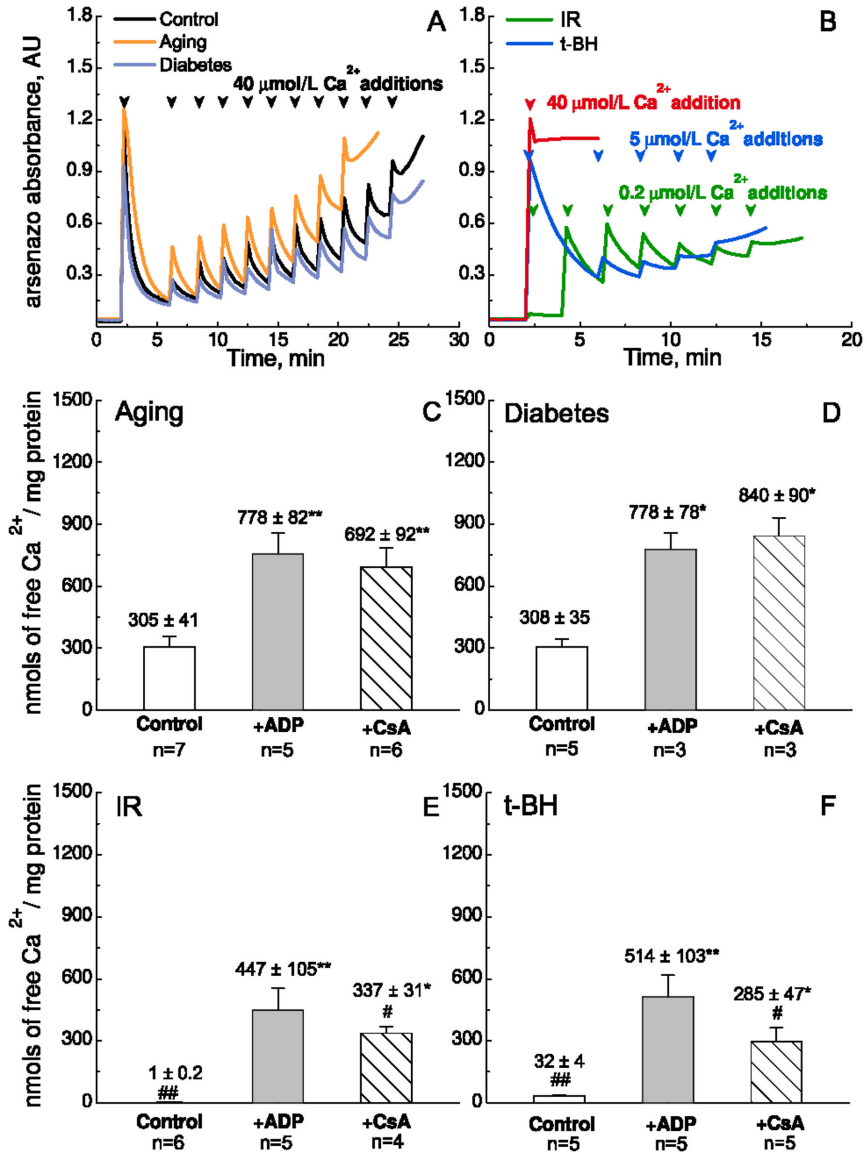

Figure 2. Ca^{2+}-uptake capacity of isolated mouse heart mitochondria from different models of chronic and acute oxidative stress. A-B: Representative raw traces of the Ca^{2+}-uptake from different models under control conditions. A. Control mice (black); Aging (orange); Diabetes (violet). Pulses of 40 µmol/L free Ca^{2+} were added as indicated by arrow heads. B. Ischemia-reperfusion, IR (green); exposure to 5 µmol/L tert-butyl hydroperoxide, t-BH, (blue). Pulses of 40 µmol/L (red), 0.2 µmol/L (green), and 5 µmol/L (blue) free Ca^{2+} were added respectively as indicated by arrow heads. C-F: Column diagrams of the averaged results under the conditions indicated below. The final concentrations of ADP and CsA are 500 µmol/L and 0.2 µmol/L, respectively. The amount of Ca^{2+} was normalized to the mitochondrial content (mg protein). All values are mean ± SEM. * and ** denote significant difference $P < 0.05$ and $P < 0.01$ respectively, between treatment and control within an animal group. # and ## denote significant difference $P < 0.05$ and $P<0.01$, respectively, between animal groups with similar treatment.

doi: 10.1371/journal.pone.0083214.g002

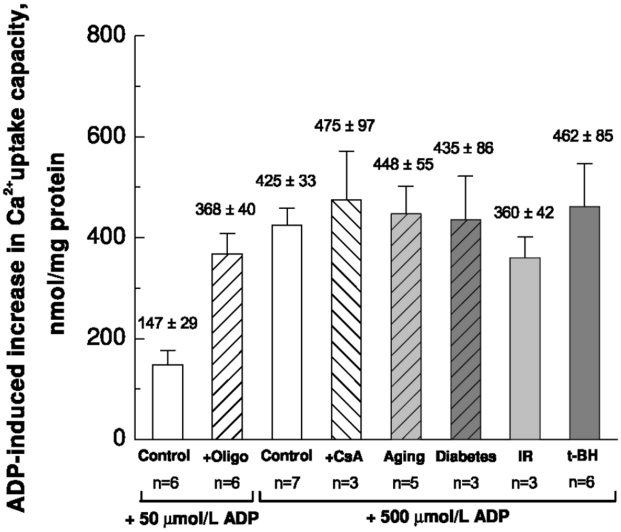

Figure 3. Increase in mitochondrial Ca^{2+}-uptake capacity induced by ADP.

doi: 10.1371/journal.pone.0083214.g003

ATPase. This, however, does not exclude an additional effect via ADP-binding to ANT.

The present study showed that the effect of ADP on CRC relates to its concentration. 500 μmol/L ADP had a signifcantly larger effect than 50 μmol/L ADP (Figure 1). Also, 50 μmol/L ADP had a significantly larger effect in the presence of oligomycin to inhibit ADP-turnover by F_1F_0-ATPase (Figure 1B-C). Thus, the effect of ADP is specific to [ADP] and not the total concentration of adenine nucleotides.

It is noticed that oligomycin on its own has a negative effect on mitochondrial Ca^{2+}-uptake capacity (Figure 1B-C). The mitochondrial membrane potential decreases as the mitochondria take up a significant amout of Ca^{2+}. It is conceivable that in the absence of oligomycin, the mitochondria will hydrolyze ATP to ADP in order to maintain their membrane potential. However, oligomycin renders the mitochondria unable to rescue their membrane potential, so that the critical potential at which mPTP opens is reached at a lower Ca^{2+}-concentration.

Ca^{2+}-sequestration has no significant effect on CRC

ADP can buffer Ca^{2+} by itself [31], and could have an additional effect on mitochondrial Ca^{2+} buffering such as the maintenance of high matrix Pi concentrations. It has been shown that ATP-Mg^{2-}/Pi^{2-} and $HADP^{2-}$/Pi^{2-} can increase matrix Ca^{2+} buffering via Ca^{2+}-Pi precipitates and thus desensitize the mPTP [32,33]. Mitochondrial Ca^{2+}-sequestration is proportional to the ADP-uptake [32]. If Ca^{2+}-sequestration played a significant role in the effect of ADP, we would expect that the Ca^{2+}-uptake capacity is increased more by 500 μmol/L ADP than by 50 μmol/L ADP in the presence of oligomycin. Our results suggest that this is not the case (Figures 1 and 3). However, the role of Ca^{2+}-sequestration should be studied further by quantifying intra- and extramitochondrial total and free [Ca^{2+}] as mitochondria take up Ca^{2+} after successive Ca^{2+}-pulses.

Similar effect of ADP on CRC in all models of oxidative stress

Oxidative stress has an unfavourable effect on mitochondrial CRC [5]. We studied the effect of ADP on CRC in different models of increased oxidative stress. Chronic oxidative stress by aging and diabetes had no significant impact on CRC or the effect of ADP. However, the acute oxidative damage caused by IR and t-BH drastically lowered CRC to the extent that mitochondrial Ca^{2+}-uptake was almost absent. It is interesting that ADP was able to restore this function (Figures 2E-F) and with an effect that was similar to that in control (Figure 3). It appears that irrespective of the healthiness of mitochondria, a certain amount of ADP increases CRC by a certain amount. This is interesting, because ADP-binding to ANT is reduced by oxidative stress [15]. Therefore, our results suggest that although ADP to some extent inhibits mPTP opening via binding to ANT, significant inhibition also occurs by some other mechanism.

ADP does not increase CRC via an effect on ROS-production in mitochondria exposed to t-BH

In addition to Ca^{2+}, ROS also effectively trigger mPTP openings. One of the aims of this study was to see whether ADP might affect mitochondrial CRC via ROS decrease in the models of oxidative stress. In our study, we used Amplex red and horseradish peroxidase as a H_2O_2 detection system. This allowed us to use the efflux of H_2O_2 from mitochondria as a

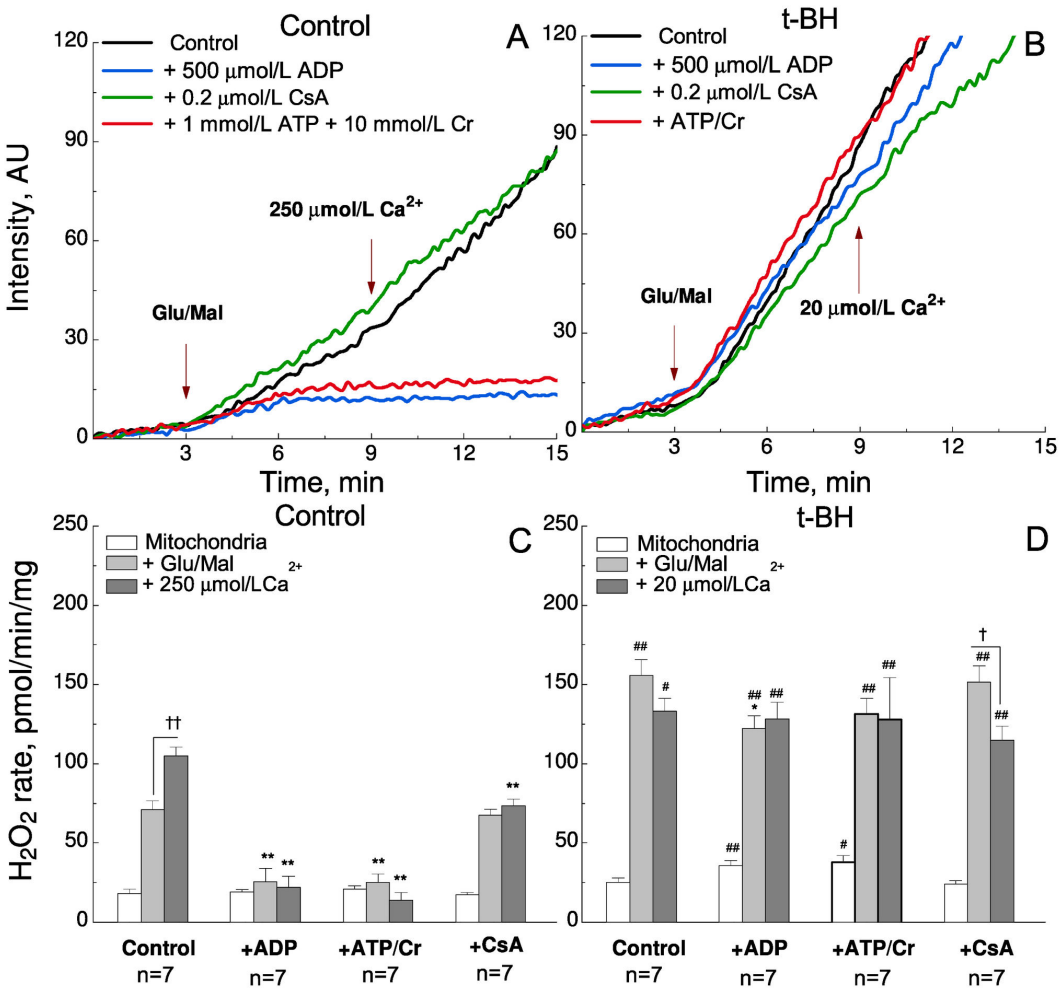

Figure 4. Rate of ROS production in mitochondria from control mice and after t-BH exposure. A-B: Representative raw traces of the ROS-recordings. The rate of hydrogen peroxide (H_2O_2) production was followed spectrofluorometrically by its reaction with Amplex Red in the presence of horseradish peroxidase. The rate of ROS production was recorded in three consecutive steps: After addition of mitochondria alone, after addition of substrates (5 mM glutamate and 5 mM malate) and after addition of one submaximal dose of Ca^{2+}. Traces are shown under control conditions (no additions; black), in the presence of 500 µmol/L ADP (blue), 0.2 µmol/L CsA (green), and 1mmol/L ATP + 10 mmol/L creatine (Cr) (red). A: control mice; B: after exposure to 5 µmol/L t-BH. C-D: Column diagrams of the averaged results under the conditions indicated below each column. Steady-state H_2O_2 production was recorded in the mitochondria alone (rate between 1-3 min; white columns), after addition of substrates (rate between 6.5-8.5 min; light grey columns), and after addition Ca^{2+} (rate between 11-15 min; dark grey columns). Treatments within each group are indicated below the columns. All values are mean ± SEM. † and †† denote significant effect of substrates and/or Ca^{2+}, $P < 0.05$, $P < 0.01$ respectively. *, ** denote significant difference $P < 0.05$, and $P < 0.01$, respectively, between control and different treatments within the group. **#**and ## denote significant difference ($P < 0.05$ and $P<0.01$, respectively) between control and t-BH with the same treatment. The number of experiments is indicated below.

doi: 10.1371/journal.pone.0083214.g004

measure of net superoxide production in the matrix. Under physiological conditions, the production of ROS and their consumption in the form of H_2O_2 is finely tuned. ROS are mainly produced as superoxide by complexes I and III in the mitochondrial electron transport chain [34]. Superoxide is dismutated to H_2O_2 by manganese superoxide dismutase (MnSOD) in the mitochondrial matrix and copper/zinc superoxide dismutase (Cu/ZnSOD) in the mitochondrial intermembrane space and cytosol. The resulting H_2O_2 can easily diffuse across membranes to be detected by the assay. However, H_2O_2 can also be consumed by matrix enzymes, e.g. glutathione peroxidases, and cause an underestimate of superoxide production by competing with the efflux of H_2O_2 [35]. By a series of redox reactions, H_2O_2 is converted to H_2O, while glutathione (GSH) is oxidized to glutathione disulfide (GSSG). GSSG is reduced back to GSH by the oxidation of pyridine nucleotides (NADH/NADPH). The GSH/GSSG ratio provides an estimate of cellular redox buffering capacity, thus playing a key role in maintaining redox homeostasis [36].

ADP can regulate mitochondrial ROS production through complexes I and III, as well as general redox state of the mitochondrial matrix (NADH/NADPH, GSH) via oxidative phosphorylation. Indeed, the addition of ADP caused a decrease in H_2O_2 export from control mitochondria (Figure 4A and C). However, in t-BH treated mitochondria the fine tuning of ROS production and consumption by ADP in mitochondria is disturbed (Figure 4B-D). t-BH treatment induces the oxidation of pyridine nucleotides [37] and GSH [38]. GSSG is not exported from the mitochondria [39] and increased GSSG formation may decrease the activity of mitochondrial redox-sensitive proteins [40–46]. As a result, H_2O_2 export is increased in t-BH mitochondria (Figure 4B-D). Although ADP does reduce ROS, it is not able to bring it down to control level (Figure 4D). Thus, the t-BH results demonstrate that ADP regulates mitochondrial CRC not only via ROS reduction, but via some other mechanisms as well.

Conclusion

ADP is well known to desensitize the mPTP to intramitochondrial Ca^{2+}, so that the mitochondria can take up more Ca^{2+}, before opening of mPTP is triggered. In the present study, we found that ADP had the same effect in severely stressed mitochondria as in control. This suggests that ADP, in addition to its regulation via ANT, exerts significant regulation of mPTP via some other mechanism. Although ADP decreases ROS production in control mitochondria, its effect is minor in t-BH-treated mitochondria. Therefore, we conclude that at least in some cases e.g. t-BH treatment, the ADP-induced increase in mitochondrial Ca^{2+}-uptake capacity is not related to a reduction in ROS. It is likely that significant regulation by ADP occurs via its internal binding site (reported in [23]), which could be on F_1F_0-ATPase [29].

From a more integrated point of view, it is very interesting that ADP is as potent an inhibitor of mPTP in severely stresssed mitochondria, and that its effect relates to the concentration. Namely, ADP concentrations increase in the diseased state due to less efficienct ATP production, depolarized mitochondrial membrane potential, Ca^{2+} overload, and a smaller pH gradient [47–49]. It is plausible that this increase in ADP concentration could protect against opening of mPTP and thus delay the injury and death of cells. This function of ADP as a regulator of mitochondrial ATP production, Ca^{2+} homeostasis, and ROS generation is shown schematically in Figure 5. Under physiological conditions, it serves as a substrate for ATP synthesis while ensuring the closure of mPTP and modest ROS generation. Under pathological conditions like IR injury, when the mitochondria are most vulnerable for mPTP opening, ADP can effectively delay mPTP opening so that mitochondrial membrane integrity can be preserved to maintain energy production. The ability of ADP to serve multiple roles as a potent mPTP blocker, a substrate for catalysing ATP generation, and an inhibitor for ROS generation, makes it a unique molecule to preserve mitochondrial function under pathophysiological conditions.

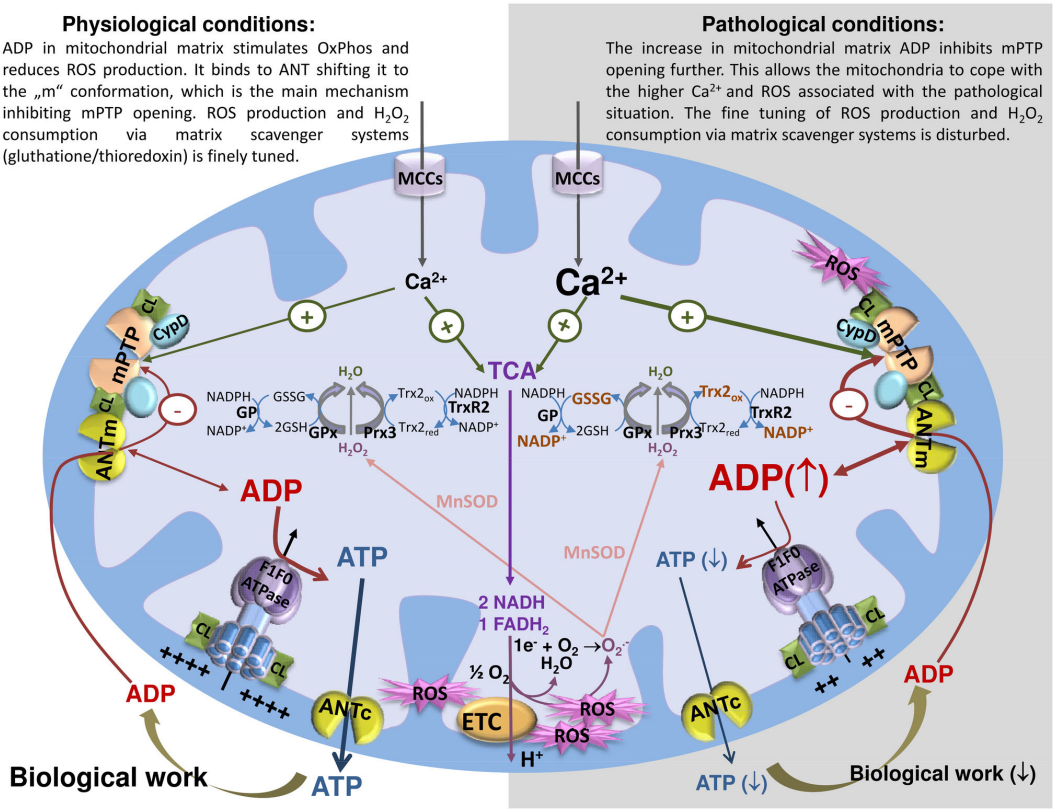

Figure 5. ADP is a master regulator of mitochondrial ATP production, Ca^{2+} homeostasis, and ROS generation. Under physiological conditions, optimal ADP concentrations in mitochondrial matrix serve effectively to maximize ATP generation while minimizing ROS. ROS production via ETC and annihilation via matrix scavenger systems (gluthatione/thioredoxin) is finely balanced. Under pathological conditions, mitochondrial Ca^{2+} and ROS increase, stimulate excessive mPTP opening and thus the signaling pathway for injury. These detrimental effects are countered by a concomitant increase in ADP, which allows the mitochondria to endure a larger load of Ca^{2+} and ROS, maintaining mitochondrial integrity and function when it is most critical.
ANTm – ANT in the “m”-conformation; ANTc – ANT in the “c”-conformation; CL - cardiolipin; CypD – cyclophilin D; ETC – electron transport chain; GR – glutathione reductase; GRx – glutathione peroxidase; GSH – reduced glutathione; GSSG – oxidized glutathione; MCCs – mitochondrial calcium channels; MnSOD – manganese superoxide dismutase; mPTP – mitochondrial permeability transition pore; Prx3 – peroxiredoxin 3; ROS – reactive oxygen species, TCA – tricarboxylic acid cycle; $Trx2_{red}$ - reduced thioredoxin 2; $Trx2_{ox}$ – oxidized thioredoxin 2; TrxR2 – thioredoxin reductase 2.
doi: 10.1371/journal.pone.0083214.g005

Acknowledgements

We thank Dr. Sergiy M Nadtochiy at the University of Rochester Medical Center (URMC) for his support on Langendorff perfusion of the mouse hearts, and Dr. Paul Brookes (URMC) for the use of spectrophotometer. We also thank the members of the Mitochondrial Research and Innovation Group (MRIG) at URMC for their comments.

Author Contributions

Conceived and designed the experiments: SSS GB NS. Performed the experiments: NS S. Pan S. Provazza. Analyzed the data: NS MV RB. Contributed reagents/materials/analysis tools: SSS GB. Wrote the manuscript: RB NS S. Pan GB SSS. Prepared all the figures: NS.

References

1. Balaban RS (2002) Cardiac energy metabolism homeostasis: role of cytosolic calcium. J Mol Cell Cardiol 34: 1259–1271. PubMed: 12392982.
2. Vendelin M, Kongas O, Saks V (2000) Regulation of mitochondrial respiration in heart cells analyzed by reaction-diffusion model of energy transfer. Am J Physiol Cell Physiol 278: C747 –C764. PubMed: 10751324.
3. Brdiczka DG, Zorov DB, Sheu S-S (2006) Mitochondrial contact sites: their role in energy metabolism and apoptosis. Biochim Biophys Acta 1762: 148–163. doi:10.1016/j.bbadis.2005.09.007. PubMed: 16324828.
4. Haworth RA, Hunter DR (2000) Control of the mitochondrial permeability transition pore by high-affinity ADP binding at the ADP/ATP translocase in permeabilized mitochondria. J Bioenerg Biomembr 32: 91–96. PubMed: 11768766.
5. Lemasters JJ, Theruvath TP, Zhong Z, Nieminen AL (2009) Mitochondrial calcium and the permeability transition in cell death. Biochim_Biophys_Acta 1787: 1395–1401.
6. Halestrap AP (2010) A pore way to die: the role of mitochondria in reperfusion injury and cardioprotection. Biochem Soc Trans 38: 841–860. doi:10.1042/BST0380841. PubMed: 20658967.
7. Baines CP (2009) The mitochondrial permeability transition pore and ischemia-reperfusion injury. Basic Res Cardiol 104: 181–188. doi: 10.1007/s00395-009-0004-8. PubMed: 19242640.
8. Di Lisa F, Carpi A, Giorgio V, Bernardi P (2011) The mitochondrial permeability transition pore and cyclophilin D in cardioprotection. Biochim Biophys Acta 1813: 1316–1322. doi:10.1016/j.bbamcr.2011.01.031. PubMed: 21295622.
9. Leung AW, Halestrap AP (2008) Recent progress in elucidating the molecular mechanism of the mitochondrial permeability transition pore. Biochim Biophys Acta 1777: 946–952. PubMed: 18407825.
10. Giorgio V, Soriano ME, Basso E, Bisetto E, Lippe G et al. (2010) Cyclophilin D in mitochondrial pathophysiology. Biochim Biophys Acta 1797: 1113–1118. PubMed: 20026006.
11. Juhaszova M, Wang S, Zorov DB, Nuss HB, Gleichmann M et al. (2008) The identity and regulation of the mitochondrial permeability transition pore: where the known meets the unknown. Ann N Y Acad Sci 1123: 197–212. doi:10.1196/annals.1420.023. PubMed: 18375592.
12. Halestrap AP, Connern CP, Griffiths EJ, Kerr PM (1997) Cyclosporin A binding to mitochondrial cyclophilin inhibits the permeability transition pore and protects hearts from ischaemia/reperfusion injury. Mol Cell Biochem 174: 167–172. doi:10.1023/A:1006879618176. PubMed: 9309682.
13. Giorgio V, Von Stockum S, Antoniel M, Fabbro A, Fogolari F et al. (2013) Dimers of mitochondrial ATP synthase form the permeability transition pore. Proc Natl Acad Sci U S A 110: 5887–5892. doi:10.1073/pnas.1217823110. PubMed: 23530243.
14. Giorgio V, Bisetto E, Soriano ME, Dabbeni-Sala F, Basso E et al. (2009) Cyclophilin D modulates mitochondrial F0F1-ATP synthase by interacting with the lateral stalk of the complex. J Biol Chem 284: 33982–33988. doi:10.1074/jbc.M109.020115. PubMed: 19801635.
15. McStay GP, Clarke SJ, Halestrap AP (2002) Role of critical thiol groups on the matrix surface of the adenine nucleotide translocase in the mechanism of the mitochondrial permeability transition pore. Biochem J 367: 541–548. doi:10.1042/BJ20011672. PubMed: 12149099.
16. Carafoli E (2010) The fateful encounter of mitochondria with calcium: how did it happen? Biochim Biophys Acta 1797: 595–606. doi:10.1016/j.bbabio.2010.03.024. PubMed: 20385096.
17. Chinopoulos C, Adam-Vizi V (2010) Mitochondrial Ca2+ sequestration and precipitation revisited. FEBS J 277: 3637–3651. doi:10.1111/j.1742-4658.2010.07755.x. PubMed: 20659160.
18. Saito A, Castilho RF (2010) Inhibitory effects of adenine nucleotides on brain mitochondrial permeability transition. Neurochem Res 35: 1667–1674. doi:10.1007/s11064-010-0228-x. PubMed: 20652632.
19. Nadtochiy SM, Tompkins AJ, Brookes PS (2006) Different mechanisms of mitochondrial proton leak in ischaemia/reperfusion injury and preconditioning: implications for pathology and cardioprotection. Biochem J 395: 611–618. doi:10.1042/BJ20051927. PubMed: 16436046.
20. Rehncrona S, Mela L, Siesjö BK (1979) Recovery of brain mitochondrial function in the rat after complete and incomplete cerebral ischemia. Stroke 10: 437–446. doi:10.1161/01.STR.10.4.437. PubMed: 505482.
21. Hoffman DL, Salter JD, Brookes PS (2007) Response of mitochondrial reactive oxygen species generation to steady-state oxygen tension: implications for hypoxic cell signaling. Am J Physiol Heart Circ Physiol 292: H101–H108. doi:10.1152/ajpheart.00699.2006. PubMed: 16963616.
22. Endlicher R, Kriváková P, Rauchová H, Nůsková H, Cervinková Z et al. (2009) Peroxidative damage of mitochondrial respiration is substrate-dependent. Physiol Res 58: 685–692. PubMed: 19093725.
23. Hunter DR, Haworth RA (1979) The Ca2+-induced membrane transition in mitochondria. I. The protective mechanisms. Arch Biochem Biophys 195: 453–459. doi:10.1016/0003-9861(79)90371-0. PubMed: 383019.
24. Haworth RA, Hunter DR (1979) The Ca2+-induced membrane transition in mitochondria. II. Nature of the Ca2+ trigger site. Arch Biochem Biophys 195: 460–467. doi:10.1016/0003-9861(79)90372-2. PubMed: 38751.
25. Hunter DR, Haworth RA (1979) The Ca2+-induced membrane transition in mitochondria. III. Transitional Ca2+ release. Arch Biochem Biophys 195: 468–477. doi:10.1016/0003-9861(79)90373-4. PubMed: 112926.
26. Griffiths EJ, Ocampo CJ, Savage JS, Stern MD, Silverman HS (2000) Protective effects of low and high doses of cyclosporin A against reoxygenation injury in isolated rat cardiomyocytes are associated with differential effects on mitochondrial calcium levels. Cell Calcium 27: 87–95. doi:10.1054/ceca.1999.0094. PubMed: 10756975.
27. Klingenberg M (2008) The ADP and ATP transport in mitochondria and its carrier. Biochim Biophys Acta 1778: 1978–2021. doi:10.1016/j.bbamem.2008.04.011. PubMed: 18510943.
28. Kokoszka JE, Waymire KG, Levy SE, Sligh JE, Cai J et al. (2004) The ADP/ATP translocator is not essential for the mitochondrial permeability transition pore. Nature 427: 461–465. doi:10.1038/nature02229. PubMed: 14749836.
29. Leung AWC, Halestrap AP (2008) Recent progress in elucidating the molecular mechanism of the mitochondrial permeability transition pore. Biochimica et Biophysica Acta (BBA) - Bioenergetics 1777: 946–952. Available online at: doi:10.1016/j.bbabio.2008.03.009
30. Bonora M, Bononi A, De Marchi E, Giorgi C, Lebiedzinska M et al. (2013) Role of the c subunit of the FO ATP synthase in mitochondrial permeability transition. Cell Cycle 12: 674–683. doi:10.4161/cc.23599. PubMed: 23343770.
31. Michailova A, McCulloch A (2001) Model study of ATP and ADP buffering, transport of Ca(2+) and Mg(2+), and regulation of ion pumps in ventricular myocyte. Biophys J 81: 614–629. doi:10.1016/S0006-3495(01)75727-X. PubMed: 11463611.
32. CARAFOLI E, Rossi CS, LEHNINGER AL (1965) UPTAKE OF ADENINE NUCLEOTIDES BY RESPIRING MITOCHONDRIA DURING ACTIVE ACCUMULATION OF CA++ AND PHOSPHATE. J Biol Chem 240: 2254–2261. PubMed: 14299656.
33. Traba J, Del Arco A, Duchen MR, Szabadkai G, Satrústegui J (2012) SCaMC-1 promotes cancer cell survival by desensitizing mitochondrial permeability transition via ATP/ADP-mediated matrix Ca(2+) buffering. Cell Death Differ 19: 650–660. doi:10.1038/cdd.2011.139. PubMed: 22015608.
34. Turrens JF (2003) Mitochondrial formation of reactive oxygen species. J Physiol (Lond) 552: 335–344. doi:10.1113/jphysiol.2003.049478.

35. Treberg JR, Quinlan CL, Brand MD (2010) Hydrogen peroxide efflux from muscle mitochondria underestimates matrix superoxide production--a correction using glutathione depletion. FEBS J 277: 2766–2778. doi:10.1111/j.1742-4658.2010.07693.x. PubMed: 20491900.
36. Schafer FQ, Buettner GR (2001) Redox environment of the cell as viewed through the redox state of the glutathione disulfide/glutathione couple. Free Radic Biol Med 30: 1191–1212. doi:10.1016/S0891-5849(01)00480-4. PubMed: 11368918.
37. Nieminen AL, Byrne AM, Herman B, Lemasters JJ (1997) Mitochondrial permeability transition in hepatocytes induced by t-BuOOH: NAD(P)H and reactive oxygen species. Am J Physiol 272: C1286–C1294. PubMed: 9142854.
38. Sies H, Moss KM (1978) A role of mitochondrial glutathione peroxidase in modulating mitochondrial oxidations in liver. Eur J Biochem 84: 377–383. doi:10.1111/j.1432-1033.1978.tb12178.x. PubMed: 25178.
39. Olafsdottir K, Reed DJ (1988) Retention of oxidized glutathione by isolated rat liver mitochondria during hydroperoxide treatment. Biochim Biophys Acta 964: 377–382. doi:10.1016/0304-4165(88)90038-4. PubMed: 3349102.
40. Hurd TR, Costa NJ, Dahm CC, Beer SM, Brown SE et al. (2005) Glutathionylation of mitochondrial proteins. Antioxid Redox Signal 7: 999–1010. doi:10.1089/ars.2005.7.999. PubMed: 15998254.
41. Taylor ER, Hurrell F, Shannon RJ, Lin T-K, Hirst J et al. (2003) Reversible glutathionylation of complex I increases mitochondrial superoxide formation. J Biol Chem 278: 19603–19610. doi:10.1074/jbc.M209359200. PubMed: 12649289.
42. Fratelli M, Demol H, Puype M, Casagrande S, Villa P et al. (2003) Identification of proteins undergoing glutathionylation in oxidatively stressed hepatocytes and hepatoma cells. Proteomics 3: 1154–1161. doi:10.1002/pmic.200300436. PubMed: 12872216.
43. Garcia J, Han D, Sancheti H, Yap L-P, Kaplowitz N et al. (2010) Regulation of mitochondrial glutathione redox status and protein glutathionylation by respiratory substrates. J Biol Chem 285: 39646–39654. doi:10.1074/jbc.M110.164160. PubMed: 20937819.
44. Odin JA, Huebert RC, Casciola-Rosen L, LaRusso NF, Rosen A (2001) Bcl-2-dependent oxidation of pyruvate dehydrogenase-E2, a primary biliary cirrhosis autoantigen, during apoptosis. J Clin Invest 108: 223–232. doi:10.1172/JCI10716. PubMed: 11457875.
45. Nulton-Persson AC, Starke DW, Mieyal JJ, Szweda LI (2003) Reversible inactivation of alpha-ketoglutarate dehydrogenase in response to alterations in the mitochondrial glutathione status. Biochemistry 42: 4235–4242. doi:10.1021/bi027370f. PubMed: 12680778.
46. Nulton-Persson AC, Szweda LI (2001) Modulation of mitochondrial function by hydrogen peroxide. J Biol Chem 276: 23357–23361. doi:10.1074/jbc.M100320200. PubMed: 11283020.
47. Metelkin E, Demin O, Kovács Z, Chinopoulos C (2009) Modeling of ATP-ADP steady-state exchange rate mediated by the adenine nucleotide translocase in isolated mitochondria. FEBS J 276: 6942–6955. doi:10.1111/j.1742-4658.2009.07394.x. PubMed: 19860824.
48. Chinopoulos C, Adam-Vizi V (2010) Mitochondria as ATP consumers in cellular pathology. Biochim Biophys Acta 1802: 221–227. doi:10.1016/j.bbadis.2009.08.008. PubMed: 19715757.
49. Wu KLH, Hsu C, Chan JYH (2009) Nitric oxide and superoxide anion differentially activate poly(ADP-ribose) polymerase-1 and Bax to induce nuclear translocation of apoptosis-inducing factor and mitochondrial release of cytochrome c after spinal cord injury. J Neurotrauma 26: 965–977. doi:10.1089/neu.2008.0692. PubMed: 19473058.

DISSERTATIONS DEFENDED AT
TALLINN UNIVERSITY OF TECHNOLOGY ON
NATURAL AND EXACT SCIENCES

1. **Olav Kongas**. Nonlinear Dynamics in Modeling Cardiac Arrhytmias. 1998.

2. **Kalju Vanatalu**. Optimization of Processes of Microbial Biosynthesis of Isotopically Labeled Biomolecules and Their Complexes. 1999.

3. **Ahto Buldas**. An Algebraic Approach to the Structure of Graphs. 1999.

4. **Monika Drews**. A Metabolic Study of Insect Cells in Batch and Continuous Culture: Application of Chemostat and Turbidostat to the Production of Recombinant Proteins. 1999.

5. **Eola Valdre**. Endothelial-Specific Regulation of Vessel Formation: Role of Receptor Tyrosine Kinases. 2000.

6. **Kalju Lott**. Doping and Defect Thermodynamic Equilibrium in ZnS. 2000.

7. **Reet Koljak**. Novel Fatty Acid Dioxygenases from the Corals *Plexaura homomalla* and *Gersemia fruticosa.* 2001.

8. **Anne Paju**. Asymmetric oxidation of Prochiral and Racemic Ketones by Using Sharpless Catalyst. 2001.

9. **Marko Vendelin**. Cardiac Mechanoenergetics *in silico*. 2001.

10. **Pearu Peterson**. Multi-Soliton Interactions and the Inverse Problem of Wave Crest. 2001.

11. **Anne Menert**. Microcalorimetry of Anaerobic Digestion. 2001.

12. **Toomas Tiivel**. The Role of the Mitochondrial Outer Membrane in *in vivo* Regulation of Respiration in Normal Heart and Skeletal Muscle Cell. 2002.

13. **Olle Hints**. Ordovician Scolecodonts of Estonia and Neighbouring Areas: Taxonomy, Distribution, Palaeoecology, and Application. 2002.

14. **Jaak Nõlvak**. Chitinozoan Biostratigrapy in the Ordovician of Baltoscandia. 2002.

15. **Liivi Kluge**. On Algebraic Structure of Pre-Operad. 2002.

16. **Jaanus Lass**. Biosignal Interpretation: Study of Cardiac Arrhytmias and Electromagnetic Field Effects on Human Nervous System. 2002.

17. **Janek Peterson**. Synthesis, Structural Characterization and Modification of PAMAM Dendrimers. 2002.

18. **Merike Vaher**. Room Temperature Ionic Liquids as Background Electrolyte Additives in Capillary Electrophoresis. 2002.

19. **Valdek Mikli**. Electron Microscopy and Image Analysis Study of Powdered Hardmetal Materials and Optoelectronic Thin Films. 2003.

20. **Mart Viljus**. The Microstructure and Properties of Fine-Grained Cermets. 2003.

21. **Signe Kask**. Identification and Characterization of Dairy-Related *Lactobacillus.* 2003

22. **Tiiu-Mai Laht**. Influence of Microstructure of the Curd on Enzymatic and Microbiological Processes in Swiss-Type Cheese. 2003.

23. **Anne Kuusksalu**. 2–5A Synthetase in the Marine Sponge *Geodia cydonium*. 2003.

24. **Sergei Bereznev**. Solar Cells Based on Polycristalline Copper-Indium Chalcogenides and Conductive Polymers. 2003.

25. **Kadri Kriis**. Asymmetric Synthesis of C_2-Symmetric Bimorpholines and Their Application as Chiral Ligands in the Transfer Hydrogenation of Aromatic Ketones. 2004.

26. **Jekaterina Reut**. Polypyrrole Coatings on Conducting and Insulating Substracts. 2004.

27. **Sven Nõmm**. Realization and Identification of Discrete-Time Nonlinear Systems. 2004.

28. **Olga Kijatkina**. Deposition of Copper Indium Disulphide Films by Chemical Spray Pyrolysis. 2004.

29. **Gert Tamberg**. On Sampling Operators Defined by Rogosinski, Hann and Blackman Windows. 2004.

30. **Monika Übner**. Interaction of Humic Substances with Metal Cations. 2004.

31. **Kaarel Adamberg**. Growth Characteristics of Non-Starter Lactic Acid Bacteria from Cheese. 2004.

32. **Imre Vallikivi**. Lipase-Catalysed Reactions of Prostaglandins. 2004.

33. **Merike Peld**. Substituted Apatites as Sorbents for Heavy Metals. 2005.

34. **Vitali Syritski**. Study of Synthesis and Redox Switching of Polypyrrole and Poly(3,4-ethylenedioxythiophene) by Using *in-situ* Techniques. 2004.

35. **Lee Põllumaa**. Evaluation of Ecotoxicological Effects Related to Oil Shale Industry. 2004.

36. **Riina Aav**. Synthesis of 9,11-Secosterols Intermediates. 2005.

37. **Andres Braunbrück**. Wave Interaction in Weakly Inhomogeneous Materials. 2005.

38. **Robert Kitt**. Generalised Scale-Invariance in Financial Time Series. 2005.

39. **Juss Pavelson**. Mesoscale Physical Processes and the Related Impact on the Summer Nutrient Fields and Phytoplankton Blooms in the Western Gulf of Finland. 2005.

40. **Olari Ilison**. Solitons and Solitary Waves in Media with Higher Order Dispersive and Nonlinear Effects. 2005.

41. **Maksim Säkki**. Intermittency and Long-Range Structurization of Heart Rate. 2005.

42. **Enli Kiipli**. Modelling Seawater Chemistry of the East Baltic Basin in the Late Ordovician–Early Silurian. 2005.

43. **Igor Golovtsov**. Modification of Conductive Properties and Processability of Polyparaphenylene, Polypyrrole and polyaniline. 2005.

44. **Katrin Laos**. Interaction Between Furcellaran and the Globular Proteins (Bovine Serum Albumin β-Lactoglobulin). 2005.

45. **Arvo Mere**. Structural and Electrical Properties of Spray Deposited Copper Indium Disulphide Films for Solar Cells. 2006.

46. **Sille Ehala**. Development and Application of Various On- and Off-Line Analytical Methods for the Analysis of Bioactive Compounds. 2006.

47. **Maria Kulp**. Capillary Electrophoretic Monitoring of Biochemical Reaction Kinetics. 2006.

48. **Anu Aaspõllu.** Proteinases from *Vipera lebetina* Snake Venom Affecting Hemostasis. 2006.

49. **Lyudmila Chekulayeva**. Photosensitized Inactivation of Tumor Cells by Porphyrins and Chlorins. 2006.

50. **Merle Uudsemaa**. Quantum-Chemical Modeling of Solvated First Row Transition Metal Ions. 2006.

51. **Tagli Pitsi**. Nutrition Situation of Pre-School Children in Estonia from 1995 to 2004. 2006.

52. **Angela Ivask**. Luminescent Recombinant Sensor Bacteria for the Analysis of Bioavailable Heavy Metals. 2006.

53. **Tiina Lõugas**. Study on Physico-Chemical Properties and Some Bioactive Compounds of Sea Buckthorn (*Hippophae rhamnoides* L.). 2006.

54. **Kaja Kasemets**. Effect of Changing Environmental Conditions on the Fermentative Growth of *Saccharomyces cerevisae* S288C: Auxo-accelerostat Study. 2006.

55. **Ildar Nisamedtinov**. Application of ^{13}C and Fluorescence Labeling in Metabolic Studies of *Saccharomyces* spp. 2006.

56. **Alar Leibak**. On Additive Generalisation of Voronoï's Theory of Perfect Forms over Algebraic Number Fields. 2006.

57. **Andri Jagomägi**. Photoluminescence of Chalcopyrite Tellurides. 2006.

58. **Tõnu Martma**. Application of Carbon Isotopes to the Study of the Ordovician and Silurian of the Baltic. 2006.

59. **Marit Kauk**. Chemical Composition of $CuInSe_2$ Monograin Powders for Solar Cell Application. 2006.

60. **Julia Kois**. Electrochemical Deposition of $CuInSe_2$ Thin Films for Photovoltaic Applications. 2006.

61. **Ilona Oja Açik**. Sol-Gel Deposition of Titanium Dioxide Films. 2007.

62. **Tiia Anmann**. Integrated and Organized Cellular Bioenergetic Systems in Heart and Brain. 2007.

63. **Katrin Trummal**. Purification, Characterization and Specificity Studies of Metalloproteinases from *Vipera lebetina* Snake Venom. 2007.

64. **Gennadi Lessin**. Biochemical Definition of Coastal Zone Using Numerical Modeling and Measurement Data. 2007.

65. **Enno Pais**. Inverse problems to determine non-homogeneous degenerate memory kernels in heat flow. 2007.

66. **Maria Borissova**. Capillary Electrophoresis on Alkylimidazolium Salts. 2007.

67. **Karin Valmsen**. Prostaglandin Synthesis in the Coral *Plexaura homomalla*: Control of Prostaglandin Stereochemistry at Carbon 15 by Cyclooxygenases. 2007.

68. **Kristjan Piirimäe**. Long-Term Changes of Nutrient Fluxes in the Drainage Basin of the Gulf of Finland – Application of the PolFlow Model. 2007.

69. **Tatjana Dedova**. Chemical Spray Pyrolysis Deposition of Zinc Sulfide Thin Films and Zinc Oxide Nanostructured Layers. 2007.

70. **Katrin Tomson**. Production of Labelled Recombinant Proteins in Fed-Batch Systems in *Escherichia coli*. 2007.

71. **Cecilia Sarmiento**. Suppressors of RNA Silencing in Plants. 2008.

72. **Vilja Mardla**. Inhibition of Platelet Aggregation with Combination of Antiplatelet Agents. 2008.

73. **Maie Bachmann**. Effect of Modulated Microwave Radiation on Human Resting Electroencephalographic Signal. 2008.

74. **Dan Hüvonen**. Terahertz Spectroscopy of Low-Dimensional Spin Systems. 2008.

75. **Ly Villo**. Stereoselective Chemoenzymatic Synthesis of Deoxy Sugar Esters Involving *Candida antarctica* Lipase B. 2008.

76. **Johan Anton**. Technology of Integrated Photoelasticity for Residual Stress Measurement in Glass Articles of Axisymmetric Shape. 2008.

77. **Olga Volobujeva**. SEM Study of Selenization of Different Thin Metallic Films. 2008.

78. **Artur Jõgi**. Synthesis of 4'-Substituted 2,3'-dideoxynucleoside Analogues. 2008.

79. **Mario Kadastik**. Doubly Charged Higgs Boson Decays and Implications on Neutrino Physics. 2008.

80. **Fernando Pérez-Caballero**. Carbon Aerogels from 5-Methylresorcinol-Formaldehyde Gels. 2008.

81. **Sirje Vaask**. The Comparability, Reproducibility and Validity of Estonian Food Consumption Surveys. 2008.

82. **Anna Menaker**. Electrosynthesized Conducting Polymers, Polypyrrole and Poly(3,4-ethylenedioxythiophene), for Molecular Imprinting. 2009.

83. **Lauri Ilison**. Solitons and Solitary Waves in Hierarchical Korteweg-de Vries Type Systems. 2009.

84. **Kaia Ernits**. Study of In_2S_3 and ZnS Thin Films Deposited by Ultrasonic Spray Pyrolysis and Chemical Deposition. 2009.

85. **Veljo Sinivee**. Portable Spectrometer for Ionizing Radiation "Gammamapper". 2009.

86. **Jüri Virkepu**. On Lagrange Formalism for Lie Theory and Operadic Harmonic Oscillator in Low Dimensions. 2009.

87. **Marko Piirsoo**. Deciphering Molecular Basis of Schwann Cell Development. 2009.

88. **Kati Helmja**. Determination of Phenolic Compounds and Their Antioxidative Capability in Plant Extracts. 2010.

89. **Merike Sõmera**. Sobemoviruses: Genomic Organization, Potential for Recombination and Necessity of P1 in Systemic Infection. 2010.

90. **Kristjan Laes**. Preparation and Impedance Spectroscopy of Hybrid Structures Based on $CuIn_3Se_5$ Photoabsorber. 2010.

91. **Kristin Lippur**. Asymmetric Synthesis of 2,2'-Bimorpholine and its 5,5'-Substituted Derivatives. 2010.

92. **Merike Luman**. Dialysis Dose and Nutrition Assessment by an Optical Method. 2010.

93. **Mihhail Berezovski**. Numerical Simulation of Wave Propagation in Heterogeneous and Microstructured Materials. 2010.

94. **Tamara Aid-Pavlidis**. Structure and Regulation of BDNF Gene. 2010.

95. **Olga Bragina**. The Role of Sonic Hedgehog Pathway in Neuro- and Tumorigenesis. 2010.

96. **Merle Randrüüt**. Wave Propagation in Microstructured Solids: Solitary and Periodic Waves. 2010.

97. **Marju Laars**. Asymmetric Organocatalytic Michael and Aldol Reactions Mediated by Cyclic Amines. 2010.

98. **Maarja Grossberg**. Optical Properties of Multinary Semiconductor Compounds for Photovoltaic Applications. 2010.

99. **Alla Maloverjan**. Vertebrate Homologues of Drosophila Fused Kinase and Their Role in Sonic Hedgehog Signalling Pathway. 2010.

100. **Priit Pruunsild**. Neuronal Activity-Dependent Transcription Factors and Regulation of Human *BDNF* Gene. 2010.

101. **Tatjana Knjazeva**. New Approaches in Capillary Electrophoresis for Separation and Study of Proteins. 2011.

102. **Atanas Katerski**. Chemical Composition of Sprayed Copper Indium Disulfide Films for Nanostructured Solar Cells. 2011.

103. **Kristi Timmo.** Formation of Properties of $CuInSe_2$ and $Cu_2ZnSn(S,Se)_4$ Monograin Powders Synthesized in Molten KI. 2011.
104. **Kert Tamm**. Wave Propagation and Interaction in Mindlin-Type Microstructured Solids: Numerical Simulation. 2011.
105. **Adrian Popp**. Ordovician Proetid Trilobites in Baltoscandia and Germany. 2011.
106. **Ove Pärn**. Sea Ice Deformation Events in the Gulf of Finland and This Impact on Shipping. 2011.
107. **Germo Väli**. Numerical Experiments on Matter Transport in the Baltic Sea. 2011.
108. **Andrus Seiman**. Point-of-Care Analyser Based on Capillary Electrophoresis. 2011.
109. **Olga Katargina**. Tick-Borne Pathogens Circulating in Estonia (Tick-Borne Encephalitis Virus, *Anaplasma phagocytophilum*, *Babesia* Species): Their Prevalence and Genetic Characterization. 2011.
110. **Ingrid Sumeri**. The Study of Probiotic Bacteria in Human Gastrointestinal Tract Simulator. 2011.
111. **Kairit Zovo**. Functional Characterization of Cellular Copper Proteome. 2011.
112. **Natalja Makarytsheva**. Analysis of Organic Species in Sediments and Soil by High Performance Separation Methods. 2011.
113. **Monika Mortimer**. Evaluation of the Biological Effects of Engineered Nanoparticles on Unicellular Pro- and Eukaryotic Organisms. 2011.
114. **Kersti Tepp**. Molecular System Bioenergetics of Cardiac Cells: Quantitative Analysis of Structure-Function Relationship. 2011.
115. **Anna-Liisa Peikolainen**. Organic Aerogels Based on 5-Methylresorcinol. 2011.
116. **Leeli Amon**. Palaeoecological Reconstruction of Late-Glacial Vegetation Dynamics in Eastern Baltic Area: A View Based on Plant Macrofossil Analysis. 2011.
117. **Tanel Peets**. Dispersion Analysis of Wave Motion in Microstructured Solids. 2011.
118. **Liina Kaupmees**. Selenization of Molybdenum as Contact Material in Solar Cells. 2011.
119. **Allan Olspert**. Properties of VPg and Coat Protein of Sobemoviruses. 2011.
120. **Kadri Koppel**. Food Category Appraisal Using Sensory Methods. 2011.
121. **Jelena Gorbatšova**. Development of Methods for CE Analysis of Plant Phenolics and Vitamins. 2011.
122. **Karin Viipsi**. Impact of EDTA and Humic Substances on the Removal of Cd and Zn from Aqueous Solutions by Apatite. 2012.
123. **David Schryer**. Metabolic Flux Analysis of Compartmentalized Systems Using Dynamic Isotopologue Modeling. 2012.
124. **Ardo Illaste**. Analysis of Molecular Movements in Cardiac Myocytes. 2012.
125. **Indrek Reile**. 3-Alkylcyclopentane-1,2-Diones in Asymmetric Oxidation and Alkylation Reactions. 2012.
126. **Tatjana Tamberg**. Some Classes of Finite 2-Groups and Their Endomorphism Semigroups. 2012.

127. **Taavi Liblik**. Variability of Thermohaline Structure in the Gulf of Finland in Summer. 2012.
128. **Priidik Lagemaa**. Operational Forecasting in Estonian Marine Waters. 2012.
129. **Andrei Errapart**. Photoelastic Tomography in Linear and Non-linear Approximation. 2012.
130. **Külliki Krabbi**. Biochemical Diagnosis of Classical Galactosemia and Mucopolysaccharidoses in Estonia. 2012.
131. **Kristel Kaseleht**. Identification of Aroma Compounds in Food using SPME-GC/MS and GC-Olfactometry. 2012.
132. **Kristel Kodar**. Immunoglobulin G Glycosylation Profiling in Patients with Gastric Cancer. 2012.
133. **Kai Rosin**. Solar Radiation and Wind as Agents of the Formation of the Radiation Regime in Water Bodies. 2012.
134. **Ann Tiiman**. Interactions of Alzheimer's Amyloid-Beta Peptides with Zn(II) and Cu(II) Ions. 2012.
135. **Olga Gavrilova**. Application and Elaboration of Accounting Approaches for Sustainable Development. 2012.
136. **Olesja Bondarenko**. Development of Bacterial Biosensors and Human Stem Cell-Based *In Vitro* Assays for the Toxicological Profiling of Synthetic Nanoparticles. 2012.
137. **Katri Muska**. Study of Composition and Thermal Treatments of Quaternary Compounds for Monograin Layer Solar Cells. 2012.
138. **Ranno Nahku**. Validation of Critical Factors for the Quantitative Characterization of Bacterial Physiology in Accelerostat Cultures. 2012.
139. **Petri-Jaan Lahtvee**. Quantitative Omics-level Analysis of Growth Rate Dependent Energy Metabolism in *Lactococcus lactis*. 2012.
140. **Kerti Orumets**. Molecular Mechanisms Controlling Intracellular Glutathione Levels in Baker's Yeast *Saccharomyces cerevisiae* and its Random Mutagenized Glutathione Over-Accumulating Isolate. 2012.
141. **Loreida Timberg**. Spice-Cured Sprats Ripening, Sensory Parameters Development, and Quality Indicators. 2012.
142. **Anna Mihhalevski**. Rye Sourdough Fermentation and Bread Stability. 2012.
143. **Liisa Arike**. Quantitative Proteomics of *Escherichia coli*: From Relative to Absolute Scale. 2012.
144. **Kairi Otto**. Deposition of In_2S_3 Thin Films by Chemical Spray Pyrolysis. 2012.
145. **Mari Sepp**. Functions of the Basic Helix-Loop-Helix Transcription Factor TCF4 in Health and Disease. 2012.
146. **Anna Suhhova**. Detection of the Effect of Weak Stressors on Human Resting Electroencephalographic Signal. 2012.
147. **Aram Kazarjan**. Development and Production of Extruded Food and Feed Products Containing Probiotic Microorganisms. 2012.
148. **Rivo Uiboupin**. Application of Remote Sensing Methods for the Investigation of Spatio-Temporal Variability of Sea Surface Temperature and Chlorophyll Fields in the Gulf of Finland. 2013.
149. **Tiina Kriščiunaite**. A Study of Milk Coagulability. 2013.

150. **Tuuli Levandi**. Comparative Study of Cereal Varieties by Analytical Separation Methods and Chemometrics. 2013.
151. **Natalja Kabanova**. Development of a Microcalorimetric Method for the Study of Fermentation Processes. 2013.
152. **Himani Khanduri**. Magnetic Properties of Functional Oxides. 2013.
153. **Julia Smirnova**. Investigation of Properties and Reaction Mechanisms of Redox-Active Proteins by ESI MS. 2013.
154. **Mervi Sepp**. Estimation of Diffusion Restrictions in Cardiomyocytes Using Kinetic Measurements. 2013.
155. **Kersti Jääger**. Differentiation and Heterogeneity of Mesenchymal Stem Cells. 2013.
156. **Victor Alari**. Multi-Scale Wind Wave Modeling in the Baltic Sea. 2013.
157. **Taavi Päll**. Studies of CD44 Hyaluronan Binding Domain as Novel Angiogenesis Inhibitor. 2013.
158. **Allan Niidu**. Synthesis of Cyclopentane and Tetrahydrofuran Derivatives. 2013.
159. **Julia Geller**. Detection and Genetic Characterization of *Borrelia* Species Circulating in Tick Population in Estonia. 2013.
160. **Irina Stulova**. The Effects of Milk Composition and Treatment on the Growth of Lactic Acid Bacteria. 2013.
161. **Jana Holmar**. Optical Method for Uric Acid Removal Assessment During Dialysis. 2013.
162. **Kerti Ausmees**. Synthesis of Heterobicyclo[3.2.0]heptane Derivatives *via* Multicomponent Cascade Reaction. 2013.
163. **Minna Varikmaa**. Structural and Functional Studies of Mitochondrial Respiration Regulation in Muscle Cells. 2013.
164. **Indrek Koppel**. Transcriptional Mechanisms of BDNF Gene Regulation. 2014.
165. **Kristjan Pilt**. Optical Pulse Wave Signal Analysis for Determination of Early Arterial Ageing in Diabetic Patients. 2014.
166. **Andres Anier**. Estimation of the Complexity of the Electroencephalogram for Brain Monitoring in Intensive Care. 2014.
167. **Toivo Kallaste**. Pyroclastic Sanidine in the Lower Palaeozoic Bentonites – A Tool for Regional Geological Correlations. 2014.
168. **Erki Kärber**. Properties of ZnO-nanorod/In_2S_3/$CuInS_2$ Solar Cell and the Constituent Layers Deposited by Chemical Spray Method. 2014.
169. **Julia Lehner**. Formation of Cu_2ZnSnS_4 and $Cu_2ZnSnSe_4$ by Chalcogenisation of Electrochemically Deposited Precursor Layers. 2014.
170. **Peep Pitk**. Protein- and Lipid-rich Solid Slaughterhouse Waste Anaerobic Co-digestion: Resource Analysis and Process Optimization. 2014.
171. **Kaspar Valgepea**. Absolute Quantitative Multi-omics Characterization of Specific Growth Rate-dependent Metabolism of *Escherichia coli*. 2014.
172. **Artur Noole**. Asymmetric Organocatalytic Synthesis of 3,3'-Disubstituted Oxindoles. 2014.
173. **Robert Tsanev**. Identification and Structure-Functional Characterisation of the Gene Transcriptional Repressor Domain of Human Gli Proteins. 2014.

174. **Dmitri Kartofelev**. Nonlinear Sound Generation Mechanisms in Musical Acoustic. 2014.
175. **Sigrid Hade**. GIS Applications in the Studies of the Palaeozoic Graptolite Argillite and Landscape Change. 2014.
176. **Agne Velthut-Meikas**. Ovarian Follicle as the Environment of Oocyte Maturation: The Role of Granulosa Cells and Follicular Fluid at Pre-Ovulatory Development. 2014.
177. **Kristel Hälvin**. Determination of B-group Vitamins in Food Using an LC-MS Stable Isotope Dilution Assay. 2014.
178. **Mailis Päri**. Characterization of the Oligoadenylate Synthetase Subgroup from Phylum Porifera. 2014.
179. **Jekaterina Kazantseva**. Alternative Splicing of *TAF4*: A Dynamic Switch between Distinct Cell Functions. 2014.
180. **Jaanus Suurväli**. Regulator of G Protein Signalling 16 (RGS16): Functions in Immunity and Genomic Location in an Ancient MHC-Related Evolutionarily Conserved Synteny Group. 2014.
181. **Ene Viiard**. Diversity and Stability of Lactic Acid Bacteria During Rye Sourdough Propagation. 2014.
182. **Kristella Hansen**. Prostaglandin Synthesis in Marine Arthropods and Red Algae. 2014.
183. **Helike Lõhelaid**. Allene Oxide Synthase-lipoxygenase Pathway in Coral Stress Response. 2015.
184. **Normunds Stivrinš**. Postglacial Environmental Conditions, Vegetation Succession and Human Impact in Latvia. 2015.
185. **Mary-Liis Kütt**. Identification and Characterization of Bioactive Peptides with Antimicrobial and Immunoregulating Properties Derived from Bovine Colostrum and Milk. 2015.
186. **Kazbulat Šogenov**. Petrophysical Models of the CO_2 Plume at Prospective Storage Sites in the Baltic Basin. 2015.
187. **Taavi Raadik**. Application of Modulation Spectroscopy Methods in Photovoltaic Materials Research. 2015.
188. **Reio Põder**. Study of Oxygen Vacancy Dynamics in Sc-doped Ceria with NMR Techniques. 2015.
189. **Sven Siir**. Internal Geochemical Stratification of Bentonites (Altered Volcanic Ash Beds) and its Interpretation. 2015.
190. **Kaur Jaanson**. Novel Transgenic Models Based on Bacterial Artificial Chromosomes for Studying BDNF Gene Regulation. 2015.